



universität
wien

DISSERTATION

Titel der Dissertation

Global in situ upper air data for climate change research

Verfasst von

Lorenzo Ramella Pralungo

angestrebter akademischer Grad

Doktor der Naturwissenschaften (Dr. rer. nat.)

Wien, 2014

Studienkennzahl lt. Studienblatt:	A 791 415
Dissertationsgebiet lt. Studienblatt:	Meteorologie und Geophysik
Betreuer:	Ao. Univ.-Prof. Dr. Leopold Haimberger

Abstract

Availability of long and homogenized time series plays a key role in climate understanding. While many studies already involve surface and upper air data (since the 1970s), an important fraction of kites, PILOT balloons and radiosondes, containing temperature and wind data, have only in the last few years been digitized and made available to the scientific community.

The lack of long homogenized upper air records has been identified as a major source of uncertainty in global analyses, causing serious limitations in our ability to diagnose climate change. This thesis is an attempt to fill this gap and its approach can be summarized in three main steps: (i) collection of all the new digitized data and organization of these data in a global archive, structured in a convenient and user-friendly time series format; (ii) homogenization of temperature and wind records; and (iii) analysis of the tropical temperature trends in the layer 1000-100hPa, directly using temperature and wind data employing the thermal wind relation, to demonstrate that the amplification of the surface temperature trend is stable and source independent.

The first part of this thesis focuses on the collection and merge of all available archives of upper air data. An automatic procedure has been developed to meld data from different sources. The result is in the most comprehensive archive of upper air temperature and wind (U and V components) data, organized in time series at 16 standard pressure levels. This archive contains data from 3217 stations, spanning from 1905 up to 2013. Although the data itself has an enormous potential for climate-related research, raw time series may be affected by many artificial shifts and jumps, which can limit their worth and interest.

The second part of this thesis is devoted to the complex task of finding and adjusting the inhomogeneities affecting the raw temperature and wind time series. The homogenization procedure that has been developed is able to locate and repair artificial shifts by using background information from the National Oceanic and Atmospheric Administration 20th Century Reanalysis (NOAA - 20CR), which has been produced using surface data only. This guarantees the complete independence between analyzed data and the background. Regarding wind time series, the majority of the breaks detected occurred before 1960, when the procedure for tracking the balloons was manual. For temperature, several significant breaks have been detected and fixed in the early and in the recent years.

The last part of this thesis is dedicated to the estimation of tropical temperature trends using zonal U-winds, employing the thermal-wind relationship. Tropical tropospheric trends have been a matter of debate in the last 20 years because of the significant discrepancies between climate models' predictions and observations coming from radiosondes and satellites. A comparison between the above-mentioned homogenized wind data and the homogenized temperature archive has been performed. A good agreement of trends derived from temperature and inferred by wind was found. Specifically, both sources are showing a surface trend amplification factor in the range 1.4-2.0 at 200hPa that is fitting within the range of CIMP5 climate model predictions, reconciling previous trend discrepancies.

The long and homogeneous archive that contains temperature and wind upper air data spanning the whole 20th century, is however, considered the main contribution of this thesis to the scientific community. This data set can be employed for climate studies and as input for global reanalysis efforts.

Zusammenfassung

Die Verfügbarkeit langer und homogener Zeitreihen ist unverzichtbar für die Klimaforschung. Viele Studien beschäftigten sich bereits mit Boden- und Atmosphärendaten (ab den 1970er Jahren), aber eine große Zahl an Temperatur- und Winddaten von Drachen, PILOT-Ballonen und Radiosonden wurde erst in den letzten Jahren digitalisiert und veröffentlicht.

Der Mangel an langen, homogenisierten Zeitreihen der freien Atmosphäre ist ein Hauptgrund für die Schwierigkeit der Detektion des Klimawandels. Die vorliegende Dissertation leistet einen Beitrag zur Verbesserung der Datenlage und besteht aus drei Teilen: (i) Sammeln und Zusammenfügen aller neu digitalisierten Daten in einem Archiv und nutzerfreundliche Verfügbarmachung als Zeitserien; (ii) Homogenisierung der Temperatur- und Winddaten; (iii) Analyse tropischer Temperaturtrends in der Schicht von 1000-100hPa mit Hilfe der thermischen Windgleichung unter Verwendung der homogenisierten Daten, um die Amplifizierung der bodennahen Temperaturtrends mit unabhängigen Daten nachzuweisen.

Der erste Teil dieser Dissertation beschäftigt sich mit dem Sammeln und Zusammenfügen aller verfügbaren Archive von Daten der freien Atmosphäre. Das Zusammenfügen von Daten aus verschiedenen Quellen wurde automatisiert. Das Ergebnis ist das zur Zeit umfassendste Datenarchiv der freien Atmosphäre und beinhaltet Wind- (u- und v-Komponenten) sowie Temperaturdaten als Zeitreihen auf 16 Standarddruckflächen. Das Archiv umfasst 3217 Stationen im Zeitraum 1905-2013. Obwohl diese Daten von großem Interesse für die Klimaforschung sind, können die Rohdaten artifizielle Sprünge und Trends aufweisen und dadurch in ihrem Wert für die Forschung gemindert werden.

Im zweiten Teil der vorliegenden Dissertation wird der aufwändige Vorgang des Auffindens und Homogenisierens der beschriebenen zeitlichen Inhomogenitäten dargestellt. Die entwickelte Homogenisierungsmethode kann artifizielle Sprünge durch Verwendung von Background-Information der National Oceanic and Atmospheric Administration 20th Century Reanalysis (NOAA-20CR), welche ausschließlich Bodenbeobachtungen assimiliert hat, auffinden und korrigieren. Dieser Umstand sichert die vollständige Unabhängigkeit der analysierten Daten von den zu korrigierenden Radiosondendaten. Die größte Zahl an Sprüngen in den Windzeitreihen wurde in den Jahren vor 1960 gefunden, als die Nachverfolgung der Ballone noch manuell erfolgte. Die Temperaturzeitreihen weisen signifikante Bruchstellen verteilt über die gesamte untersuchte Periode auf.

Der letzte Teil dieser Dissertation beschäftigt sich mit der Abschätzung des tropischen Temperaturtrends unter Verwendung der u-Windkomponente und der thermischen Windgleichung. Über den Temperaturtrend der tropischen Troposphäre wird seit vielen Jahren debattiert, da beträchtliche Diskrepanzen zwischen Modellvorhersagen und Beobachtungen von Radiosonden und Satelliten bestehen. Ein Vergleich zwischen Trends aus homogenisierten Winddaten und Trends aus homogenisierten Temperaturdaten zeigt, dass die Ergebnisse aus diesen unabhängigen Beobachtungen gut übereinstimmen. Trends aus Wind und Temperatur zeigen beide einen Amplifizierungsfaktor im Bereich von 1.4 bis 2.0 in 200hPa, in Übereinstimmung mit Ergebnissen der CMIP5-Modellergebnisse. Frühere Trenddiskrepanzen konnten nun also beseitigt werden.

Das lange und homogenisierte Archiv der Wind und Temperaturdaten der freien Atmosphäre, im 20. Jahrhundert wird jedoch als wichtigster Beitrag dieser Dissertation für die wissenschaftliche Gemeinschaft angesehen. Diese Daten können für Klimaforschung und als Input für künftige Reanalyseprojekte verwendet werden.

Contents

Abstract	i
Zusammenfassung	iii
1 Introduction	1
2 A global radiosonde and tracked balloon archive on 16 pressure levels (GRASP) back to 1905 - Part 1: Merging and interpolation to 00:00 and 12:00 GMT	13
3 A global radiosonde and tracked balloon archive on 16 pressure levels (GRASP) back to 1905 - Part 2: Homogeneity adjustments for PILOT and radiosonde wind data	31
4 New estimates of tropical mean temperature trend profiles from zonal mean historical radiosonde and pilot balloon wind shear observations	53
5 Conclusions	81
6 Outlook	95
Bibliography	97
Acknowledgments	103
Curriculum vitae	105

1 Introduction

The understanding of climate variability requires observed long time series of the climate state quantities not only at the Earth's surface but also the free atmosphere, since climate anomalies and climate change have a three-dimensional spatial structure. One of the main limitations and sources of uncertainty affecting the climate change estimation with upper air records like radiosondes and pilot balloons is the lack of long homogenized series, as identified by the Intergovernmental Panel on Climate Change (IPCC) 4th assessment report (Solomon et al. (2007); Le Treut et al. (2007)).

The primary intention of this thesis is to overcome the mentioned limitation by creating long and homogeneous temperature and wind time series involving all the currently available in situ upper air data sets.

The project can be split in three strongly related sections:

- (i) Generation of a comprehensive archive merging the existing fragmentary archives of upper air data;
- (ii) Development of a unified automatic homogenization system that analyzes and adjusts upper air temperature, wind and humidity data-sets together, using available reanalysis background departure data;
- (iii) Analysis of the temperature trends over the tropic belt (20N-20S) using the archive generated in (i) and the adjustments in (ii). The trends are evaluated directly employing temperature data and indirectly using wind time series processed through thermal wind relation. The goal is to find a robust amplification of the surface trends reconciling the discrepancy existing between observations and the outcomes from the climate models.

The point (i) finds incentive on the fact that in the last years an increasing number of upper air data has been digitized but not yet integrated in a common format that would make them valuable for climate analysis. Not surprisingly, there are very few upper air wind climatologies that go back beyond 1958, and most of them work with monthly data although thousands of ascents are available since 1920s. Some studies have reconstructed the flow fields during special climatological events such as the Dust Bowl drought in the 1930s (Brönnimann et al. (2009)); some other works have characterized climate anomalies in troposphere and stratosphere in association with the particularly strong El Niño event registered between 1940-42 (Brönnimann and Luterbacher (2004)). The first section of this thesis describes the approach to improve data availability, via the generation of an archive that includes temperature and wind time series as far back as such data exist, but only on standard pressure levels

(10, 20, 30, 50, 70, 100, 150, 200, 250, 300, 400, 500, 700, 850, 925, 1000 hPa). Data on altitude levels are interpolated to standard pressure levels using temperature and geopotential information from the NOAA Twentieth Century Reanalysis (NOAA-20CR, Compo et al. (2011)). It is required that the time series are from ascending balloons (not kites or tethered balloons) and are at least 300 days long. The availability of a unified source of information that merges all the fragmentary existing archives is high desirable.

The point (ii) refers to the fact that time series homogeneity remains an open topic and each future study will benefit from high quality input data. Up to the beginning of the satellite era in the late 1970s, tracked balloons, and, from the 1940s onwards, radiosondes were practically the only upper-air wind observing system, and these are still now an essential component of the observing network. While radiosonde temperature has been extensively globally homogenized (Haimberger et al. (2008), Haimberger et al. (2012)), the pioneering radiosonde wind data homogenization (Gruber and Haimberger (2008)) has not got much attention and covered only the period 1958-2001. The availability of the freshly digitized PILOT and radiosondes soundings allows for the extension of the time series further back and opens new challenging horizons on the homogenization of full data sets, back till the beginning of the observation record.

Point (iii) contributes to the debate, that was very popular a few years ago (Trenberth et al. (2007); Douglass et al. (2007); Santer et al. (2008)), focused on the tropospheric temperature trend discrepancy between observations (mainly radiosonde) and the results of climate model simulations: while the former were showing no amplification of surface temperature trends the latter depicted a strong amplification of the surface trends in the layer 200-500hPa. It was demonstrated by Allen and Sherwood (2008) that employing radiosonde wind data, recognized as less biased than temperature, and employing the thermal wind relation, was possible to reconstruct a temperature trend profile comparable with climate model outputs, even if with large uncertainty bounds. Still at our days this subject is matter of interest (Thorne et al. (2011); Hartmann et al. (2013); Mitchell et al. (2013)) and only in the most recent comparison Mitchell et al. (2013) were able to prove for the first time that homogenized temperature trends (obtained with the recent effort of Haimberger et al. (2012)) and the Coupled Climate Model Intercomparison Project phase 5th CMIP5 predictions agree to a satisfactory degree in the tropics. However there is still room for improvements.

The surface temperature observations started shortly after the invention of the thermometer in the early 1600s; the first meteorological network was installed in northern Italy in 1650s (Kington (1988)) and, already by the latter part of the 19th century, systematic observations of the weather were being made in almost all inhabited areas of the world.

The upper air observations began only in the second half of the 19th century using the meteo-graph, a recording device measuring pressure and temperature, which flew secured by a rope to

a kite. The measured data were regained after the experiment. This practice was particularly challenging because the kites were linked to the ground and were very difficult to maneuver in windy conditions. Additionally, the sounding was limited to low altitudes due to the rope. For the first time in the 1892, a balloon was used in France to fly a meteograph and 6 years later these balloons were launched daily (DuBois et al. (2002)). The collected data were then used to demonstrate that the temperature decreased with height up to certain altitude, which varied with the season, and then stabilized above this altitude. In 1902 the discovery of the tropopause and stratosphere was announced at the French Academic of Sciences (Hoinka (1997)). During the next years there was a fast spread of those new instruments that allowed the collection of valuable data for meteorological and aviation purposes.

The name “radiosonde” was coined in 1929 in France and refers to a balloon-borne instruments that transmits atmospheric data (at the beginning only temperature and pressure, and then wind speed and direction, and humidity) to a receiver-recorder on the ground. At the same time, an independent project in Russia designed the first radiosonde device able to convert the sensor readings to Morse code, making the tool particularly easy to use (DuBois et al. (2002)). In the following years the radiosonde was rapidly adopted by the weather bureaus of all the industrialized nations and their colonies, and became an important instrument for scientific campaigns in the most remote regions of the world.

The impact of this device to the advance of meteorology can hardly be exaggerated: it contributed to the discovery of Rossby waves and baroclinic waves and still contributes to the systematization of the weather observations. Notable is also its the contribution to improve the accuracy of the weather forecasts, atmospheric knowledge and it directly affects aeronautics and agriculture.

Already at the end of the 1940s the USA upper air observing system was fully operative and in the next 10 years the coverage reached almost the whole globe (even if with some notable gaps, especially in equatorial and south Africa, South America and Antarctica). Unfortunately, the observation practices were not standardized: different observation times and altitude levels, and different data formats made this valuable information difficult to be used. The observation practice became standardized only after the 1958, when, in the occasion of the International Geophysical Year (IGY, with the main focus of establish interchange between East and West scientific communities that had been seriously interrupted during the cold war) the World Meteorological Organization (WMO¹) introduced uniform criteria in the meteorological practice throughout the world (therefore the IGY is often taken as starting point for climatological studies relying on radiosondes).

¹ <http://www.wmo.int/pages/prog/www/IMOP/publications/IOM-80/CatalogRadiosond.pdf>

The lack of long and homogeneous time series is a serious problem that does not allow to pull out the in situ upper air data (PILOT balloons and radiosondes) full potential and worth. In the last years, many data rescue campaigns have been carried out and different log books have been digitized, bringing to light a huge amount of new data to the scientific community. Those archives contain invaluable temperature, wind, geopotential and humidity information but usually they are quite fragmentary, not reporting the information in a common format, which makes the reconstruction of the complete series more problematic .

The first section of this study is fully dedicated to create the most comprehensive and uniform collection of temperature and wind data coming from PILOT balloons and radiosonde merging the following source archives:

- * The Comprehensive Historical Upper-Air Network (CHUAN) data set version 1.7 (Stickler et al. (2010) and Wartenburger et al. (2013)) and the ERA-CLIM Historical Upper-Air Data (Stickler et al. (2014)). These archives have been recently digitized and contain mainly historical upper-air data prior to the IGY. The data sets consist of 20 million measurement values organized in around 5000 ASCII files (with additional metadata) that represent ca. 2000 stations with geopotential, temperature, wind and humidity data. The first record goes back to 1900. The data are mainly at altitude levels and a-synoptic times, and have never been actively assimilated (only passively (Poli et al. (2013))).
- * The Integrated Global Radiosonde Archive (IGRA, Durre et al. (2006)), updated until 2012, contains data (temperature, wind and humidity) on standard and significant pressure levels and sometimes, complementary altitude levels (not used in this work, since they do not add information to the pressure data). The archive is structured in ASCII files. It is quite comprehensive and goes back to 1938. However, this data set has its geographical focus on America and partially lacks Europe prior to the mid-1960s.
- * The ERA-40 observation input data set (Uppala et al. (2005)). This data set is available in BUFR format and contains temperature, wind and humidity observations. It has an important overlap with IGRA but also additional data over Europe, Japan and Antarctica. The ERA-40 data set starts in late 1957 and ends in 2002.
- * The ERA-Interim observation input data set (Dee et al. (2011)). This is the natural replacement of the ERA-40 archives. It covers the period from 1979 up to now and it is updated in near real time. It is available in the far more convenient ODB format. The ERA-Interim is preferred when overlapping with others archives since more robust quality control have been applied to the data.

Each single archive contains a big fraction of unique information, but only by merging all archives it is possible to achieve complete overview of the full upper air data set with the longest time series obtainable.

Unfortunately, those input archives are in different formats: they identify stations with different names or codes (just the station name, WBAN² code, WMO code), the data can be recorded in different altitude or pressure levels, and either in single ascents or in time series reporting one or several observations per day. In order to make the information completely transparent for climate purposes, those formal inhomogeneities have to be removed:

- (i) Each station needs to be identified with the unique WMO IDs. While ERA-Interim, ERA-40 and IGRA already provides WMO IDs, the CHUAN and ECUD archives are given with geographical coordinates and/or station names and/or WBAN code, but only in rare cases WMO ID.
- (ii) Vertical interpolation: from altitude to pressure and if required, from pressure to standard pressure levels;
- (iii) Time interpolation from the a-synoptic observation time to the standard time 00 and 12GMT³;

After the interpolation process, the spatial, temporal and vertical resolutions are guaranteed to be constant within all the stations. To achieve the points (ii) and (iii), a reference temperature and geopotential profile is essential and the NOAA-20CR has been employed as background (for the vertical and time interpolation), since it is the only reanalysis available back to 1871 (apart from ERA-20C (Poli et al. (2013)) which came too late for this study). Thus, even the earliest upper air data can be matched (the longest record goes back to April 1900 and it belongs to Lindenberg station (WMO 10393), which reports temperature). Since the NOAA-20CR is a surface pressure only reanalysis, it is completely independent from the upper air data sets and it can be actively used as reference for the time series homogenization, as it is described in the second part of this work.

For the simple time series visualization, a dedicated Java-Script-based time series viewer has been developed. It is a polyvalent tool that allows quick on line monitoring, comparison of single and multiple time series, and detection of outliers and shifts. The Viewer is available at the page http://srvx7.img.univie.ac.at/~lorenzo/DEVL_rrvis_2.0/html/ and full documentation can be found at <https://reanalyses.org/observations/raobcorerich-visualization>.

The Fig.1 and Fig.2 present two of the longest and most complete time series contained in the Global Radiosonde and tracked balloon Archive on 16 Standard Pressure levels (GRASP) archive, obtained joining the input archives. Fig1 shows, for the station Moscow (Russia) at

² Weather Bureau, Air Force and Navy, <http://www.ncdc.noaa.gov/homr/reports/platforms>

³ Greenwich Mean Time

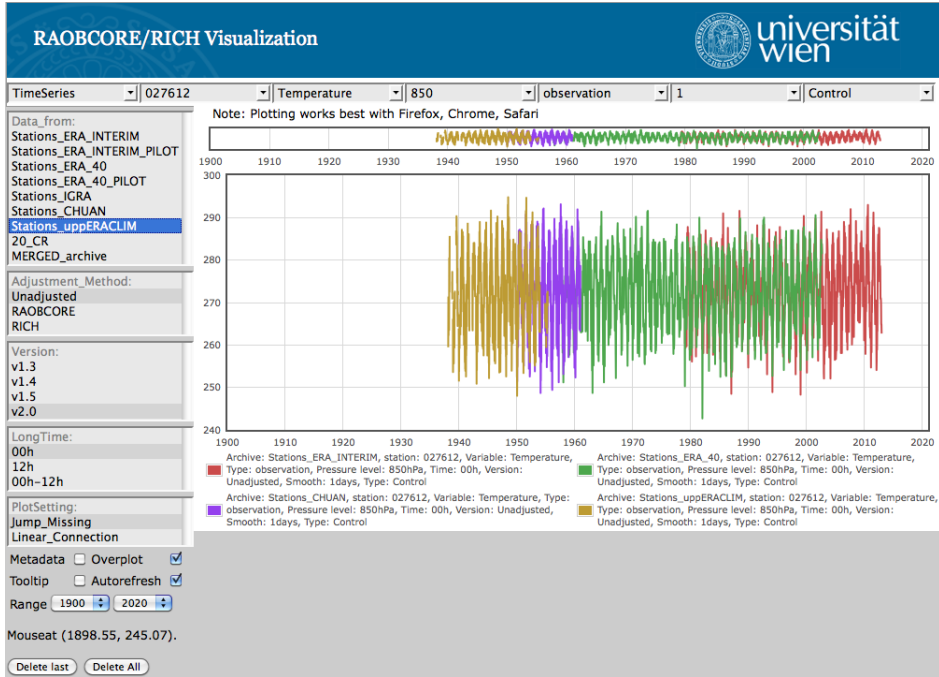


Figure 1: Station 27612, Moscow, Russia. Observed temperature at 850hPa, at 00 GMT. The plot shows the longest and complete temperature time series in the Merged archive, from 1938 up to now: red is ERA-Interim, green ERA-40, violet CHUAN and yellow ECUD. The plot is produced by the time series viewer.

850hPa and 12GMT, the temperature time series that can be fully reconstructed using the information contained in four different archives which partially overlapping. Globally it spans more than 70 years of continuous observations. In the merging procedure in case of multiple data for the same day, a source priority has been set: ERA-Interim, ERA-40, IGRA, CHUAN and ECUD (from the highest to lowest, according to the most robust quality control criteria that the archives themselves guarantee). Fig.2 displays the U-Wind component time series for Denver (USA) at 700hPa and 00GMT. To obtain the complete time series, the CHUAN, IGRA and ERA-Interim archives have been joined to spans more than 80 years of continuous observations. Since the GRASP archive has been intended as a fully suitable input for homogenization purposes, for each station, variable and time series (pressure layer, observation time and available day), it has been equipped with the so-called “*innovation = observations - background*” (also known as *background departures*). These quantities are an essential and integral part of the data set that can facilitate the homogenization procedure. Long observed time series are the best candidates to investigate climate change, but they need to be made free of artificial shifts. This kind of behavior is well documented in the Fig.3(a), in which the observed wind direction time series for the station Bismarck (072764, North Dakota, USA) is plotted at 400, 500, 700 and 850hPa. Well visible is an anomalous shift present in the period 1938-1948 that affects, with comparable behaviors, all the pressure levels. If the shift can be flagged as artificial, i.e.

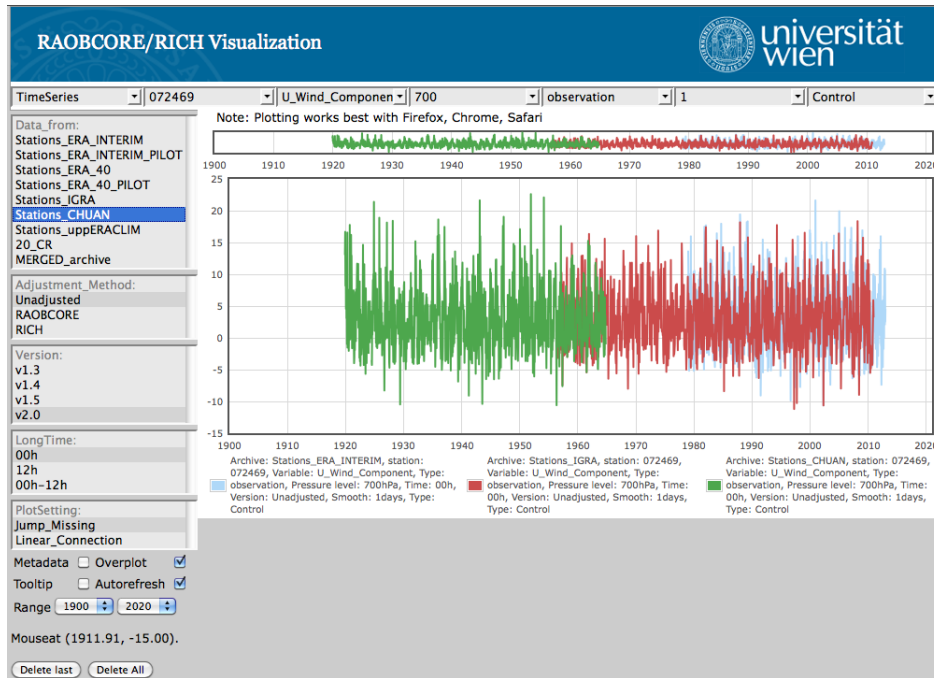


Figure 2: Station 72469 , Denver, Colorado, USA. Observed Wind, U-Component at 700hPa, at 00 GMT. The plot shows the longest and complete Wind (here plotted the U-component) time series in the Merged archive from 1920 up to now: light blue is ERA-Interim, red IGRA and green CHUAN.

as caused by some artifact related with the observation practice itself (human or instrumental), then it should be removed from the original series, otherwise, when assimilated, it may lead to spurious results.

The procedure to remove artificial breaks and trends is referred to as homogenization procedure. The second aim of this work is the development of a unified automatic homogenization system with daily resolution that is able to detect and adjust artificial breaks of the upper air temperature, and wind time series, using surface data only reanalysis as reference. The system has been named **RAOBCORE 2.0** since it has been designed on the basis of the RAOBCORE (Radiosonde OBservation COrrrection using REanalyzes, Haimberger et al. (2008)) homogenization system, in which, for the first time, background time series from reanalysis were used effectively to analyze and fix radiosonde temperature breaks. RAOBCORE was the first successful attempt to homogenize automatically the global radiosonde temperature network for the period 1958-2008, but it had the disadvantage to depend on background information (ERA-Interim and ERA-40) that were dependent themselves on the radiosonde data. The more recent RICH method (Radiosonde Innovation Composite Homogenization, Haimberger et al. (2012)) uses the breakpoints date information from RAOBCORE but it employs neighbor station information for the break adjustments. The new NOAA-20CR is a surface-pressure-only reanalysis; thus it is independent of upper air observations and it has reasonably realistic temperature fields up to stratospheric levels and winds through the whole vertical profile. This product can be

used to reconstruct extreme weather events occurring over the past 140 years in a physically plausible manner (Brönnimann et al. (2013)). Even though, it contains some wind (see Fig. 3 of part I in Stickler and Brönnimann (2011)) and temperature (Compo et al. (2011)) biases, the NOAA-20CR is currently the best product to use as reference in the homogenization of all in situ upper air datasets.

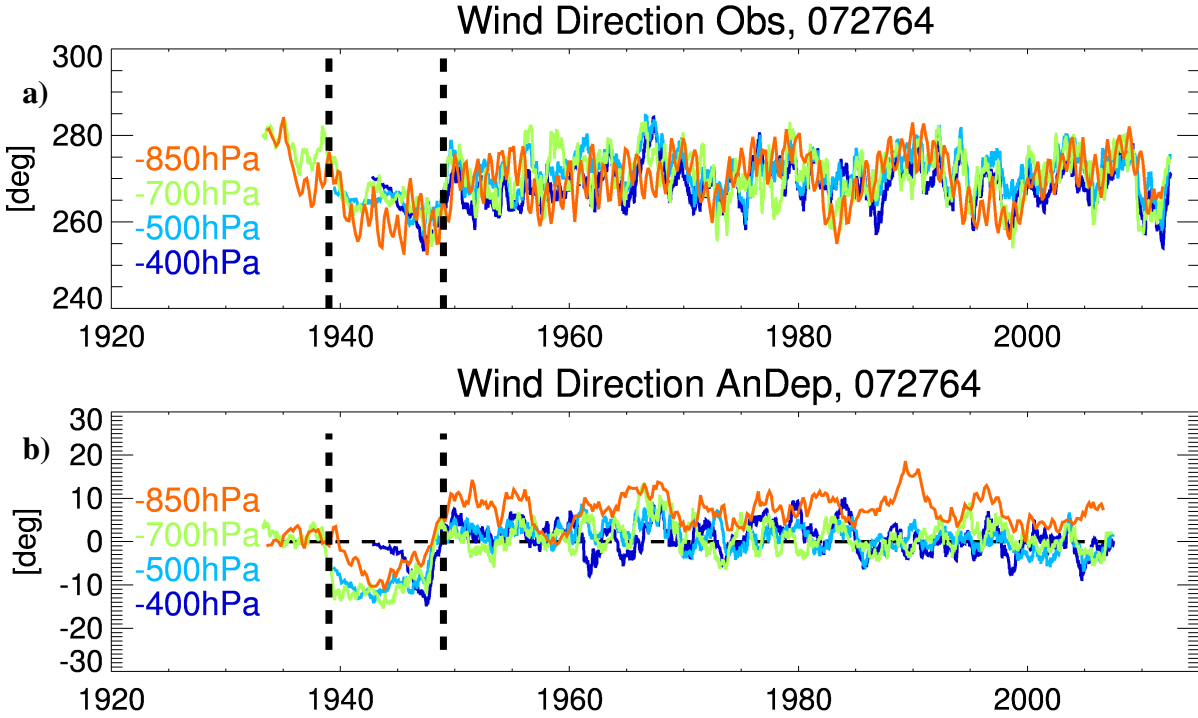


Figure 3: Wind direction observations (a) and innovations (b) for Bismarck (WMO ID 072764, North Dakota, USA), at 00GMT and 700 (orange), 500 (green), 300 (light blue) and 200 (dark blue) hPa levels, respectively. A 365 days running mean has been applied to all time series. Note the shifts in 1938 and 1948. The 850hPa time series in the panel (a) has been shift of $+30^\circ$.

A reliable reference allows the production of robust innovation time series than can easily point out suspicious trends or shifts in the observed data. In the ideal case, the departures average over a large number of realizations in a certain period should be close to zero. Every significant deviation from the expected null value indicates an anomaly in the innovations time series that, theoretically, can be attributed to the observations, under the hypothesis of robust and reliable reference. Fig.3(b) shows the innovations time series obtained from the observation shown in 3(a): the shift in the years 1938-1948, already visible in the raw observations time series, has been cleaned up and it turns out to be more evident and almost equal in size at all the pressure levels.

Following the idea presented in Haimberger et al. (2008), a variant of the Standard Normal Homogeneity Test (SNHT, Alexandersson and Moberg (1997)) is used to detect the breaks by analyzing the innovation time series. Under the null hypothesis of homogeneity, the SNHT time series can be obtained using a Monte Carlo simulation. Thus a critical factor C can be de-

rived to distinguish between natural accepted deviations and artificial shifts. When the SNHT is applied on a real innovation time series, if it responds with a value higher than the selected C , this maximum value is flagged as a potential break. All the detected potential breaks are tested with robustness criteria, which are different for temperature and wind, since the types of inhomogeneity are strictly related to the observation type. While the simultaneous treatment of temperature and wind would allow for combined break detection, in this study it has been found that temperature and wind breaks rarely occur at the same time, with the potential exception of station relocation. Therefore each variable is treated separately for break detection and adjustment:

- * Temperature: the typical bias affecting temperature is radiation error, which is visible as a pervasive tendency to cooling in daytime compared to nighttime observations due to the daytime solar heating on the instrument (Sherwood et al. (2005)). To smooth such inhomogeneity, the mean innovations time series before and after the potential break are calculated at each available pressure level, ensuring that the annual cycle is sampled equally before and after the break. The difference of the means at every pressure level gives the estimated profile of the breaks. After estimating the break at each level, its significance is tested using Student's t test. Only profiles in which at least two pressure levels contain breaks that are significant at the 95% level are adjusted. If a break profile is considered significant, adjustments have been applied at all levels, even if the adjustments have been below the significance threshold at some pressure levels. The adjustment is calculated as the difference of the innovations before and after the break.
- * Wind direction: the most common reason for wind direction breaks is the wrong north alignment. If this explanation is the source of breaks then shifts are expected to be constant in time and for all pressure levels. A break is flagged significant if its magnitude is larger than 1.96 times the standard deviation of the innovation time series. Additionally, in order to accept only unambiguous breaks, it is required that the mean break size along the vertical profile is greater than 3° , and that at least 4 time series (2 pressure levels at both 00GMT and 12GMT times or 4 pressure levels at the same time) are available. Under these conditions, the break is adjusted at both 00 and 12GMT. Since there are cases (especially before 1960) in which the device changes between the observation at 00 and 12GMT (for example, pilot balloon at 00GMT and radiosonde at 12GMT), independent break profiles at different times are allowed. For such cases, the significance test has been performed at both times separately.
- * Wind speed: in what concerns wind speed, the breaks are not constrained physically to the same extent as for wind direction. Large biases are expected only where wind speed is high and typically these occur where jet streams are located (7-12 km above sea level

for the polar jet and 10-16 km for the subtropical jet, where wind speed up to 300km/h can be recorded). At a given pressure level, a break is considered significant if its size is larger than 1.96 times the standard deviation of the innovation time series. If the criterion is fulfilled for least at two levels, the break point is classified as significant and afterward adjusted. For each pressure level, a constant factor λ is estimated from comparing wind speeds and wind speed innovations before and after the break. The adjustment factors remain constant in amplitude between the breakpoints.

For each variable, the break adjustment procedure works backward in time, from the most recent to the earliest break point. In this way, a progressively shorter section of the time series is adjusted. After these procedures, the breaks due to changes in the measurement biases of the observed wind time series should be largely removed. However, since only anomaly time series are adjusted, some records of these homogenized datasets may still have a constant bias.

The last section of the thesis presents a new estimation of the vertical profile of the tropical mean temperature trends from radiosonde and PILOT temperature and wind observations, employing the thermal wind relation.

This subject was a matter of debate in the previous years and became popular at the beginning of the 2000s when the climate models, forced by anthropogenic drivers, were predicting an amplification of the warm surface trend in the tropic belt (defined as 20S, 20N). Inexplicably, this result was not confirmed by the radiosondes and satellites measurements (Trenberth et al. (2007); Douglass et al. (2007); Santer et al. (2008)). The trends amplification was interpreted as a response to the human-caused increases in the greenhouse gases and the mismatch with the observed values to the poor quality of the radiosonde temperature observation and as lack of satisfactory performances of homogenization techniques.

Even after the generous RAOBCORE homogenization effort carried out by Haimberger et al. (2008), the stratospheric radiosondes temperature trends in the tropical regions were still too weak (ERA-Interim, used as background reference in RAOBCORE, ingests itself part of the tropical radiosonde network, shows too weak tropospheric temperature trends). The turning point came in the 2008 when Allen and Sherwood (2008) proposed a novel approach which implies the use of radiosonde observed winds to infer temperature trends under the thermal wind relation hypothesis. The method founds its strength on the more reliable quality of the wind data in comparison with temperature data. These authors found a maximum warming trend at 200hPa of $0.65 \pm 0.47 K$ in the tropical belt for the period 1979-2005 that, when compared with the HadCRUTv4 surface temperature trend of $0.15 \pm 0.23 K$ returned an amplification value of ca. 4 times with a quite large uncertainty. Such amplification factor looks too large when compared to the climate models (CMIP⁴, Meehl et al. (2007)) that predict an amplification factor of

⁴ <http://cmip-pcmdi.llnl.gov/>

ca. 2 times (Santer et al. (2005, 2008)). Already with the recent RICH homogenization procedure (Haimberger et al. (2012)), a satisfactory agreement between observation and the CMIP5 was found for the tropic belt, up to 300hPa (Mitchell et al. (2013)).

Due to the inclusion of the freshly digitalized radiosonde and PILOT data in the GRASP, a much more comprehensive upper air wind archive is available from 1920s, with sufficient coverage of the Tropics region from the 1958 onward. The second big advantage is the presence of homogeneity adjustments for wind and temperature with daily resolution. These are substantial differences with Allen and Sherwood (2008) approach, who have (1) assumed unbiased radiosonde wind profiles; and (2) relied only on radiosondes without including PILOT balloons that help to increase the poor data coverage in the tropical regions.

Not only the input data, but also the numerical calculation method can be improved by employing second order finite differences to calculate the vertical and horizontal discretization of wind shear and temperature trends. Particular care has been adopted also in the uncertainty estimation.

This progress made in the availability and quality of input data should allow to improve the results of Allen and Sherwood (2008), reconciling the gap between climate model predictions and observations, stressing the central role of reliable long and homogeneous time series for climate studies.

The project has been carried out with the productive collaboration of the European Center for Medium Weather Forecast (ECMWF⁵) and the Climatology Research Group⁶ of the University of Bern.

For each of the above-mentioned main points, novel results have been produced and published in peer-reviewed journals.

In the following sections, three journal articles (sections 2, 3 and 4) are presented and introduced by a brief preface. Section 5 wraps up the main results and offers comments. In the last section (6th) a short outlook is given.

⁵ <http://www.ecmwf.int/>

⁶ http://www.geography.unibe.ch/content/forschungsgruppen/klimatologie/index_eng.html

2 A global radiosonde and tracked balloon archive on 16 pressure levels (GRASP) back to 1905 - Part 1: Merging and interpolation to 00:00 and 12:00 GMT

This article presents the effort to merge the newly digitalized (CHUAN and ECUD) with the well known (IGRA, ERA-40 and ERA-Interim) upper air data sets (PILOT balloons and radiosondes) in a comprehensive archive (named GRASP) that contains Temperature, Wind (as U and V wind components) data organized in time series with daily resolution (00 and 12GMT) at the 16 standard pressure level.

The paper describes the work to combine the not uniform information stored in the input archives (associate at each record the WMO ID, and, if necessary, interpolate in time and converting from altitude to pressure data). The NOAA-20CR has been employed as reference for the procedure and for the robustness check. Since the archive has been designed to be employed for homogenization purposes, each observation has been complemented with the corresponding *innovation*. The GRASP and the input archives are stored as Network Common Data Form (NetCDF⁷) files and they are available at the PANGAEA⁸ web portal.

My contributions to this work were to write the *FORTRAN* code from scratch to merge the archives. I have also developed the *JavaScript* code for the Time Series Viewer⁹. I also prepared all the *IDL* visualizations employed for this publication. The text has been produced in collaboration with Leopold Haimberger, who also helped in the beginning when I was dealing with computational issues.

Ramella-Pralungo, L. and Haimberger, L. and Stickler, A. and Brönnimann, S., 2014:
A global radiosonde and tracked balloon archive on 16 pressure levels (GRASP) back to 1905 - Part 1: Merging and interpolation to 00:00 and 12:00 GMT,
Earth System Science Data (ESSD),
doi:10.5194/essdd-6-837-2013

⁷ <http://www.unidata.ucar.edu/software/netcdf/http://www.unidata.ucar.edu/software/netcdf/>

⁸ <http://doi.pangaea.de/10.1594/PANGAEA.823617>

⁹ http://srvx7.img.univie.ac.at/~lorenzo/DEVL_rvis.2.0/html/



A global radiosonde and tracked balloon archive on 16 pressure levels (GRASP) back to 1905 – Part 1: Merging and interpolation to 00:00 and 12:00 GMT

L. Ramella Pralungo¹, L. Haimberger¹, A. Stickler^{2,3}, and S. Brönnimann¹

¹Department of Meteorology and Geophysics, University of Vienna, Althanstrasse 14, 1090 Vienna, Austria

²Oeschger Centre for Climate Change Research, Bern, Switzerland

³Institute of Geography, University of Bern, Switzerland

Correspondence to: L. Ramella Pralungo (lorenzo.ramella-pralungo@univie.ac.at)

Received: 5 December 2013 – Published in Earth Syst. Sci. Data Discuss.: 23 December 2013

Revised: 7 April 2014 – Accepted: 12 April 2014 – Published:

Abstract. Many observed time series of the global radiosonde or PILOT networks exist as fragments distributed over different archives. Identifying and merging these fragments can enhance their value for studies on the three-dimensional spatial structure of climate change.

The Comprehensive Historical Upper-Air Network (CHUAN version 1.7), which was substantially extended in 2013, and the Integrated Global Radiosonde Archive (IGRA) are the most important collections of upper-air measurements taken before 1958. CHUAN (tracked) balloon data start in 1900, with higher numbers from the late 1920s onward, whereas IGRA data start in 1937. However, a substantial fraction of those measurements have not been taken at synoptic times (preferably 00:00 or 12:00 GMT) and on altitude levels instead of standard pressure levels. To make them comparable with more recent data, the records have been brought to synoptic times and standard pressure levels using state-of-the-art interpolation techniques, employing geopotential information from the National Oceanic and Atmospheric Administration (NOAA) 20th Century Reanalysis (NOAA 20CR). From 1958 onward the European Re-Analysis archives (ERA-40 and ERA-Interim) available at the European Centre for Medium-Range Weather Forecasts (ECMWF) are the main data sources. These are easier to use, but pilot data still have to be interpolated to standard pressure levels.

Fractions of the same records distributed over different archives have been merged, if necessary, taking care that the data remain traceable back to their original sources. If possible, station IDs assigned by the World Meteorological Organization (WMO) have been allocated to the station records. For some records which have never been identified by a WMO ID, a local ID above 100 000 has been assigned. The merged data set contains 37 wind records longer than 70 years and 139 temperature records longer than 60 years. It can be seen as a useful basis for further data processing steps, most notably homogenization and gridding, after which it should be a valuable resource for climatological studies.

Homogeneity adjustments for wind using the NOAA-20CR as a reference are described in Ramella Pralungo and Haimberger (2014). Reliable homogeneity adjustments for temperature beyond 1958 using a surface-data-only reanalysis such as NOAA-20CR as a reference have yet to be created.

All the archives and metadata files are available in ASCII and netCDF format in the PANGAEA archive doi:10.1594/PANGAEA.823617.

1 Introduction

The radiosonde and pilot balloon network was practically the only global upper-air observing system up to the late 1970s and is still a valuable source of meteorological and climatological information, although there are now plenty of other observations such as satellite or aircraft data (Dee et al., 2011). While several global radiosonde archives exist and are publicly available, such as the Integrated Global Radiosonde Archive (Durre et al., 2006) or CHUAN (Stickler et al., 2010, 2014), they only partly fulfil the needs of climate scientists due to inhomogeneities in the data and since wind data from tracked balloons are often not available on standard pressure levels.

Almost all homogenized radiosonde data sets published so far, most notably Radiosonde Atmospheric Temperature Products for Assessing Climate (RATPAC) (Free et al., 2005), manually and automatically homogenized versions of the Hadley Centre Atmospheric Temperature (HadAT) (Thorne et al., 2005, 2011), Iterative Universal Kriging (IUK) (Sherwood et al., 2008) as well as Radiosonde Observation Correction using Reanalyses (RAOBCORE) (Haimberger, 2007; Gruber and Haimberger, 2008) and Radiosonde Innovation Composite Homogenization (RICH) (Haimberger et al., 2012), only go back to 1958 since radiosonde and pilot launch times had not been standardized to synoptic times (mostly 00:00 and 12:00 GMT). While radiosonde data are reported on significant pressure levels (levels where the vertical temperature gradient changes) and often have been interpolated to standard pressure levels (10, 20, 30, 50, 70, 100, 150, 200, 250, 300, 400, 500, 700, 850, 1000 hPa), wind data from tracked balloons are mostly given on altitude levels. These altitude levels are relative to the sea level. Without additional temperature information at least every 12 h, it is not possible to interpolate those wind data to standard pressure levels accurately enough to make them suitable for climate analysis.

Not surprisingly there are very few upper-air wind climatologies so far that go back beyond 1958, and most of them work with monthly data although thousands of ascents are available back to the 1920s. Some studies have analysed the flow fields during special climatological events such as the Dust Bowl drought in the 1930s (Brönnimann et al., 2009). In a pioneering study, Brönnimann and Luterbacher (2004) used the data presented in “A historical upper air-data set for the 1939–1944 period” (Brönnimann, 2003) to characterize climate anomalies in troposphere and stratosphere in association with the particularly strong El Niño event of 1940–1942. Grant et al. (2009) studied low-frequency variability and trends of upper-air temperature and geopotential but not winds.

The present study intends to improve the data availability by providing temperature and wind time series as far back as such data exist, but only on standard pressure levels. Data on altitude levels are interpolated to standard pressure levels us-

ing temperature information from the NOAA Twentieth Century Reanalysis (20CR) (Compo et al., 2011). It is required that the time series are from ascending balloons (not kites or tethered balloons) and are at least 300 days long. As such the data set is smaller than CHUAN (Stickler et al., 2014) but is easier to use for time-series analysis. The source data sets are described in the next section. Details on the interpolation methods to standard time/pressure are given in Sect. 3, and data counts and some results are presented in Sect. 4.

2 Input data

Creating a uniform radiosonde data set is challenging. There exist many different data sources, and various digitization efforts around the globe have yielded valuable data, but in different formats. However, one can build on the results of earlier integration efforts. These are

- the Comprehensive Historical Upper-Air Network (CHUAN) data set version 1.7 (Stickler et al., 2010; Wartenburger et al., 2013) and the ERA-CLIM Historical Upper-Air Data (Stickler et al., 2014). The ERA-CLIM historical upper-air data set (termed ECUD here) contains upper-air data collected and digitized within the EU 7th Framework Programme project ERA-CLIM. These archives contain mainly historical upper-air data prior to the International Geophysical Year 1957. The data sets consist of 20 million balloon measurement values in around 5000 files that represent ca. 2000 stations with geopotential, temperature, wind and humidity data. The first record goes back to 1900. Those data, as well as some post 1957 data, have never been actively assimilated.
- the Integrated Global Radiosonde Archive (IGRA) (Durre et al., 2006), updated until 2012. IGRA contains data on standard and significant pressure levels and, sometimes, complementary altitude levels (not used in this work, since they do not add information to the pressure data). It is quite comprehensive and goes back to 1938. However, this data set has its geographical focus on America and lacks a lot of data over Europe prior to the mid-1960s.
- the ERA-40 observation input data set. This data set in BUFR format has lots of overlap with IGRA but contains additional data over Europe, Japan and Antarctica that are missing in IGRA. The ERA-40 data set starts in late 1957 and ends in 2002, however only data from 1958–1978 are used.
- the ERA-Interim observation input data set (Dee et al., 2011). It is equivalent with ERA-40 observation input from 1979 to 2012 but is available in the far more convenient ODB format. The ERA-Interim input data set goes

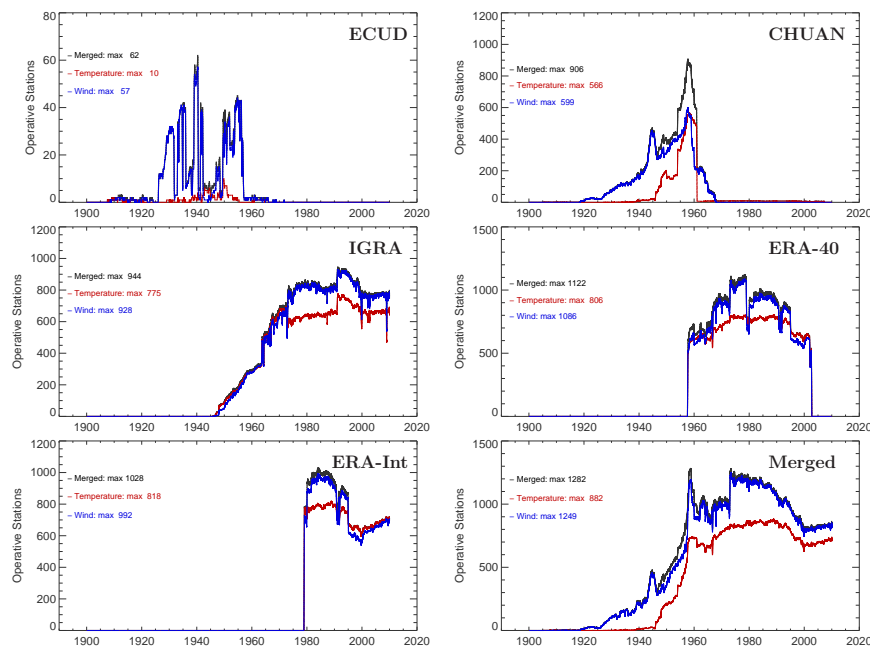


Figure 1. Time series of the numbers of active stations from the respective archives considered in this study. Only data from those stations are counted that have at least 365 ascents. The bottom right picture is the merged archive.

up to present and is preferred to ERA-40 from 1979 onward.

- the NOAA 20th century reanalysis (Compo et al., 2011). It does not contain radiosonde information but its geopotential field can be used to calculate pressure information for altitude levels. Since it is available back to 1871, even the earliest upper-air data can be brought to pressure levels. In this work, it has been used as auxiliary data set for time/pressure interpolation and for quality control purposes.

Not only the observation input data are used from the reanalysis data sets. Analyses and background forecasts from ERA-40, ERA-Interim and the NOAA 20th century reanalysis archives all provide valuable reference fields for comparison with radiosonde/pilot data. Observation minus analysis departures (obs – an) from the NOAA-20CR have been calculated for all observations used. In addition observation minus background departures (obs – bg) have been extracted for both ERA-40 and ERA-Interim back to 1958. These are an integral part of the data set prepared here, and they can greatly facilitate homogenization efforts as has been demonstrated by Haimberger (2007); Haimberger et al. (2008); Gruber and Haimberger (2008); Haimberger et al. (2012).

Figure 1 shows the number of records as function of time in the different archives. While the data count in ECUD and CHUAN prior to 1958 is small compared to the period after 1958, the information content of these archives is very high since practically no other upper-air information is available

at this time. Figures 2 and 10 show also the spatial extent of the data sets. ECUD contains some very valuable early data at remote places such as northern Russia and India, and the data count will soon increase in the future since several not yet digitized upper-air data have recently been identified and will be digitized in ongoing efforts (Allan et al., 2011; Jourdain and Roucaute, 2013).

Our next step is now to merge all those archives to get long time series, spanning the whole operative time of all the available stations.

3 Station identification

The station identification procedure is crucial in order to be able to join different records coming from the same station but stored in different archives. For data assimilated in ERA-40 or ERA-Interim, this is relatively straightforward since the data must have World Meteorological Organization (WMO) number and precise coordinates (latitude, longitude, altitude and time) in order to be assimilated. The IGRA offers WMO ID numbers and coordinates for all its station records as well. The situation is much more difficult for CHUAN and ECUD archives where only around 42 % of the station records have a WMO ID and 74 % have at least a WMO and/or Weather Bureau Army Navy (WBAN) ID number. It has been recognized that many of the unknown station records can be related to WMO ID numbers because of the available geographical information. Nevertheless automatic methods to

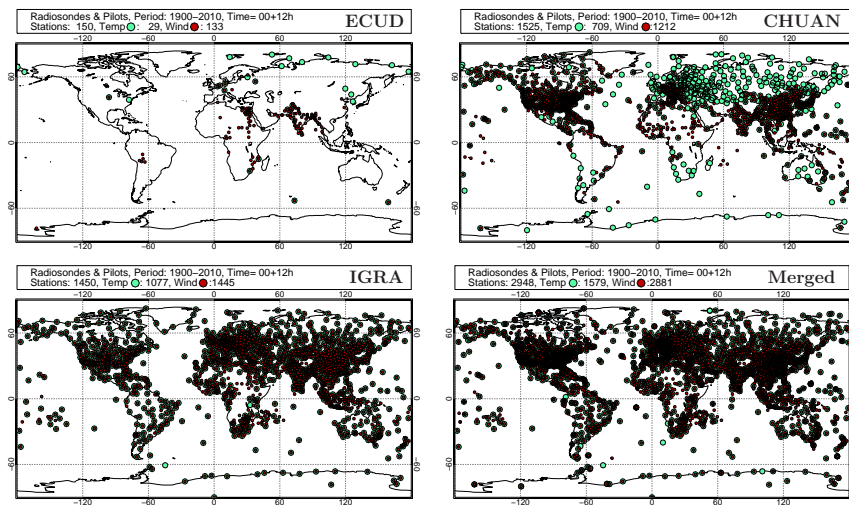


Figure 2. Spatial distributions of stations with at least 365 days of data, at the pressure levels of 850, 700 and 500 hPa, in the different data sets used in this study. The bottom right panel shows the distribution in the merged archive. Only WMO stations have been used.

assign the correct WMO numbers to these stations are complex, if not impossible, for the following reasons:

- the station names differ in different archives, and sometimes they are reported in local language including non-standard ASCII characters.
- In many cases the station ID was changed even when the station was relocated only by a few kilometres, which ended the old record and started a new one. In those cases it is possible to join those records without introducing inhomogeneities.
- In other cases different stations were operative simultaneously (pilot at daytime and radiosonde at nighttime, for instance) in the same area/city; even if they are close to each other, they should be identified as independent stations at first since the data have to be processed differently. Only after the pilot data have been brought from altitude levels to standard pressure levels, merging is possible.
- Cases of erroneous coordinates (typos, exchanged signs etc.) were detected.
- While CHUAN also contains some aircraft, kite and tethered balloon data, these have not been included in the merged data set because of their different characteristics (staying at the same height, often for hours) compared to ascending balloons.

The following four station metadata files (they can be downloaded from doi:10.1594/PANGAEA.823609) have been consulted to manually identify the station records:

- WMO Observing Stations and WMO Catalogue of Radiosondes

- radiosonde comprehensive metadata catalogue (Texas University)
- ERA40 radiosonde list with metadata events
- NOAA WBAN and WMO collection.

Since none of the above metadata file is complete, all of them are essential to assign and validate stations WMO ID numbers. If the lat/long information in the four listed station inventory files were incoherent, a manual check via Google Maps was made, and the wrong entries were discarded. In most cases the most recent station location was trusted. If WMO ID number and lat/long were perfectly matching (most of the cases), the station identification was straightforward. When the station name was the same (considering the different languages and typos) and lat/long were almost (within $< 0.5^\circ$) but not perfectly matching, the station location was monitored with Google Maps. In the majority of cases, a relocation of the station within the same area/city (e.g. from university to airport, from an airport to another) was the reason, and the most recent WMO ID was kept. Stations with implausible lat/long (wrong sign, inverted digits) were highlighted, and, after a double check (if possible), their metadata were corrected. Where the localization was unsafe, no WMO ID number was assigned. As a result of those efforts, roughly 95 % of the CHUAN stations could be identified with a WMO ID number. Nevertheless, the stations not identified were analysed and stored if their records were long enough. A table with station identifiers (file station_list.txt) is presented in the supplements section of the PANGAEA website. Where the latitude and/or the longitude are missing or are unrealistic in the station list inventory, the station was rejected.

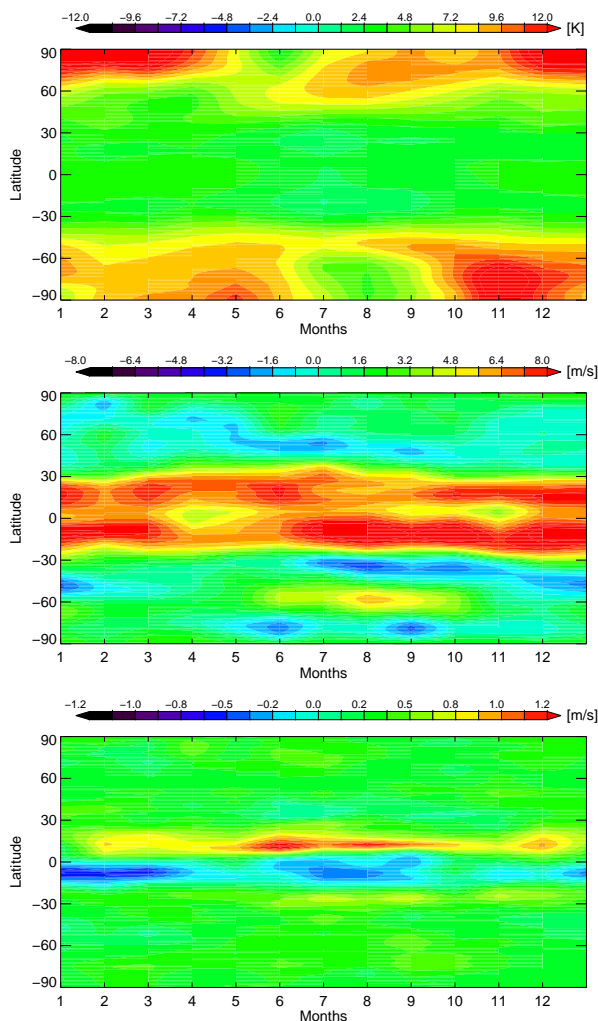


Figure 3. Zonal mean temperature (top), U (middle) and V (bottom) wind biases of NOAA-20CR compared to ERA-Interim at 150 hPa averaged over 00:00 and 12:00 UTC and over each month of the year 1979. Note different scales for U and V components.

4 Interpolation from altitude to standard pressure levels

The pilot balloons used for upper-air wind measurements were tracked using theodolites or RADAR. Both instruments report geometrical height as vertical coordinate. In both CHUAN and ECUD, the wind observations are reported on altitude levels (m a.s.l.). An accurate interpolation from altitude to pressure (most likely not standard) and, in a second step, from non-standard pressure to standard pressure levels requires either temperature plus humidity or geopotential information. Using standard atmosphere temperature values would introduce unnecessarily large errors.

Geopotential information is available globally every 6 h on a $2^\circ \times 2^\circ$ grid from the NOAA 20CR. These are interpolated bilinearly to the respective station locations (latitude/longitude). While the NOAA 20CR analysis fields are means of an ensemble, and thus spatially relatively smooth, they represent a substantial improvement compared to climatological fields or the standard atmosphere. There are some biases of temperature (and thus geopotential) fields at high tropospheric/low stratospheric levels especially in the polar regions (see Fig. 3a). However, they introduce a small bias, especially before the 1950s since only few ascents reached levels higher than 500 hPa. This can be seen also from Fig. 5.

At the station location we can now find the interpolation weight a from the formula

$$\phi_x = a \cdot \phi_1 + (1 - a) \cdot \phi_2, \quad (1)$$

where $\phi_1 < \phi_x < \phi_2$, where ϕ_1 and ϕ_2 are geopotential values at NOAA-20CR model levels at the station location and ϕ_x is the reported altitude of the measurement multiplied by g . Now it is possible to determine the corresponding pressure at the station location p_x as $\ln p_x = a \cdot \ln p(\phi_2) + (1 - a) \cdot \ln p(\phi_1)$. In order to obtain values on standard pressure levels, we perform again a linear interpolation from pressure ϕ_x levels to standard levels. The latter procedure is necessary also for assimilated pilot (from ERA-40 and ERA-Interim input data) since those are only available on significant levels but not standard levels.

5 Time interpolation

Not all radiosonde and pilot stations report at 00:00 and 12:00 GMT. Particularly before 1958 the launch times were not standardized. In order not to discard too many observations at asynoptic times, also a time interpolation has been implemented that allows backwards continuation of many records. To take into account the diurnal cycle in the temperature and wind fields, we assume that the difference between observation and the reference NOAA 20CR is constant within ± 6 h of the observations. This assumption is justifiable for wind, since wind measurement biases as well as NOAA 20CR biases are not expected to depend strongly on the observation hour, at least not in the vertical mean. The analysis value at the time of the observation t_{obs} is gained by cubic interpolation. Then it is assumed that the analysis departure at time t_{obs} is still (already) valid at 00:00 or 12:00 GMT.

The observations are divided in three time categories as outlined in Table 1. The time offset is at most 6 h, which is crude. It could, in principle, be reduced to 3 h if four synoptic times per day were considered instead of just two. Using the departure definition,

$$\tau(t_{\text{obs}}) = \text{obs}(t_{\text{obs}}) - 20\text{CR}(t_{\text{obs}}), \quad (2)$$

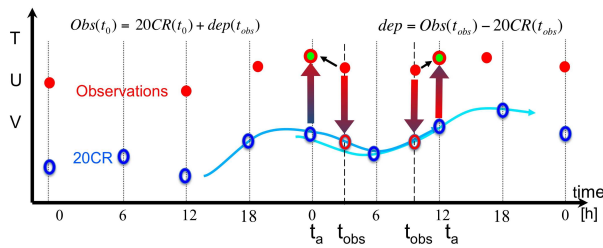


Figure 4. Time interpolation. When there are no observations available at 00:00 or 12:00 UTC but only at other times, a reference value at the time of the asynchronous observation t_{obs} is calculated from the NOAA 20CR, employing a cubic interpolation with the four closest values. The difference $\text{dep}(t_{\text{obs}}) = \text{Obs}(t_{\text{obs}}) - 20\text{CR}(t_{\text{obs}})$ is assumed constant between t_{obs} and the closest synoptic time t_a . The observation at time t_a is obtained by adding the departure $\text{dep}(t_{\text{obs}})$ to $20\text{CR}(t_a)$.

Table 1. Assignment strategy for observations for interpolation to the nearest synoptic time.

Observation	Closest synoptic time
< 06:00 UTC	00:00 UTC
≥ 06:00 UTC and ≤ 18:00 UTC	12:00 UTC
> 18:00 UTC	00:00 UTC (day after)

we estimate the observation at the synoptic time 00:00 and 12:00 UTC as

$$\begin{aligned} \text{obs}(t_0) &= 20\text{CR}(t_0) + \tau(t_{\text{obs}}), \\ \text{obs}(t_{12}) &= 20\text{CR}(t_{12}) + \tau(t_{\text{obs}}). \end{aligned} \quad (3)$$

Figure 4 summarizes the idea: the first two observations at synoptic time have not been manipulated. The third one has been reported at 03:00 UTC, and we would like to shift it to 00:00 UTC. For this purpose we interpolate cubically, using the four closest analysis data, the NOAA 20CR (it could be temperature or U or V wind component) to the observation time, and we calculate the departure observation minus reference. In a second step, we add the departure to the NOAA 20CR value at 00:00 UTC (in this case, t_a in the picture), obtaining the reconstructed observation at the standard time 00:00 UTC. We take care that the same observation is not duplicated at 00:00 and 12:00 UTC.

While the time interpolation method may be sufficient for wind, it is certainly problematic for temperature. The diurnal cycle of the NOAA-20CR temperatures may not always be realistic and the temperature measurement biases of the early radiosondes can be large and can change quickly with local time, particularly at dawn or dusk (Nash and Schmidlin, 1987; Andrae et al., 2004; Redder et al., 2004). In order to facilitate the implementation of an improved interpolation or homogenization procedure that may be able to take into account these sharp transitions, the merged data set contains not

only the (new) standardized launch times but also the original launch times.

The quality of the interpolation procedure can be assessed by comparing the interpolated values from the CHUAN archive with data from the same stations in the ERA-40 archive, which has been possible at least for the years 1957/58. ERA-40 used “first guess at appropriate time” (Upala et al., 2005), meaning that the background was compared to an observation at the time of the observation and not at the nearest synoptic time. Also the analysis and background forecast quality was higher because upper-air data were assimilated. Nevertheless, the mean difference between temperatures interpolated to standard pressure levels is very small (rms difference less than 0.1 K), as expected, since the source data should be the same in CHUAN and ERA-40. There is only a vertically constant difference of 0.05 K (not shown), which is likely attributable to a different conversion from °C to K. In this work, the constant 273.15 has been employed.

6 Merging the different archives

The good agreement between the time series stemming from ECUD, CHUAN, IGRA, ERA-40 and ERA-Interim suggests that it is generally safe to merge these archives into a global one, in order to get longer, more complete and usable time series.

Figure 1 shows the temporal development of the upper-air temperature and wind station numbers in the different archives. While systematic wind observations begin in the 1920s (data stored in the ECUD and CHUAN archives), the systematic upper-air temperature observations start only after 1940 (CHUAN and IGRA). The ECUD record of Meteorologisches Observatorium Lindenberg/Richard-Aßmann Observatorium (ID 10393) in Germany, where also the GRUAN (Seidel et al., 2009) lead centre is located, holds the earliest data with the first ascent dated 4 April 1900. Regular ascents, started in 1905, making the Lindenberg series the longest, continuous upper-air series in the world (Adam and Dier, 2005).

In order to merge all the stations and to ensure efficiency, the following rules have been adopted:

- Station WMO ID must be the same.
- Station location (latitude, longitude and altitude) must be the same (with $\pm 0.5^\circ$ tolerance) in the source archives.
- A data priority has been set: (1) ERA-Interim, (2) ERA-40, (3) IGRA, (4) CHUAN and (5) ECUD. This means the following: if ERA-Interim data were available, they were used except for those found erroneous in the quality control step outlined below. Then, ERA-40 was used to fill the gaps left by ERA-Interim, then IGRA, then CHUAN and finally ECUD. Thus the ECUD data are

2 A global radiosonde and tracked balloon archive on 16 pressure levels (GRASP) back to 1905 - Part 1: Merging and interpolation to 00:00 and 12:00 GMT

L. Ramella Pralungo et al.: A global radiosonde and tracked balloon archive

7

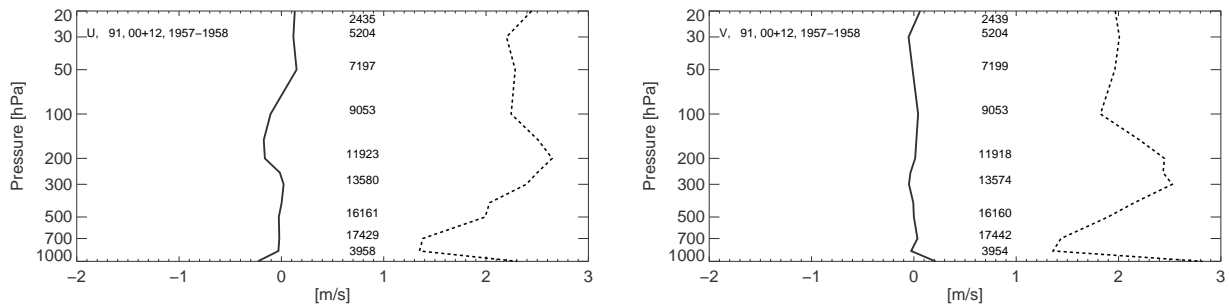


Figure 5. Mean (solid) and rms (dashed) U (left panel) and V (right panel) difference between observations interpolated to standard pressure levels in CHUAN and ERA-40, averaged over 91 stations at 00:00 and 12:00 UTC, for the period 1957–1958 in North America. The total number of observations at each pressure level is also reported. Differences come mostly from different temperatures used for interpolation to pressure levels. Only WMO stations have been used.

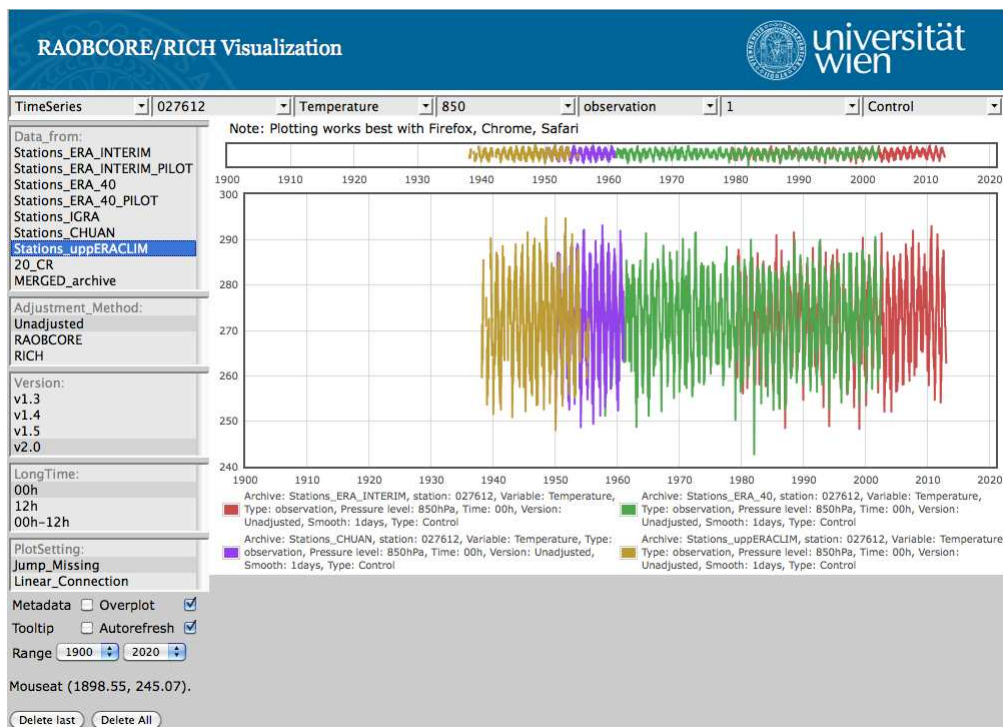


Figure 6. Observed temperature time series at station Moscow (027612, Russia) at 850 hPa, at 00:00 UTC. The plot shows the longest and complete temperature time series in the merged archive (1938–2012): red is ERA-Interim, green ERA-40, violet CHUAN and yellow ECUD. The imperfect overlap between the common parts of the archives is a JavaScript artifact which applies a smoothing function if the number of points exceeds the plot resolution. If one zooms in with the time-series viewer, the discrepancies vanish.

used only if they were found in none of the above data sets. The merge procedure is done for every measurement; that is a record for a particular day can consist of values from different archives.

- After the merger, only merged stations with more than 365 days have been kept.

The time series of Moscow in Fig. 6 is an example of a time series that has unique contributions from each of the data sets. It is also one of the very few stations that have temperature data before 1940. One can see the overlap between data sets. The data in the plot do not exactly overlap because the time series are individually sampled, and not the same days are picked for the different data sets.

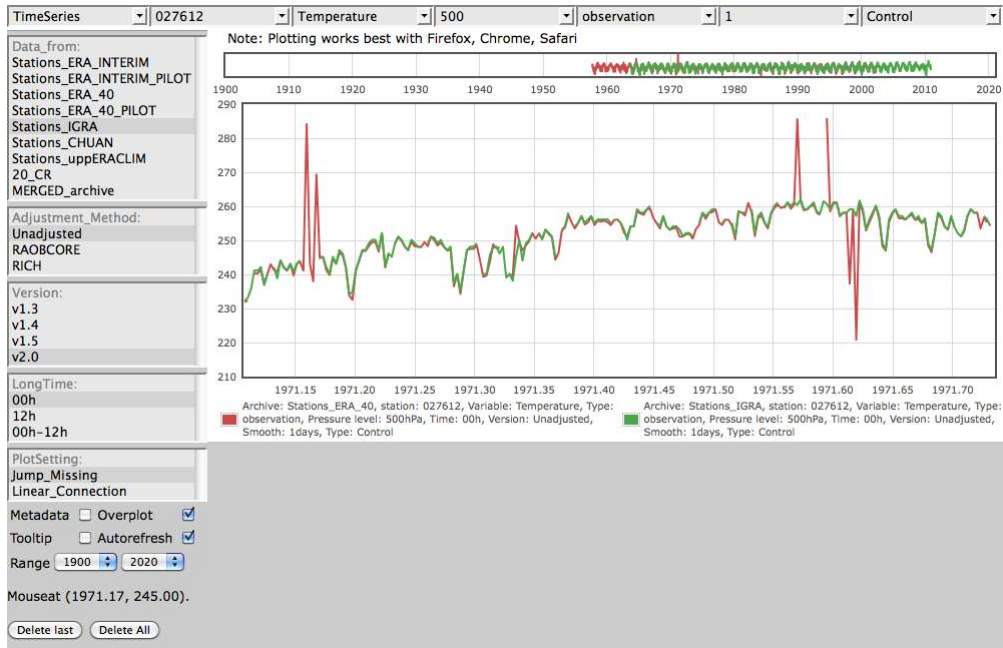


Figure 7. Temperature observation time series of station Moscow at 500 hPa and at 00:00 UTC green curve IGRA archive, red curve ERA-40 station archive. The early spikes show a case where no data are available in the IGRA archive and where the data in the ERA-40 are suspicious. The later spikes are caused by four suspicious values reported by the ERA-40 archive. The IGRA archive contains more plausible values on these days.

The U and V wind components over the US also show good agreement between CHUAN and ERA-40 (Fig. 5). The shown differences originate from the different adopted methods for the conversion of altitude to standard pressure levels. The biases are negligible; the largest rms departures are located around 300 and 150 hPa, where there are large vertical wind gradients and the known temperature biases in the NOAA 20CR reanalysis may also lead to geopotential biases that affect the interpolation quality. One also has to bear in mind that the NOAA-20CR analysis fields are estimated to be as accurate as modern 4-day forecasts (Compo et al., 2011). Thus variability due to uncertainty in the analyses also adds to the found rms departures. Newer surface-data-only reanalyses such as ERA-20C (Poli et al., 2013) or the planned Sparse Input Reanalysis for Climate Applications (SIRCA, Compo et al., 2012) are expected to have smaller temperature biases, which should further improve the interpolation quality for both temperature and wind.

For each observed value at day i (a day) at station j for parameter ϕ (temperature, wind) denoted as $^{i}\text{obs}_{\phi}^j$, there also exists an interpolated analysis value $^{i}20\text{CR}_{\phi}^j$ from the NOAA-20CR. The analysis departures from the NOAA 20CR can thus be written as

$$^{i}\tau_{\phi}^j = ^{i}\text{obs}_{\phi}^j - ^{i}20\text{CR}_{\phi}^j. \quad (4)$$

A simple quality control has been performed on the raw data:

- Date and time limits must be plausible ($00:00 < \text{time} < 23:59$; we assume $24:00 = 00:00$ of the next day, Gregorian calendar).
- Temperature must be between -100 and $+60^{\circ}\text{C}$ or the equivalent in K.
- Wind speed must be between 0 and 200 m s^{-1} .
- Wind direction must be between 0 and 360° .

Inside those ranges, the observations may still contain very unlikely/wrong values due to many possible causes, the most likely being typos in the log books and digitization mistakes. The observation was dropped during the merging procedure if its analysis departure $^{i}\tau_{\phi}^j$ was larger than 4 times the standard deviation σ of the departures for the considered pressure level. Before this criterion was applied, the NOAA-20CR was adjusted for its climatological biases, which are strongest in polar regions (see Brönnimann et al., 2012, but can be found also at some locations in the tropics (Stickler and Brönnimann, 2011)).

These have been quantified from mean differences between the NOAA-20CR and ERA-Interim in the year 1979. ERA-Interim is considered as one of the most reliable reanalyses (Blunden and Arndt, 2013). Figure 3 shows as an example the global temperature, U and V wind component difference ERA-Interim minus NOAA-20CR at 150 hPa, averaged over 00:00 and 12:00 UTC, for the year 1979. There is

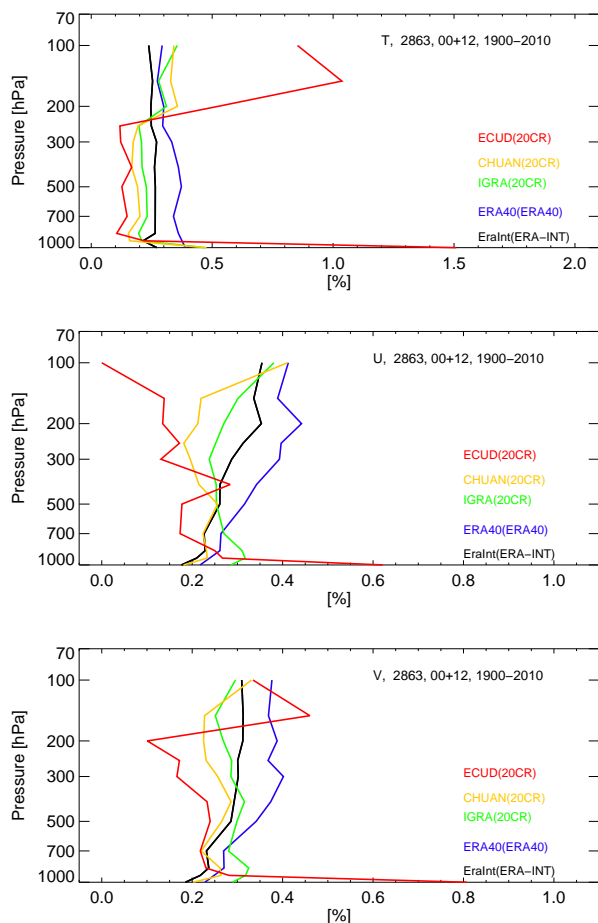


Figure 8. Temperature (upper panels) and U (middle panels) and V (bottom panels) wind component spike frequency (%) as function of pressure, for the whole period 1900–2010. The legend contains the archive names and the departure types (in brackets). Values with deviations larger than 4σ from the respective background forecasts or analyses are counted as spikes.

a warm bias at high latitudes (beyond 60° N and 60° S, reaching up to 12 K), which also has a strong annual cycle. The strongest biases in the U wind component (up to 8 m s^{-1}) are concentrated in the tropical regions, with only a weak annual cycle. The zonal mean V wind component, which is small anyway, does not show strong biases. NOAA-20CR temperatures have been shifted by the difference between ERA-Interim and NOAA-20CR. NOAA-20CR wind components have been scaled to match those in ERA-Interim.

Figure 7 highlights the presence of spikes in the raw time series of some archives. Those erroneous values are not propagated to the merged archive. Results of a more comprehensive spike evaluation can be found in Fig. 8, showing that almost all archives exhibit spike densities below 0.5 % for all pressure levels. An exception is ECUD for temperature at 150 hPa: there, the spike rate is 1 %. The ECUD tempera-

ture measurements were made prior to 1957 and mostly stem from Siberia. Their special location may explain the different frequency of spikes at high levels. Spikes in the wind time series are relatively rare.

7 The merged archived

The union of all data sets gives a total of 3217 stations (land stations and anchored weather ships that use radiosondes, tracked balloons, with time series longer than 365 days), where 3020 have been recognized as WMO stations with a valid WMO ID. A total of 1598 (1596 with WMO ID) stations contain temperature observations, and 3152 (2957 with WMO ID) stations contain wind observations (as U and V components). The Lindenberg (WMO ID 10393) series starts already in 1900, but it contains several gaps. The longest continuous upper-air temperature record comes from Moscow with data available from 1938 onward.

Figure 9 shows three temperature departure time series at 500 hPa for Moscow (WMO ID 26712, Russia). The longest series (observation minus NOAA-20CR analysis) goes as far back as the observations. Of course it already shows much smaller variance than the observation time series in Fig. 6. The deviations are generally below 1 K back until 1955, although the NOAA-20CR has not assimilated those data. Since at 00:00 GMT most ascents are nighttime ascents, the radiation error in those soundings is likely small. Only before 1955 the deviations are larger, which indicates an inhomogeneity either in the observations (possibly the pressure sensor) or in the NOAA-20CR. From 1958 onwards also ERA-40 background departures are available. These show even smaller variance, partly because upper-air data have been assimilated. Interestingly, the NOAA-20CR and ERA-40 background departures are highly correlated and show synchronous dips such as around 1969, which clearly indicates inhomogeneities in the observations rather than in the analyses/background forecasts. From such a simple comparison one can immediately see the benefit of having different (and largely independent) departure time series at one's disposal. If the same fluctuations are visible in all background departure time series, the likelihood for inhomogeneities in the observations is dramatically increased. The ERA-Interim background departures in Fig. 9 are again smaller than those from ERA-40, most likely due to the substantially improved data assimilation system compared to ERA-40. Of course any detected inhomogeneity raises the desire for proper homogenization of the observation records, as it is undertaken in Ramella Pralungo and Haimberger (2014) at least for wind data.

The global upper-air network time coverage and distribution are presented in Figs. 2 and 1. In order to explore the development of the global upper-air network, it is interesting to examine, decade by decade, the number and the positions of the operative stations. In Fig. 10 the development

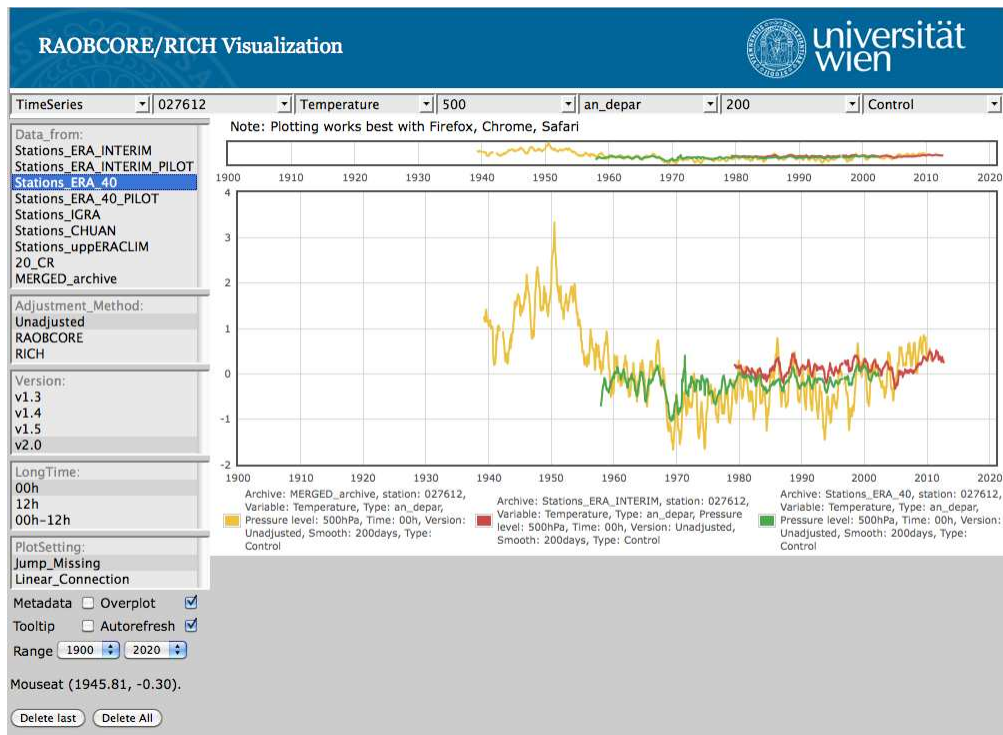


Figure 9. Time series of 500 hPa, 00:00 GMT departures between observations at Moscow and reference data sets derived from reanalysis efforts: obs-NOAA 20CR analysis (yellow); obs-ERA-40 (green) 6h background forecasts, obs-ERA-Interim 12h background forecasts (red).

of the upper-air observing network is displayed, where only stations with more than 5 years of observations for the selected decade have been plotted. The first systematic wind observations are dated 1920 over the United States, and they become denser from 1935 onward. In the years 1945/1950 in Europe, Russia (even if in Moscow temperature observations have been maintained since 1938), and Japan, a rudimentary upper-air observation network was present. In Australia, New Zealand, Hawaii, Polynesia, and Africa, a very small number of stations was active. Also stationary weather ships were operative in the Atlantic and Pacific oceans. The global coverage becomes satisfactory already in the decade 1950–1960 in the Northern Hemisphere. Good spatial coverage has been maintained over the whole globe, but observations remain scarce over central Africa and South America.

The global radiosonde network reached its maximum extent, in terms of number of stations, in 1957/58, during the International Geophysical Year with more than 1600 active stations (roughly 1200 reported wind and 900 reported temperature). In December 2012, 825 stations were active: 713 reported temperature and 804 reported wind.

Table 2 summarizes how the single archives contribute to the merged archive. For temperature ECUD and CHUAN data, 66.3 and 45.1 %, respectively, of the available observations have been ingested in the merged archive. The per-

centages are not higher because the most recent data stored in these archives are partly overlapping with IGRA and/or ERA-40, and those have higher data priority. For wind, more than 70 % of the ECUD and CHUAN data flow into the merged archive. The newly digitized and compiled (ECUD and CHUAN) data contribute roughly 4.8 % (temperature) and 10.4 % (wind) to the merged archive.

After the merging procedure, 37 station records contain more than 70 years of continuous observations, which makes them extremely interesting and valuable for further studies. When analysing those data, one has to be aware of the changing quality of the observations. The nominal precision of temperature measurements is ± 0.2 K (GCOS, 2007), but the actual precision is likely less, especially for the earlier measurements, which used relatively thick, slowly responding sensors. In addition, the precision of the pressure measurements as well as of the interpolation procedure has to be taken into account. Thus it is not surprising that Wartenburger et al. (2013) found much larger observation errors on the order of 1 K for soundings in the 1940s and 1950s. Only for the modern GPS-based sounding systems, the nominal precision is actually reached. While the actual increase of precision with time depends on the radiosonde type used as well as on the altitude of the measurements, it is very likely not better than ± 0.5 K in the 1980s, as can be seen also from

2 A global radiosonde and tracked balloon archive on 16 pressure levels (GRASP) back to 1905 - Part 1: Merging and interpolation to 00:00 and 12:00 GMT

Table 2. Data contribution of different archives to the merged archive. The order of data sets is also the order of preference when merging. Thus the 66.3 % of data used from ECUD are data found only in ECUD.

	Temperature				
	ERA-Int	ERA-40	IGRA	CHUAN	ECUD
% data used	99.9	48.5	13.8	45.1	66.30
% data respect total	52.4	32.8	10.0	4.7	0.1

	Wind				
	ERA-Int	ERA-40	IGRA	CHUAN	ECUD
% data used	99.9	53.7	13.9	78.8	70.4
% data respect total	48.2	32.7	8.8	9.7	0.7

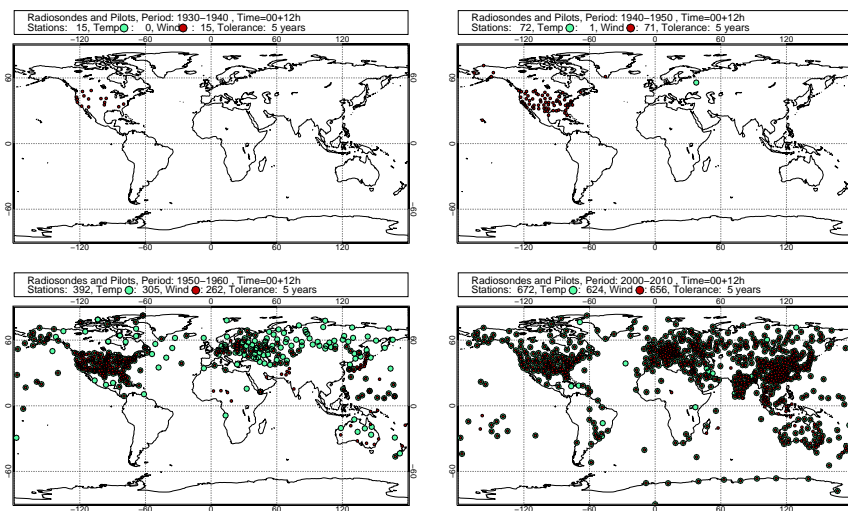


Figure 10. Decadal distribution of upper-air stations in the merged archive with at least 5 years of data in the range 850–500 hPa, starting 1930–1940 (upper left) to 2000–2010 (bottom right). Only WMO stations have been used.

the early radiosonde intercomparison experiments (Nash and Schmidlin, 1987). The time series of background departures can also serve as an upper bound for the precision of the measurements, although their variance is determined not only by measurement precision but also by representativeness errors and the quality of the analyses or background forecasts used. Figure 9 shows how the background departures have decreased over time. Regarding measurement accuracy (also called trueness or bias), the quality depends even more on radiosonde type for temperature. Biases larger than 1 K above 100 hPa are common for many radiosonde types still used in the 1990s (Haimberger et al., 2008). One should keep that in mind when using the merged data, which are given with four decimal places (10^{-4} K) to be able to trace them back to the original measurements (often given in $^{\circ}\text{C}$ or $^{\circ}\text{F}$).

Regarding wind data, the situation is similar. Not only measurement reliability but also precision has improved when switching from theodolites to RADAR and then further to GPS-based soundings. It is nowadays of the order of 1 m s^{-1} for wind speed and 5° for wind direction with a ver-

tical resolution of 200 m (GCOS, 2007). When using theodolites, the precision was worse, but not more than a factor of 2, as can be seen from time series of background departures of wind in the 1940s and 1950s (see Ramella Pralungo and Haimberger, 2014). Nevertheless, the numbers in the netCDF files have not been rounded to ensure clean conversion of units (kt , km h^{-1} to m s^{-1}).

8 The time-series viewer

For simple time-series visualization, a JavaScript-based time-series viewer, (available at the page http://srvx7.img.univie.ac.at/~lorenzo/DEVL_rrvis_2.0/html/) was developed. It allows quick monitoring of the data archive, which permits visual detection of outliers and shifts. One can choose between observed variables (temperature and wind speed, direction, U and V components) and departures from different background series (NOAA 20CR, ERA-Interim and ERA-40). Observation time (00:00, 12:00 and 00:00–12:00 UTC difference) and the pressure level can be

selected from the self-explanatory menu. More details about the viewer can be found at <http://reanalyses.org/observations/raobcorerich-visualization>.

9 Conclusions

The presented merged data set contains upper-air temperature and wind records on standard pressure levels back to the 1920s. It is specifically targeted for advanced quality control and bias adjustments and, of course, climatological analysis. It complements existing upper-air data sets (ECUD, CHUAN, IGRA, ERA-40 input, ERA-Interim input) that are in total perhaps more complete (they contain altitude and/or pressure levels and also short time series with less than 300 days with observations) but also more difficult to use and not always aligned as time series. It contains not only the raw observations but also departures from the NOAA 20th century reanalysis and ERA-40/ERA-Interim background forecasts. As such the data set is particularly suitable as a basis for a homogenized temperature and wind data set that uses RAOBCORE (Haimberger, 2007) technology for bias adjustments. The homogeneity adjustments for wind and their effect on the time series and global mean trends are described in part 2 of this paper (Ramella Pralungo and Haimberger, 2014). The archive is available in convenient NetCDF format and can be visualized with a simple online plotting tool. The archive will be updated once a year shortly after a full year has been completed in ERA-Interim.

The altitude to standard pressure level conversion involved the use of NOAA 20CR geopotential information. The time resolution is relatively coarse, and future surface-pressure-only reanalyses, such as ERA-20C (Poli et al., 2013), will help to improve this aspect since the upper-air data have been passively assimilated at the correct time which consequently yields background departures at the right time. Future surface-data-only reanalyses also may have smaller temperature and wind biases than the NOAA-20CR.

Appendix A: NetCDF file structure

All input data archives as well as the merged archive have been written as NetCDF files that contain the time series with daily resolution (00:00 and 12:00 UTC ascents) at 16 standard pressure levels (10, 20, 30, 50, 70, 100, 150, 200, 250, 300, 400, 500, 700, 850, 925 and 1000 hPa). One file is written for each variable (temperature, U wind and V wind components) and station.

The file names are self-explanatory:

123456_V_t.nc. (A1)

The first digit is either 0 or 1:

- 0 indicates that the station has been identified as a WMO station.
- 1 indicates that the station has been identified as a NO WMO station.

The next five digits are the WMO station identification number, if the first is a 0; otherwise they are the progressive number with which the station has been saved in the respective archive (CHUAN or ECUD, since only those two archives contain unknown stations). The V refers to the variable reported in the file, and it can be

- $T \rightarrow$ temperature
- $U \rightarrow$ U wind component
- $V \rightarrow$ V wind component.

The $_t$ refers to time series, as is the form in which the data have been stored. In the file are defined 13 dimensions, 18 variables and the global attributes. The variable list is composed of (type \rightarrow name)

- integer \rightarrow stations \rightarrow station ID, it works as the first six digits in the file name (according to A1)
- float \rightarrow lat \rightarrow station latitude, in degrees north, range $[-90^\circ, 90^\circ]$
- float \rightarrow long \rightarrow station longitude, in degrees east, range $[-180^\circ, 180^\circ]$
- float \rightarrow alt \rightarrow station altitude, in in m.a.s.l., range $[-400, 8000]$ m
- integer \rightarrow pressure_layers(16) \rightarrow array with the 16 standard pressure levels
- integer \rightarrow obs_time(2) \rightarrow array with launch times (00:00 and 12:00) UTC

- integer \rightarrow date(45000) \rightarrow progressive day index from 1900-01-01 with Gregorian calendar, range [19000101, 20230316]
- integer Varno \rightarrow the variable number identifier following the ECMWF line guides (Upper Air Temperature 2 [K]; U component of wind 3 [m s^{-1}]; V component of wind 4 [m s^{-1}])
- integer \rightarrow index_days \rightarrow progressive (from 1). Date(index_days) returns the corresponding day that refers to index_days for the selected station.
- float \rightarrow obs \rightarrow The observations array could be named, in agreement with the variable reported in the file name:
 - Temperature \rightarrow temperature
 - U_Wind \rightarrow U wind component
 - V_Wind \rightarrow V wind component

The arrays have dimensions obs(obs_time, pressure_layers, index_days) In this way, we use the minimum number of days in order to map the time series.

After the observed time series, the departure (background departures from ERA-Interim, ERA-40 and analysis departures from NOAA 20CR) flags and measurement system type information are stored as follows:

- float \rightarrow bias correct \rightarrow bias correct(obs_time, pressure_layers, index_days), only available for ERA-Interim and ERA-40 archives, where bias correction procedure has been performed by ECMWF (Haimberger and Andrae, 2011; Andrae et al., 2004);
- float \rightarrow fg_depar \rightarrow fg_depar(obs_time, pressure_layers, index_days), only available for ERA-Interim and ERA-40 archives, where it has been performed as Observation-Forecast first guess (ECMWF forecast);
- float \rightarrow an_depar \rightarrow an_depar(obs_time, pressure_layers, index_days), for ERA-Interim and ERA-40 archives it has been performed as Observation-Analysis (ERA-40 or ERA-Interim Reanalysis ECMWF); for IGRA, CHUAN, ECUD and merged archive, the analysis comes from NOAA 20CR fields (updated to 2010);
- integer \rightarrow sonde_type \rightarrow sonde_type(index_days) contains information about the WMO measurement system type (see <http://www.wmo.int/pages/prog/www/IMOP/meetings/Upper-Air/Radiosonde-netw/Doc5-3.pdf>)
- integer \rightarrow status \rightarrow status(obs_time, pressure_layers, index_days) contains the data source archive for the current obs_time, pressure_layers, index_days:

- status=1 → ERA-Interim input
- status=2 → ERA-40 input
- status=3 → IGRA archive
- status=4 → CHUAN archive
- status=5 → ECUD.
- integer → anflag anflag(obs_time, pressure_layers, index_days) flag, reserved for future use;
- integer → event1 event1(obs_time, pressure_layers, index_days) flag, reserved for future use.

The file is equipped with global attributes:

- conventions = “CF-1.4” → NetCDF files conventions
- title → project title
- institution → file owner "University of Vienna"
- history → when the file was produced
- data type → “RADIOSONDE INPUT DATA”
- source → source archive
- references: → www.univie.ac.at/theoret-met/research/raobcore.

Routines for reading the archived NetCDF files are available in FORTRAN and IDL and can be downloaded from [doi:10.1594/PANGAEA.823609](https://doi.org/10.1594/PANGAEA.823609).

2 A global radiosonde and tracked balloon archive on 16 pressure levels (GRASP) back to 1905 - Part 1: Merging and interpolation to 00:00 and 12:00 GMT

L. Ramella Pralungo et al.: A global radiosonde and tracked balloon archive

15

Acknowledgements. This work has been funded by projects P21772-N22 and P25260-N29 of the Austrian Fonds zur Förderung der wissenschaftlichen Forschung (FWF), as well as by the EU 7th Framework Programme collaborative project ERA-CLIM (grant no. 265229) and by the Swiss National Science Foundation (project EVALUATE). The authors thank the collaborators within ERA-CLIM, most notably Hans Hersbach and Alexander Sterin for their support and constructive comments.

Edited by: G. König-Langlo

References

- Adam, W. K. and Dier, H.: Lange Messreihen zur Wetter- und Klimaforschung am Meteorologischen Observatorium Lindenberg, *ProMet*, 31, 159–170, 2005.
- Allan, R., Brohan, P., Compo, G. P., Stone, R., Luterbacher, J., and Brönnimann, S.: The international atmospheric circulation reconstructions over the earth (ACRE) initiative, *B. Am. Meteorol. Soc.*, 92, 1421–1425, doi:10.1175/2011BAMS3218.1, 2011.
- Andrae, U., Sokka, N., and Onogi, K.: The radiosonde temperature bias correction in ERA-40, Volume 15 of ERA-40 Project Report Series, ECMWF, 2004.
- Blunden, J. and Arndt, D. S.: State of the climate in 2012, *B. Am. Meteorol. Soc.*, 94, S1–S258, doi:10.1175/2013BAMSStateoftheClimate.1, 2013.
- Brönnimann, S.: A historical upper air-data set for the 1939–44 period, *Int. J. Climatol.*, 23, 769–791, 2003.
- Brönnimann, S. and Luterbacher, J.: Reconstructing northern hemisphere upper-level fields during World War II, *Clim. Dynam.*, 22, 499–510, doi:10.1007/s00382-004-0391-3, 2004.
- Brönnimann, S., Stickler, A., Griesser, T., Ewen, T., Grant, A. N., Fischer, A. M., Schraner, M., Peter, T., Rozanov, E., and Ross, T.: Exceptional atmospheric circulation during the “Dust Bowl”, *Geophys. Res. Lett.*, 36, L08802, doi:10.1029/2009GL037612, 2009.
- Brönnimann, S., Grant, A. N., Compo, G. P., Ewen, T., Griesser, T., Fischer, A. M., Schraner, M., and Stickler, A.: A multi-data set comparison of the vertical structure of temperature variability and change over the arctic during the past 100 years, *Clim. Dynam.*, 39, 1577–1598, doi:10.1007/s00382-012-1291-6, 2012.
- Compo, G. P., Whitaker, J. S., Sardeshmukh, P. D., Matsui, N., Allan, R. J., Yin, X., Gleason, B. E., Vose, R. S., Rutledge, G., Bessemoulin, P., Brönnimann, S., Brunet, M., Crouthamel, R. I., Grant, A. N., Groisman, P. Y., Jones, P. D., Kruk, M. C., Kruger, A. C., Marshall, G. J., Maugeri, M., Mok, H. Y., Nordli, Å., Ross, T. F., Trigo, R. M., Wang, X. L., Woodruff, S. D., and Worley, S. J.: The twentieth century reanalysis project, *Q. J. Roy. Meteor. Soc.*, 137, 1–28, doi:10.1002/qj.776, 2011.
- Compo, G. P., Whitaker, J. S., Sardeshmukh, P. D., and Giese, B.: Developing the sparse input reanalysis for climate applications (SIRCA) 1850–2014, http://conference2011.wcrp-climate.org/orals/B4/Compo_B4.pdf (last access: 12 May 2014), WMO, 2012.
- Dee, D. P., Uppala, S. M., Simmons, A. J., Berrisford, P., Poli, P., Kobayashi, S., Andrae, U., Balmaseda, M. A., Balsamo, G., Bauer, P., Bechtold, P., Beljaars, A. C. M., van de Berg, L., Bidlot, J., Bormann, N., Delsol, C., Dragani, R., Fuentes, M., Geer, A. J., Haimberger, L., Healy, S. B., Hersbach, H., Hólm, E. V., Isaksen, I., Kallberg, P., Köhler, M., Matricardi, M., McNally, A. P., Monge-Sanz, B. M., Morcrette, J. J., Park, B. K., Peubey, C., de Rosnay, P., Tavolato, C., Thépaut, J. N., and Vitart, F.: The ERA-Interim reanalysis: configuration and performance of the data assimilation system, *Q. J. Roy. Meteor. Soc.*, 137, 553–597, doi:10.1002/qj.828, 2011.
- Durre, I., R. Vose, and D. B. Wuertz, 2006: Overview of the Integrated Global Radiosonde Archive. *J. Climate*, 19, 53–68.
- Free, M., Seidel, D. J., Angell, J. K., Lanzante, J., Durre, I., and Peterson, T. C.: Radiosonde atmospheric temperature products for assessing climate (RATPAC): A new data set of large-area anomaly time series, *J. Geophys. Res.*, 110, D22101, doi:10.1029/2005JD006169, 2005.
- GCOS, 2008: GCOS Reference Upper-Air Network (GRUAN): Justification, requirements, siting and instrumentation options. Technical document 1379, WMO, 2007.
- Grant, A., Brönnimann, S., Ewen, T., and Nagurny, A.: A new look at radiosonde data prior to 1958, *J. Climate*, 22, 3232–3247, 2009.
- Gruber, C. and Haimberger, L.: On the homogeneity of radiosonde wind time series, *Meteorol. Z.*, 17, 631–643, 2008.
- Haimberger, L.: Homogenization of radiosonde temperature time series using innovation statistics, *J. Climate*, 20, 1377–1403, 2007.
- Haimberger, L. and Andrae, U.: Radiosonde temperature bias correction in ERA-Interim, ERA report series, 8, http://old.ecmwf.int/publications/library/ecpublications/_pdf/era_report_series/RS_8.pdf (last access: 19 May 2014), 2011.
- Haimberger, L., Tavolato, C., and Sperka, S.: Towards elimination of the warm bias in historic radiosonde temperature records – some new results from a comprehensive intercomparison of upper air data, *J. Climate*, 21, 4587–4606, 2008.
- Haimberger, L., Tavolato, C., and Sperka, S.: Homogenization of the global radiosonde temperature dataset through combined comparison with reanalysis background series and neighboring stations, *J. Climate*, 25, 8108–8131, 2012.
- Jourdain, S. and Roucaute, E.: Historical upper air data rescue at meteo-france for ERA-CLIM, in: EMS Annual Meeting Abstracts, Volume 10, <http://meetingorganizer.copernicus.org/EMS2013/EMS2013-97.pdf> (last access: 12 May 2014), 2013.
- Nash, J. and Schmidlin, F. J.: WMO International Radiosonde Intercomparison: Final Report, WMO/TD No. 195, WMO, Geneva, 1987.
- Poli, P., Hersbach, H., Tan, D., Dee, D., Thépaut, J. N., Simmons, A., Peubey, C., Laloyaux, P., Komori, T., Berrisford, P., Dragani, R., Tremolet, Y., Holm, E., Bonavita, M., Isaksen, I., and Fisher, M.: The data assimilation system and initial performance evaluation of the ECMWF pilot reanalysis of the 20th-century assimilating surface observations only (ERA-20C), ECMWF, 2013.
- Ramella Pralungo, L. and Haimberger, L.: A global radiosonde and tracked balloon archive on 16 pressure levels (GRASP) back to 1905 – Part 2: Homogeneity adjustments for PILOT and radiosonde wind data, *Earth Syst. Sci. Data Discuss.*, 7, 335–383, doi:10.5194/essdd-7-335-2014, 2014.
- Redder, C. R., Luers, J. K., and Eskridge, R. E.: Unexplained discontinuity in the U.S. radiosonde temperature data. part II: Stratosphere, *J. Atmos. Ocean. Tech.*, 21, 1133–1144, 2004.

- Seidel, D. J., Berger, F. H., Immler, F., Sommer, M., Vömel, H., Diamond, H. J., Dykema, J., Goodrich, D., Murray, W., Peterson, T., Sisterson, D., Thorne, P., and Wang, J.: Reference upper-air observations for climate: Rationale, progress, and plans, *B. Am. Meteor. Soc.*, 90, 361–369, 2009.
- Sherwood, S. C., Meyer, C. L., Allen, R. J., and Titchner, H. A.: Robust tropospheric warming as revealed by iteratively homogenized radiosonde data, *J. Climate*, 21, 5336–5352, 2008.
- Stickler, A. and Brönnimann, S.: Significant bias of the ncep/ncar and twentieth century reanalyses relative to pilot balloon observations over the west african monsoon region (1940–57), *Q. J. Roy. Meteor. Soc.*, 137, 1400–1416, doi:10.1002/qj.854, 2011.
- Stickler, A., Grant, A. N., Ewen, T., Ross, T. F., Vose, R. S., Comeaux, J., Bessemoulin, P., Jylhä, K., Adam, W. K., Jeannet, P., Nagurny, A., Sterin, A. M., Allan, R., Compo, G. P., Griesser, T., and Brönnimann, S.: The comprehensive historical upper air network (CHUAN), *B. Am. Meteor. Soc.*, 91, 741–751, doi:10.1175/2009BAMS2852.1, 2010.
- Stickler, A., Brönnimann, S., Jourdain, S., Roucaute, E., Sterin, A., Nikolaev, D., Valente, M. A., Wartenburger, R., Hersbach, H., Ramella-Pralungo, L., and Dee, D.: Description of the ERA-CLIM historical upper-air data, *Earth Syst. Sci. Data*, 6, 29–48, doi:10.5194/essd-6-29-2014, 2014.
- Thorne, P. W., Parker, D. E., Tett, S. F. B., Jones, P. D., McCarthy, M., Coleman, H., and Brohan, P.: Revisiting radiosonde upper-air temperatures from 1958 to 2002, *J. Geophys. Res.*, 110, D18105, doi:10.1029/2004JD005753, 2005.
- Thorne, P. W., Brohan, P., Titchner, H. A., McCarthy, M. P., Sherwood, S. C., Peterson, T. C., Haimberger, L., Parker, D. E., Tett, S. F. B., Santer, B. D., Fereday, D. R., and Kennedy, J. J.: A quantification of uncertainties in historical tropical tropospheric temperature trends from radiosondes, *J. Geophys. Res.*, 116, D12116, doi:10.1029/2010JD015487, 2011.
- Uppala, S.M., P.W. Kållberg, A.J. Simmons, U. Andrae, V. da Costa Bechtold, M. Fiorino, Gibson, J. K., Haseler, J., Hernandez, A., Kelly, G. A., Li, X., Onogi, K., Saarinen, S., Sokka, N., Allan, R. P., Andersson, E., Arpe, K., Balmaseda, M. A., Beljaars, A. C. M., van de Berg, L., Bidlot, J., Bormann, N., Caires, S., Chevallier, F., Dethof, A., Dragosavac, M., Fisher, M., Fuentes, M., Hagemann, S., Hólm, E., Hoskins, B. J., Isaksen, I., Janssen, P. A. E. M., Jenne, R., McNally, A. P., Mahfouf, J. F., Morcrette, J. J., Rayner, N. A., Saunders, R. W., Simon, P., Sterl, A., Trenberth, K., Untch, A., Vasiljevic, D., Viterbo, P., and Woollen, J.: The ERA-40 Re-analysis, *Q. J. Roy. Meteor. Soc.*, 131, 2961–3012, 2005.
- Wartenburger, R., Brönnimann, S., and Stickler, A.: Observation errors in early historical upper-air observations, *J. Geophys. Res.*, 118, 12012–12028, doi:10.1002/2013JD020156, 2013.

3 A global radiosonde and tracked balloon archive on 16 pressure levels (GRASP) back to 1905 - Part 2: Homogeneity adjustments for PILOT and radiosonde wind data

This paper presents the procedure named RAOBCORE 2.0 employed to homogenize the wind records stored in the GRASP archive. Artificial breaks and shifts arise from the undocumented changes in the instruments/tools, station relocation or more general from each unknown source that can corrupt the observations. These biases are directly affecting the data quality and the results of climatological studies.

The main goal of the work is to detect the breaks using a modified version of the Standard Normal Homogeneity Test and possibly adjust them in a not invasive way. Particular emphasis has been given on the early years (before 1960) when, so far, no other global homogenization effort has been attempted due, most probably, to the station sparsity.

The adjustments, stored station by station as NetCDF files, are available at the PANGEA¹⁰ archive.

My contributions to this work were to write the *FORTTRAN* program that is able to homogenize temperature (not mentioned in the paper) and wind data-sets together. As inspiration source, I have used the well known RAOBCORE procedure, but all the code has been revisited, integrated and optimized to allow more flexibility. The adjustment method for sampling biases has been developed by me from scratch. I have also developed the *IDL* visualization routines used. Leopold Haimberger participated actively with hints, solutions and ideas on the crucial points, offering his wide experience in this field with helpful brainstorm sessions.

The paper text has been written with “four hands”: myself and Leopold Haimberger.

RamellaPralungo, L. and Haimberger, L., 2014:

A global radiosonde and tracked balloon archive on 16 pressure levels (GRASP) back to 1905 - Part 2: homogeneity adjustments for pilot balloon and radiosonde wind data,

Earth System Science Data (ESSD),

doi:10.5194/essd-6-297-2014

¹⁰ <http://doi.pangaea.de/10.1594/PANGAEA.823617>



A "Global Radiosonde and tracked-balloon Archive on Sixteen Pressure levels" (GRASP) going back to 1905 – Part 2: homogeneity adjustments for pilot balloon and radiosonde wind data

L. Ramella Pralungo and L. Haimberger

Department of Meteorology and Geophysics, University of Vienna, Althanstrasse 14, 1090 Vienna, Austria

Correspondence to: L. Ramella Pralungo (lorenzo.ramella-pralungo@univie.ac.at)

Received: 11 April 2014 – Published in Earth Syst. Sci. Data Discuss.: 15 May 2014

Revised: 4 August 2014 – Accepted: 6 August 2014 – Published: 9 September 2014

Abstract. This paper describes the comprehensive homogenization of the “Global Radiosonde and tracked balloon Archive on Sixteen Pressure levels” (GRASP) wind records. Many of those records suffer from artificial shifts that need to be detected and adjusted before they are suitable for climate studies.

Time series of departures between observations and the National Atmospheric and Oceanic Administration 20th-century (NOAA-20CR) surface pressure only reanalysis have been calculated offline by first interpolating the observations to pressure levels and standard synoptic times, if needed, and then interpolating the gridded NOAA-20CR standard pressure level data horizontally to the observation locations. These difference time series are quite sensitive to breaks in the observation time series and can be used for both automatic detection and adjustment of the breaks.

Both wind speed and direction show a comparable number of breaks, roughly one break in three stations. More than a hundred artificial shifts in wind direction could be detected at several US stations in the period 1938/1955. From the 1960s onward the wind direction breaks are less frequent. Wind speed data are not affected as much by measurement biases, but one has to be aware of a large fair-weather sampling bias in early years, when high wind speeds were much less likely to be observed than after 1960, when radar tracking was already common practice. This bias has to be taken into account when calculating trends or monthly means from wind speed data.

Trends of both wind speed and direction look spatially more homogeneous after adjustment. With the exception of a widespread wind direction bias found in the early US network, no signs of pervasive measurement biases could be found. The adjustments can likely improve observation usage when applied during data assimilation. Alternatively they can serve as a basis for validating variational wind bias adjustment schemes. Certainly, they are expected to improve estimates of global wind trends.

All the homogeneity adjustments are available in the PANGAEA archive with associated doi:10.1594/PANGAEA.823617.

1 Introduction

From the 1900s tracked balloons, and from the 1940s also radiosondes, were practically the only upper-air wind observing system with global or regional coverage up to the beginning of the satellite era in the late 1970s. Despite the rapidly increasing amounts of satellite data since then (Dee et al.,

2011), balloons and radiosondes remain an essential component of the observing network. While the vertical extent of the records was limited to mostly below 400 hPa before 1940, it reached the stratosphere from the 1950s onward (Scherhag, 1962). Since the 1970s, 10 hPa are regularly reached by most balloons.

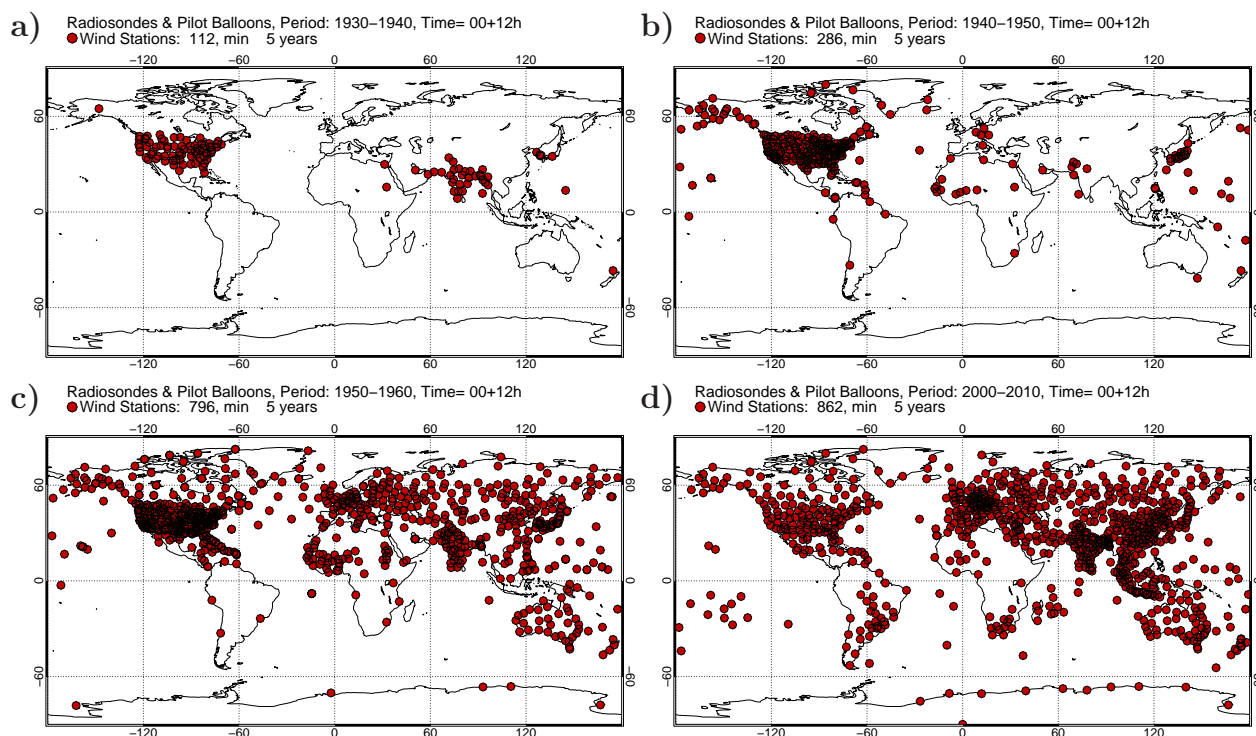


Figure 1. Maps of upper-air stations of the GRASP data set with at least 5 years of data per decade in the range of 850–500 hPa for different decades.

Early upper-air wind data have been used to reconstruct climate anomalies in the early 20th century, such as the Dust Bowl drought in the 1930s (Ewen et al., 2008b), and were instrumental in discovering the quasi-biennial oscillation (Graystone, 1959). More modern in situ upper-air wind data have helped attributing regional wind stilling in the Northern Hemisphere to increased surface roughness (Vautard et al., 2010). There is also increased interest in wind speed trends due to increasing installations of wind turbines. Allen and Sherwood (2008) have used wind data as a temperature proxy, applying the thermal wind equation to calculate temperature (gradient) trends. Interestingly, they found much larger warming trends than those estimated from radiosonde temperature measurements which are long known to be biased (Santer et al., 1999, 2005; Thorne et al., 2005).

Long and homogeneously observed time series are an essential source to diagnose the three-dimensional pattern of climate change. They are also precious input data for reanalysis efforts, particularly if they go back to before the satellite era (Kistler et al., 2001; Uppala et al., 2005; Ebita et al., 2011). Reanalyses have proved extremely fruitful for climate research and are essential input for studies in many disciplines (Hartmann et al., 2013). Reanalysis performance and homogeneity are highly dependent on the available input data and their quality. Any improvement there will increase the accuracy of the estimated climate state and will be directly

beneficial for future studies related to it. This fact triggered several efforts to digitize surface data and early upper-air data in many countries (Allan and Ansell, 2006; Allan et al., 2011; Brönnimann, 2003; Ewen et al., 2008a; Stickler et al., 2014). The present study builds upon these efforts. In part I of this study (Ramella-Pralungo et al., 2014) a new radiosonde and pilot balloon wind data set at 16 standard pressure levels, called GRASP, has been developed. Figure 1 shows maps of global coverage with wind data for different decades in this data set.

Upper-air wind time series from balloons have traditionally been assumed to be temporally relatively homogeneous compared to temperature or humidity. While biases are not as pervasive as for temperature, wind biases have been occasionally detected by monitoring the output of data assimilation systems (Hollingsworth et al., 1986). As an example, Fig. 2 shows the observed wind direction time series for the station Bismarck (North Dakota USA WMO ID 072764) at 00:00 UTC at different pressure levels. Already in these time series there are indications that, in around 1948, they are affected by artificial shifts in wind direction, caused by wrong north alignment of the station. Imperfect tracking of the horizontal motion, wrong height assignment or the inertness of the ascending balloon can also cause biases. These biases are hard to detect without a reliable reference if they are smaller

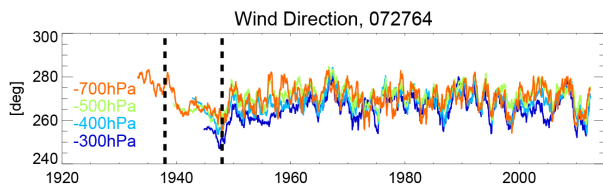


Figure 2. Time series of wind direction observations at station Bismarck (072764, North Dakota, USA), at the 700 (orange), 500 (green), 300 (light blue) and 200 (dark blue) hPa levels, respectively. A 365-day running mean has been applied to all time series. Note shifts in 1938 and 1948.

than in this example. That reference may be neighboring stations or, since recent times, reanalysis data.

Haimberger (2007) showed that background departure time series from reanalyses can be used effectively to detect and adjust breaks in radiosonde temperature time series. An automatic homogenization method (RADiosonde OBServation CORrection using REanalyses, RAOBCORE) showed some skill in adjusting the global radiosonde temperature data set. Subsequent refinements of the method also employed composites of neighboring radiosondes that allowed more accurate adjustment of breaks without sacrificing the independence of the adjusted radiosonde data from satellite data (Haimberger et al., 2008, 2012).

This method has been successfully applied to the global radiosonde wind data set back to 1958 as well (Gruber and Haimberger, 2008). While wind direction errors could be safely identified in their paper, there were concerns that wind speed background departures may not be independent enough from the assimilating model (ERA-40 (European Centre for Medium-Range Weather Forecasts (ECMWF) Re-Analysis) at this time (Uppala et al., 2005), which has some known inhomogeneities). This study also did not consider pilot balloon winds and was restricted to the period 1958–2002.

Since then, the availability of newly digitized data as well as the advent of the National Atmospheric and Oceanic Administration 20th-Century Reanalysis (NOAA-20CR; Compo et al., 2011) improved the prospects for a comprehensive homogenization of upper-air wind data back to the beginning of balloon observations. The NOAA-20CR is well suited as reference since it is independent of upper-air observations and since it has reasonably realistic temperature fields up to stratospheric levels. While some wind biases are evident in this reanalysis (see Fig. 3 of Part 1 and Stickler and Brönnimann, 2011), these are temporally quite stable, at least over the midlatitudes from 1950 onward, as will be shown below. It has been used for interpolating the global pilot balloon wind data set from geometric height to standard pressure levels in Part 1. The present paper describes how this combined radiosonde plus pilot balloon data set is homogenized using analysis departure information from the NOAA-20CR.

The next section describes the input data, and Sect. 3 outlines the homogenization method. Section 4 explains how sampling biases can translate into monthly mean biases and what is done to avoid that. Section 5 presents results, and conclusions are drawn in Sect. 6.

2 Input data

The GRASP data set as described in Part 1 is the main input to be homogenized. Its main sources are the ERA-Interim observation input and observation feedback data set (Dee et al., 2011), the ERA-40 observation input and feedback data set (Uppala et al., 2005), the Integrated Global Radiosonde Archive (IGRA) (Durre et al., 2006), updated until 2012 and supplemented with analysis departures from the NOAA-20CR, and the Comprehensive Historical Upper-Air Network (CHUAN; Stickler et al., 2010) including the ERA-CLIM (European Reanalysis of Global Climate Observations) Historical Upper-Air Data (Stickler et al., 2014).

The archive contains daily records at 00:00 and 12:00 UTC from 2924 wind stations with a WMO identifier, distributed all over the world, with data starting in 1905 at Lindenberg (10 393) for temperature and in Hamburg (10 148) for wind and with longer time series over the US starting in 1915 (e.g., Omaha 72 553). Figure 1 shows the wind network development and distribution of those stations that have at least 5 years of observations. Already in the 1930s, a network of stations was operating mainly in the US and in India. In the 1940s the distribution was already global, albeit sparse. The global coverage over land masses was constantly improved in the 1950s, particularly in the International Geophysical Year (IGY) 1958 when several new radiosonde stations also started operating in South America, southern Africa and the Pacific Islands. The network of radiosonde and pilot balloon observations in the 1950s is much denser than the radiosonde network only (compare with Fig. 10 in Part 1). Since the IGY, the radiosonde network has not changed much in size, peaking in the 1970s and since then slowly decreasing in density.

In addition to the observations at standard pressure levels, the GRASP data set contains the so-called *innovations* or *analysis departures*, i.e., observation minus analysis from the NOAA-20CR, collocated at each station location and each available observation time (00:00 and 12:00 UTC), and standard pressure levels. For homogenization the analyzed fields from the NOAA-20CR have been chosen again since they are independent of upper-air data and since NOAA-20CR goes back to 1872 so that analysis departures exist even for the earliest upper-air data. While background departures from ERA-40 and ERA-Interim have smaller variance, they are not completely independent of upper-air data, and they also do not reach back far enough. Evaluations of NOAA-20CR have found some biases in its wind field (Stickler et al., 2010) and several inhomogeneities have been detected by Ferguson and Villarini (2013), particularly in ensemble spread. Despite

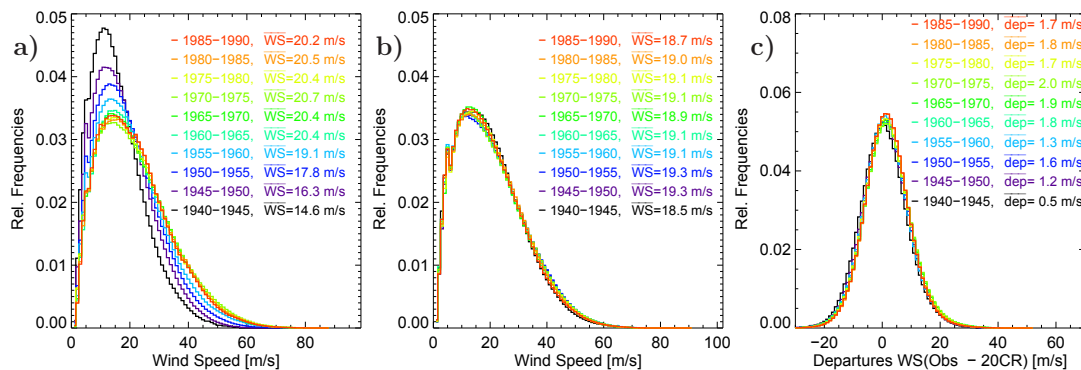


Figure 3. Histogram for several decades of (a) wind speed observations, (b) analyzed wind speeds and (c) innovations (obs-NOAA-20CR) at 300 hPa and 00:00 UTC for the same subset of stations as in Fig. 12. The histograms have been normalized so that the integral is 1.

these caveats one has to acknowledge that the NOAA-20CR reproduces the comprehensive global atmospheric circulation and also the surface temperatures in the 20th century quite well, given the reduced set of input data it assimilates. In many ways it is unique, and similar upcoming products such as ERA-20C (Poli et al., 2013) have yet to demonstrate significantly better temporal homogeneity than the NOAA-20CR.

3 Methods

The radiosonde wind homogenization system presented here is based on the methodology referred to as Radiosonde Observation Correction using Reanalysis (RAOBCORE). It was introduced by Haimberger (2007) and was originally applied only to temperature time series. Gruber and Haimberger (2008) demonstrated that the RAOBCORE's technique can be, when properly modified, applied also to wind data with promising results. In that pioneering study only radiosondes data collected during ERA-40 (Uppala et al., 2005), complemented with radiosonde data from the IGRA (Durre et al., 2006), were used, spanning the time interval 1958–2002.

The system used here, referred to as RAOBCORE 2.0, analyzes temperature, wind speed and wind direction simultaneously. In contrast to the original RAOBCORE, it uses NOAA 20th-Century Reanalysis data as reference. While the simultaneous treatment of temperature and wind would allow for combined break detection, we found that temperature and wind breaks rarely occur at the same time, the exception being perhaps station relocations. Therefore each variable is treated separately for break detection and adjustment. Metadata are an important source of information for homogenization purposes, and they can and have been used in the break detection procedure by assigning higher a priori probabilities to a break given particular events (Haimberger, 2007) or for applying certain adjustments (Luers and Eskridge, 1995). A new, promising version of upper-air metadata has recently become available (Tschudin and Schroeder, 2013). However,

the metadata have been collected mainly for temperature and humidity adjustment. For wind, the metadata information is rather sparse and most likely incomplete. At this stage, metadata have therefore not been used for wind homogenization.

3.1 Construction of reference time series

The NOAA-20CR zonal (U) and meridional (V) wind values used as reference are already stored in GRASP as departure time series, i.e., the NOAA-20CR values can be calculated simply by adding the departures to the observations. For homogenization purposes is often advantageous to represent wind information in polar coordinates (speed ff and direction dd). North alignment shifts in wind direction, which are a major source of biases affecting the whole vertical profile, are visible much better in wind direction time series than in U or V time series. Following the notation of Haimberger et al. (2012), we define the wind direction difference (τ) between an observation (obs) at time t_i (where i is index of day) at a given station and the NOAA-20CR analysis (an) interpolated to this as

$$\tau_{dd}(t_i) = \text{obs}_{dd}(t_i) - \text{an}_{dd}(t_i). \quad (1)$$

In cases where this difference is not in the range of $[-180^\circ, 180^\circ]$, we set

$$\begin{aligned} -\tau_{dd}(t_i) &= \tau_{dd}(t_i) - 360^\circ & \text{if } \tau_{dd}(t_i) > 180^\circ \\ -\tau_{dd}(t_i) &= 360^\circ + \tau_{dd}(t_i) & \text{if } \tau_{dd}(t_i) < -180^\circ. \end{aligned}$$

Wind direction departures are not necessarily Gaussian distributed, and care must be taken particularly at low wind speeds. Therefore, they are considered valid only if the wind speeds in both observations and in the reanalysis are higher than 1 m s^{-1} and if the wind direction differences are smaller than 90° . Now one can take the average over a time interval a (denoted by an overbar) which yields

$$\bar{\tau}_{dd}(a) = \overline{\text{obs}_{dd}}(a) - \overline{\text{an}_{dd}}(a). \quad (2)$$

The wind speed departures Δff are defined as

$$\bar{\tau}_{ff}(a) = \overline{\text{obs}}_{ff}(a) - \overline{\text{an}}_{ff}(a). \quad (3)$$

$\bar{\tau}_u(a)$ and $\bar{\tau}_v(a)$ can be defined in a similar way. All these averages exist at 00:00 and 12:00 UTC at the 16 standard pressure levels. The standard length of the intervals a, b is 2 years for break detection (to be able to separate two nearby breakpoints) and 8 years (for better accuracy) for break adjustment. It can be reduced to 200 days at the beginning and end of the time series and near gaps. At least 200 valid observations in each interval are required for valid averages.

3.2 Break detection

As discussed by Haimberger (2007), a variant of the standard normal homogeneity test (SNHT; Alexandersson, 1986) can be applied to the innovation time series $\tau_x(t_i)$ (where x can be u, v, dd, ff) in order to find possible break candidates.

The SNHT variant considered here calculates a test statistic Q_k for each potential breakpoint k . The intervals are then chosen as $a = [k - N/2, k]$ and $b = [k, k + N/2]$, with $N = 1460$ (2 years before, 2 years after a potential break) as default choice. We now define Q_k as

$$Q_k = N/2 \left\{ [\bar{\tau}_x(a) - \bar{\tau}_x(a, b)]^2 + [\bar{\tau}_x(b) - \bar{\tau}_x(a, b)]^2 \right\} / \sigma_x(a, b), \quad (4)$$

where $\sigma(a, b)$ is the standard deviation of the $\tau_x(t_i)$ over the interval $[a, b]$ and $\bar{\tau}_x(a, b)$ is the mean $\tau_x(t_i)$ over the whole interval $[a, b]$. The maximum number of missing data admitted in one subinterval of length $N/2$ is an important parameter. It is set to 650. With so many data allowed to be missing, special care is needed to ensure the equal sampling of the annual cycle in the interval before and after a potential breakpoint k , particularly in the case of data gaps. This is done by deleting data for a month that is missing in one interval also in the other interval. This simple measure minimizes false break detections at stations with strong annual cycles (Haimberger, 2007). This SNHT variant yields time series of Q_k for all k where there are enough data. The Q_k time series exist at each pressure level, and significant maxima are not reached at each level and not at the same k values. Thus one has to combine the breakpoint probability information from all levels to get unique breakpoints. The composite series of all the Q_k is obtained as a mean along all the pressure levels and times:

$$\langle Q_k(t_m) \rangle = \frac{1}{n_p} \frac{1}{n_t} \sum_{n_p, n_t} Q_k(p_l, t_m) \text{ with } p_l = 100, 150, \dots, 850 \text{ hPa.}$$

$$t_m = 00, 12 \text{ UTC}$$

Under the null hypothesis (homogeneous time series), the distribution of $\langle Q_k \rangle$ can be obtained from Monte Carlo simulations, taking possible autocorrelation into account. From these, a critical value Q_{crit} can be derived. It is a reasonable idea to set Q_{crit} not too high, since weaker breaks can be

eliminated later by applying robustness criteria (explained in the next section). Depending on the value set for Q_{crit} , the time series $\langle Q_k \rangle$ is converted into break “probabilities”, with range $[0, 1]$, in the same manner as Haimberger (2007), except that the a priori probability time series is flat (no use of metadata). If, on a given day, the maximum break probability exceeds 0.5, the date is recorded as a *possible* break. If it passes the robustness tests, it is adjusted as explained below. If there is a break, the $\langle Q_k \rangle$ are typically larger than Q_{crit} over a certain time interval (see, e.g., Fig. 6). The break location is set at the maximum $\langle Q_k \rangle$ value. Local $\langle Q_k \rangle$ maxima have to be separated by at least a year to be recognized as separate breakpoints.

3.3 Break adjustment

As mentioned, a common reason for breaks in wind direction is the wrong north alignment: in this case the wind direction error is expected to be constant in time and also in the vertical. The break size estimate at a given pressure level at 00:00 or 12:00 UTC at date k is defined as

$$\overline{\Delta \tau}_{dd}^k(a, b) = \bar{\tau}_{dd}^k(b) - \bar{\tau}_{dd}^k(a). \quad (5)$$

The intervals a, b are generally chosen to be longer (up to 8 years, as explained above) than the intervals used for break detection with SNHT, above. We consider a break significant if its magnitude is larger than 1.96 times the standard deviation of the $\bar{\tau}_{dd}$. We require that the vertical mean of the break sizes $\langle \overline{\Delta \tau}_{dd}^k(a, b) \rangle$ must be greater than 3° and that the break size estimates at individual pressure levels must not change sign in the vertical. At least four time series (two pressure levels at both 00:00 and 12:00 UTC times or four pressure levels at the same time) must be available in order for them to be accepted. In this case the break is adjusted at both 00:00 and 12:00 UTC. Since there are cases in which the device changes between the observation at 00:00 and 12:00 UTC (for example, pilot balloon at 00:00 UTC and radiosonde at 12:00 UTC), one may get different and independent break profiles at different times. For such cases, the significance test has been performed at both times separately. The breaks at station Bismarck as shown in Fig. 6 are typical examples. Others, like the Russian station Aktyubinsk (now known as Aktobe, but for historical reason here called Aktyubinsk, WMO ID 35229) or Marion Island (WMO ID 68994), highlighted by Gruber and Haimberger (2008), have been revisited for comparison purposes. The obtained mean break profiles agree well with those presented in Gruber and Haimberger (2008), although the variance of the estimates is larger because the scatter of the departures from surface data only reanalysis used as reference is larger when compared to background departures from full reanalyses such as ERA-Interim, particularly in remote regions.

The approach for wind speed is slightly different, since there are no such strong physical constraints available as

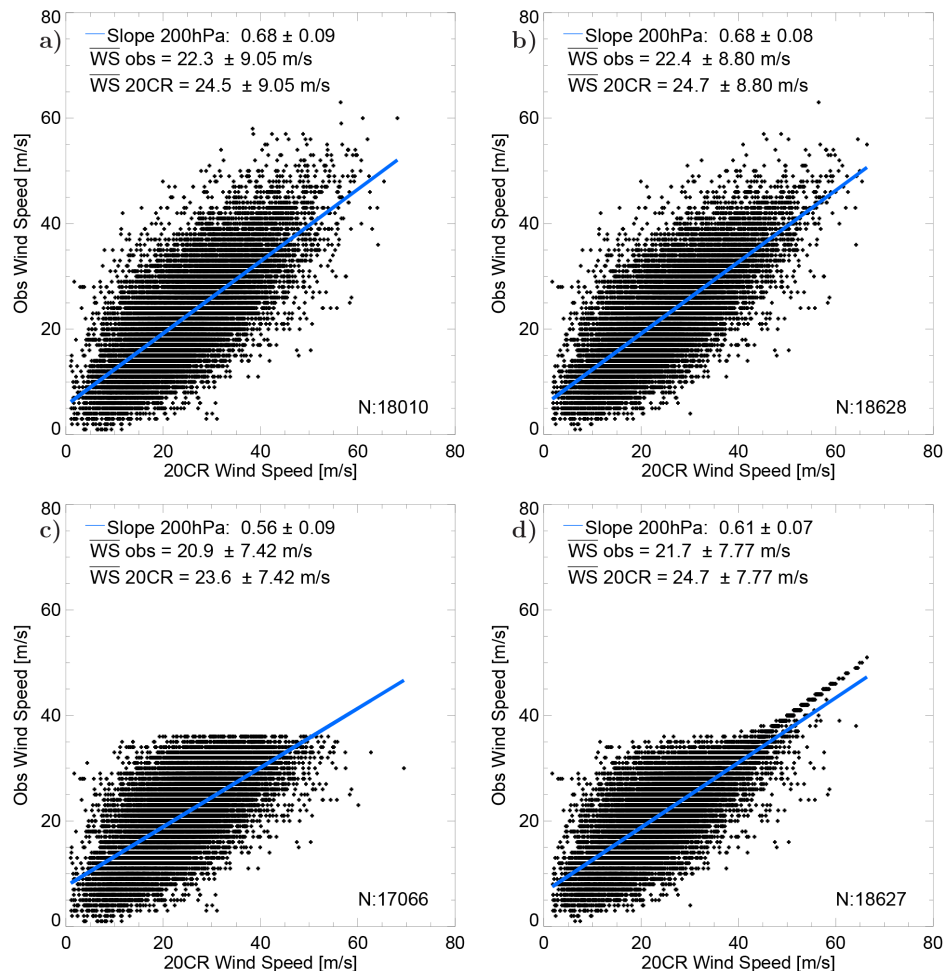


Figure 4. Scatterplots of observed wind speed vs. NOAA-20CR at station 72764 at 200 hPa with different treatment of high wind speeds during the period 1960–2010. **(a)** original observed wind speed; **(b)** observed wind speed, missing values replaced by scaled NOAA-20CR wind speeds; **(c)** observed wind speed, all values above 60 % of the maximum observed wind speed set to “missing”; **(d)** as **(c)**, but values set to missing in **(c)** are replaced with scaled NOAA-20CR wind speeds. Mean wind speeds as well as the linear relationship between observed and NOAA-20CR wind speeds are given in inset legends.

there are for wind direction. Larger biases may occur only at some pressure levels; thus, each single level is analyzed independently. In particular, it is well known that the largest inhomogeneities occur at high wind speeds, i.e., where the jet streams are located (7–12 km above the sea level for the polar jet and 10–16 km for the subtropical jet). A break at a given level is considered significant if its size is larger than 1.96 times the standard deviation of the $\bar{\tau}_{ff}$. If this criterion is fulfilled at least at two levels at a potential breakpoint, the wind speed profile is adjusted.

While the individual wind direction values are adjusted by a vertically constant value, the wind speeds at a given pressure level are adjusted by a factor λ such that high wind speed values are adjusted more than low wind speeds. Otherwise low wind speeds might become negative.

Before adjusting the observations, the NOAA-20CR wind speeds, which are known to be biased (Compo et al., 2011), have been adjusted by another constant factor λ_{20CR} , which has been derived from the mean wind speed quotient between the most recent part of the observation time series and the corresponding NOAA-20CR analysis time series:

$$\lambda_{20CR} = \overline{WS}_{obs} / \overline{WS}_{20CR}. \quad (6)$$

The λ_{20CR} factor is calculated for each pressure level and for each station using linear regression to reflect different biases in different climate zones. Only wind speeds larger than 1 m s^{-1} in the NOAA-20CR and after 1960 have been taken into account when calculating this factor. In general, the method delivers reasonable factors in the range of 0.9–1.2, assuming there are sufficient data available (at least

1000 values). One example is the ratio of the mean wind speeds given in Fig. 4a. Before 1960, the mean values of the observations in Fig. 3a are higher by this factor than the NOAA-20CR winds in Fig. 3b.

As has been described in Haimberger (2007) and Haimberger et al. (2012), the breakpoint adjustment procedure works backward in time, from the most recent to the earliest one; in this way, a progressively shorter section of the time series is adjusted. The default averaging interval for the break size estimation has been set to 8 years. If only a shorter time series is available (because of the next earlier break or because of a data gap), this parameter is reduced accordingly. The adjustment factors remain constant in amplitude between the breakpoints. After these procedures, the breaks due to changes in the measurement biases of the observed wind time series should be largely removed.

3.4 Calculation of unbiased monthly means

The early wind measurement systems used theodolites to track the ascending balloons, which worked only if there was good visibility and upper-level winds were not too strong. While, under fair weather conditions, the balloons could be tracked up to 200 hPa or higher, the balloons were sometimes lost below 2 km in stormy conditions. As a result, winds during disturbed weather conditions are underrepresented. While the single measurements are unbiased, their monthly mean is biased since only the low-wind part of the distribution is well sampled. Figure 3a shows histograms of observed wind speed for long records over the US at the 300 hPa level. Whereas there are very few measured wind speeds over 40 m s^{-1} in the 1940s, they are quite common from 1960 onward. When taking the mean, the 5-year averaged wind speeds increase from 14.6 m s^{-1} to more than 20 m s^{-1} in the above time frame. This increase is almost solely due to decreasing sampling bias. After the introduction of radar tracking in the 1960s, only very few observations were missing and the sampling bias vanished.

In contrast to the observations, the mean wind speed departures from the NOAA-20CR changed only slightly. Observed winds tend to be higher than NOAA-20CR winds by 0.5 m s^{-1} in the 1940s and 1.8 m s^{-1} from the 1960s onwards. The mean is positive since the NOAA-20CR has a predominantly low bias below 150 hPa in wind speed (Compo et al., 2011); see also Fig. 3 of Part 1 (U wind is a very good proxy for wind speed in the zonal mean). It increases slightly over time since the departures tend to be larger during high-wind conditions, which are undersampled in the early years. The increase is, therefore, not necessarily a sign of inhomogeneities in the measurements. The constant mean departures from the 1960s onward indicate that the low bias of NOAA-20CR is practically constant throughout these decades. Thus, it can be expected to be constant also earlier on, the exception being perhaps the period 1900–1940, when

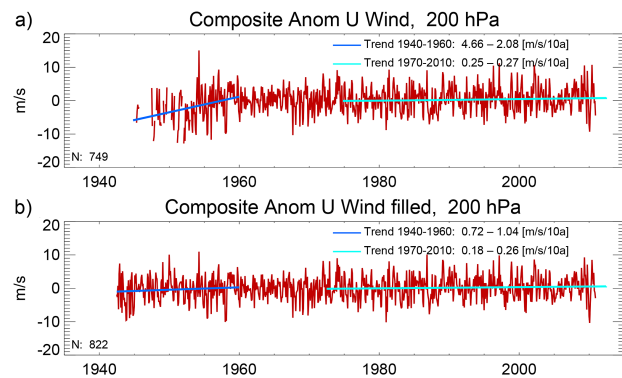


Figure 5. Monthly mean wind speed at 200 hPa, averaged over WMO stations with IDs between 70 000 and 75 000 (mostly USA and Canada), (a) without filling, (b) with missing data replaced with NOAA-20CR scaled wind values.

different background error variances have been used in the NOAA-20CR assimilation system (Compo et al., 2011).

There are several options to avoid a sampling bias in, e.g., monthly means. The simplest one is to calculate the means only if a very large fraction of observations are available (e.g., less than two observations missing per month). Such a strict requirement leads to very few monthly means being calculated in the early years. As a second option, one can substitute missing observations with analyzed winds from NOAA-20CR. We did this for months where at least 15 observations were available at a given observation time (00:00 or 12:00 UTC). The scaled NOAA-20CR winds (as explained before) are, of course, used for the substitution. Figure 4a, b show the effect of the filling at a station where only few data were missing. The filling procedure increases the observation count from 18 010 in (a) to 18 628 in (b). The mean wind speed is slightly increased through the filling in this case. To put more stress on the filling algorithm, we artificially set all high wind speed values to “missing” in panel (c), which reduces the mean wind speed by 1.4 m s^{-1} . Substitution of the values set to missing in (c) by scaled NOAA-20CR values reduces this artificial sampling bias to 0.6 m s^{-1} in panel (d).

A composite of monthly mean anomaly time series of stations with WMO numbers between 70 000 and 75 000 are shown in Fig. 5. The earliest part of the time series in (a) is affected by the sampling bias without filling. Complementing the daily data with scaled NOAA-20CR values before taking the monthly averages makes it possible to remove or at least reduce the spurious trends due to undersampling (lower panel). There may be room for further improvement in the treatment of the sampling bias, but the example demonstrates that the sampling bias cannot be ignored at all if one wants to consider time series going back before the 1960s.

Despite this encouraging performance of the filling method, we decided not to use it for homogenization

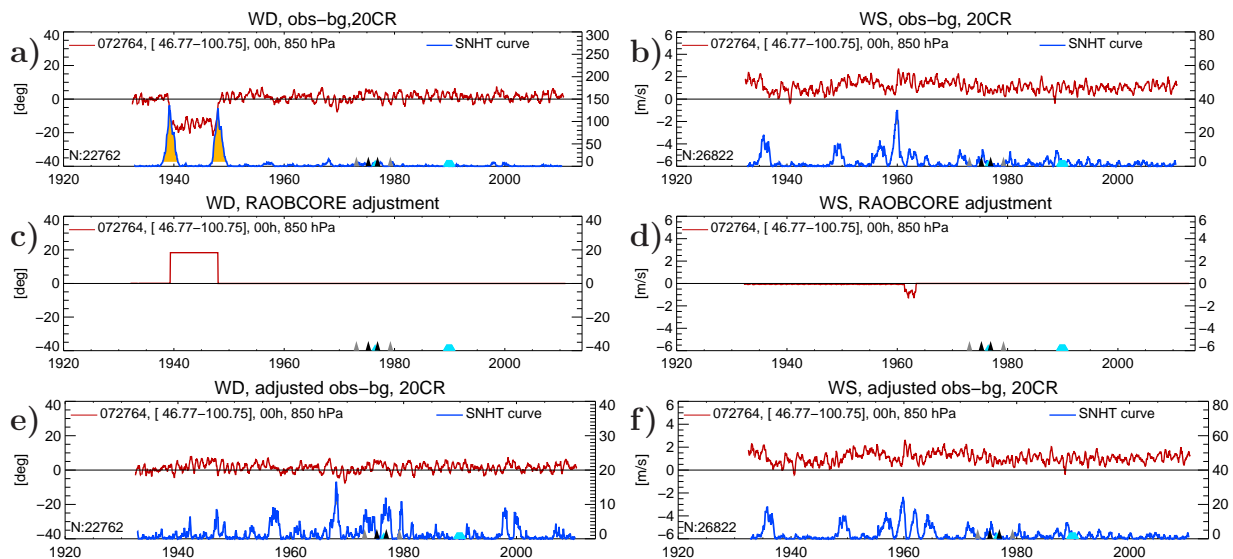


Figure 6. Upper row: (a) wind direction and (b) wind speed analysis departure (Obs-NOAA-20CR) time series at time 00:00 UTC at 850 hPa at station Bismarck (red curves). The blue curves (right axes) show the Q_k time series as defined in Eq. (4). Q_k values above $Q_{crit} = 10$ are statistically significant and are shaded. The small colored triangles on the x axes indicate changes in the radiosonde type. For dd , Q_{crit} has been set to 20. The mean of the wind speed differences is positive since NOAA-20CR wind speeds over the US are generally biased low. Metadata from IGRA are indicated as light blue trapezoids or triangles. Middle row: (c) wind direction and (d) wind speed adjustments calculated by RAOBCORE from analysis of the departure time series in upper row. Wind direction biases are constant in pressure and time between breakpoints. Wind speed adjustments occur only after 1960 at this station. They depend on observed wind speeds and are, therefore, not constant. Lower row: analysis departures after adding the adjustments in middle row to upper row. Note smaller right axis scales compared to the upper panel, indicating better homogeneity.

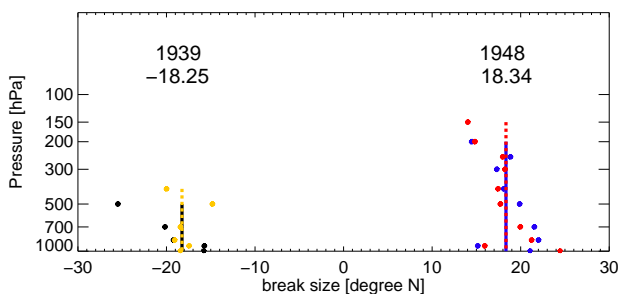


Figure 7. Vertical profiles of wind direction break size estimates at Bismarck (WMO ID 72764) for breaks in 1939 and 1948. The bullets are the estimated differences detected at each pressure level (black and blue at 00:00 UTC, yellow and red at 12:00 UTC). The solid and dotted lines are the respective vertically constant adjustment mean values for the whole vertical profiles

purposes. The most important reason is that the filling compromises the independence between observation and the reference. Thus, it would become harder to detect breaks when analyzing time series containing an appreciable amount of values from the reference series. Even if we did an adjustment, it would be underestimated for the observed values but overestimated for the filled values. This would re-

main a problem even if we had a more accurate reanalysis than the NOAA-20CR at our disposal. As such, one should use the filling approach only after homogenization.

In the following we display only results with data where the sampling bias is low so that the filling is essentially unnecessary. This is the case for the early period at lower pressure levels (< 500 hPa) and for the period after 1960.

Also, on PANGAEA, we only provide homogeneity adjustments (daily and monthly) but no filled values. It is important for the reader to understand that we removed the non-climatic shifts but that we only highlighted the presence of the sampling bias without actually removing it.

4 Results

4.1 Individual series analysis

As mentioned above, the main purpose of this paper is to find and possibly fix breaks, especially in the period before 1958, where other more sophisticated techniques (RICH (Radiosonde Innovation Composite Homogenization) and its versions (Haimberger et al., 2008), for example) are not applicable, mainly due to the low station density that makes the construction of reliable reference time series from neighboring stations rather difficult.

3 A global radiosonde and tracked balloon archive on 16 pressure levels (GRASP) back to 1905 - Part 2: Homogeneity adjustments for PILOT and radiosonde wind data

L. Ramella Pralungo and L. Haimberger: Homogeneity adjustments for pilot balloon and radiosonde wind data

305

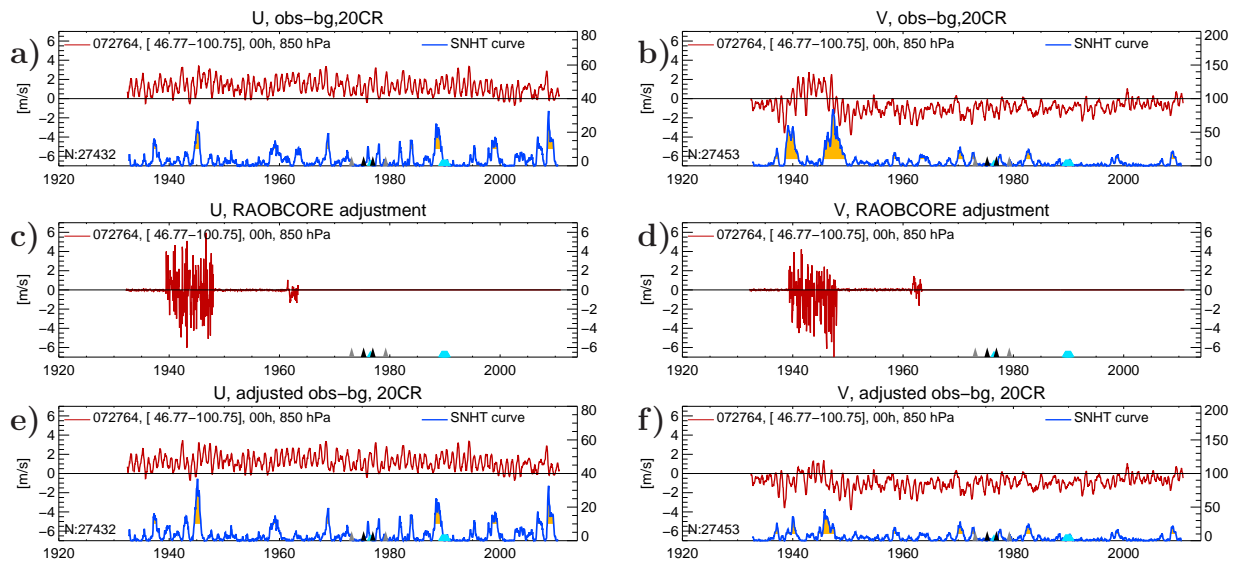


Figure 8. (a) *U* and (b) *V* wind innovations, (c, d) wind adjustments and (e, f) adjusted innovations at the 850 hPa level. Note that a positive adjustment of wind direction as shown in Fig. 6c translates to negative *V* adjustments, depending on the strength of the predominantly westerly winds.

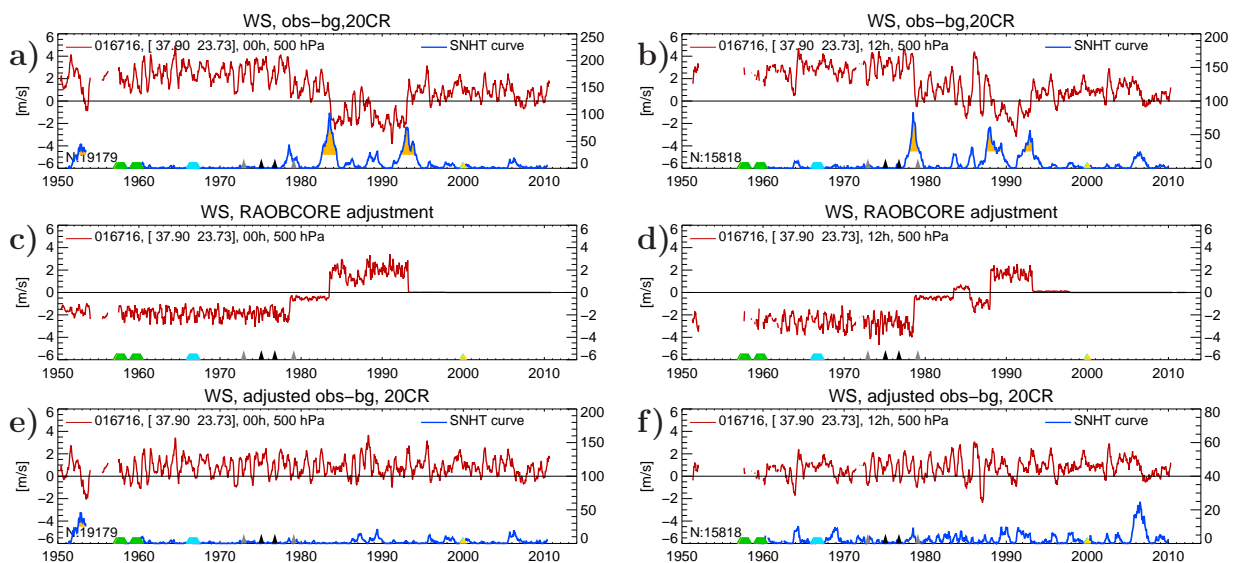


Figure 9. Wind speed innovations (upper row, red curves) at Athens, Greece, WMO ID 016716, at 300 hPa, at (a) 00:00 UTC and (b) 12:00 UTC. Blue curves are SNHT time series, (c, d) are corresponding adjustments and (e, f) are corresponding adjusted innovations.

While the US wind network was established already very early with up to 60 stations in the 1930s, it had some problems with measuring the wind direction. The raw observations show visible shifts, e.g., in the wind direction time series of station 072764 (Bismarck, North Dakota, USA) in Fig. 2. Shifts are visible at all the available pressure levels in the years 1938 and 1948. The shifts are much more clearly visible in Fig. 6a. It shows the wind direction innovations

$\tau_{dd}(t_i)$ time series with the NOAA-20CR winds as reference at 850 hPa for (a) wind direction and (b) wind speed. The SNHT test statistic reaches very high values for wind direction. The breaks are very similar for wind direction at other levels (Fig. 7). In these early years the ascents did not reach very high levels and already at 500 hPa the SNHT (blue line, right axis) can be calculated only after 1945. After those

3 A global radiosonde and tracked balloon archive on 16 pressure levels (GRASP) back to 1905 - Part 2: Homogeneity adjustments for PILOT and radiosonde wind data

306

L. Ramella Pralungo and L. Haimberger: Homogeneity adjustments for pilot balloon and radiosonde wind data

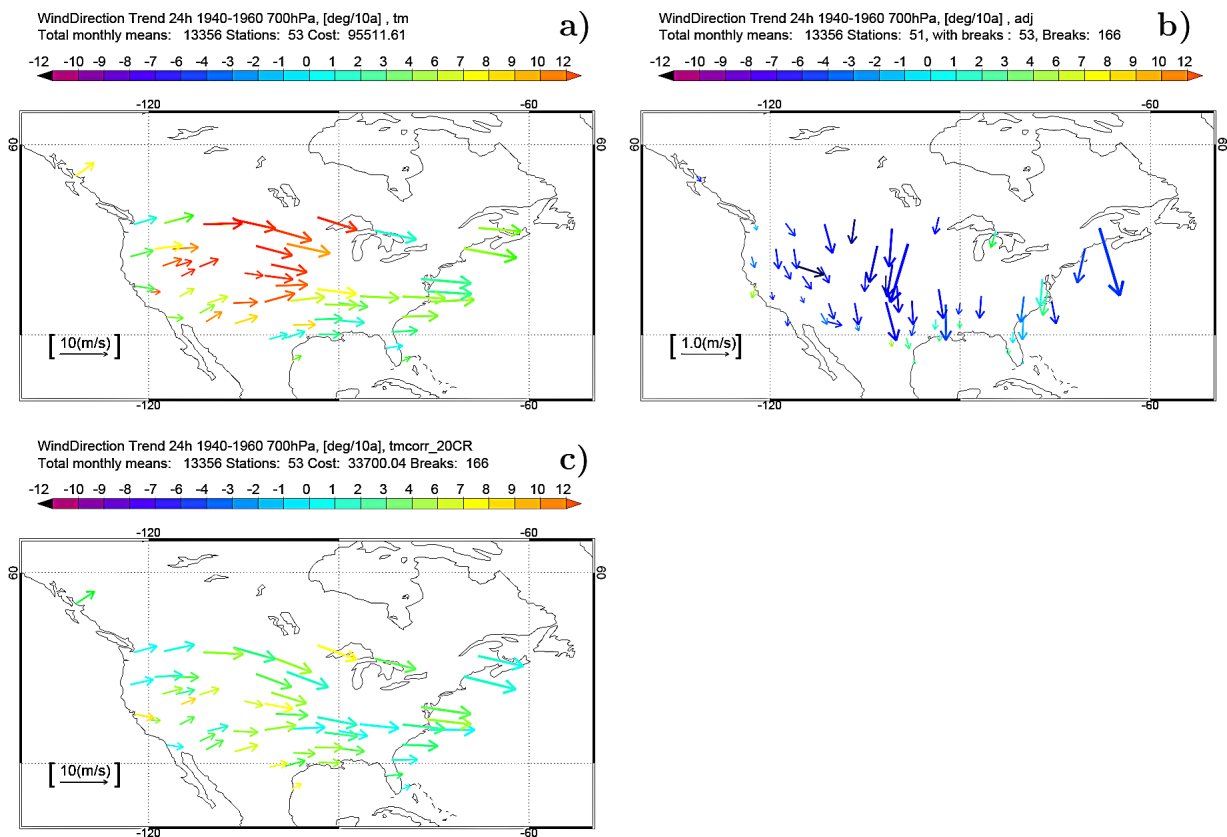


Figure 10. (a) Raw wind direction trends at 700 hPa at US stations (WMO numbers between 71 000 and 73 000) for the period 1940–1960 averaged over both 00:00 and 12:00 UTC (most stations reported twice daily). Arrows depict the mean wind speed and direction over this period. Arrow color indicates wind direction trend over the investigated period. Only stations with less than 1 year of missing values are shown. (b) Wind direction adjustments ($\Delta \bar{U}$, $\Delta \bar{V}$) as estimated by RAOBCORE 2.0. The arrows show size and direction of the adjustments; the colors show how much the wind direction trend has been changed due to the adjustments. Note scale difference in arrow length compared to (a). 174 shifts have been adjusted in total. (c) shows wind direction trends after adjustment. The cost function measuring spatial-trend heterogeneity (see Haimberger, 2007; Haimberger et al., 2012) has been reduced by a factor of 3 compared to (a).

breaks in early years, the wind direction departures seem quite homogeneous with no obvious shift.

Figure 6b shows the wind speed innovations $\tau_{ff}(t_i)$ and the SNHT time series. In the years 1930–1960, the time series are homogeneous. Weak shifts are visible in 1960, 1963 (for unknown reasons) and in 1973, which can be attributed to a station relocation according to S. Schroeder’s metadata database (Tschudin and Schroeder, 2013).

Panels 6c, d shows= the different adjustments calculated with RAOBCORE 2.0. They reduce the detected jumps, as can be seen from the adjusted innovation time series in Fig. 6e, f, which are definitely more homogeneous than the raw series presented in Fig. 6a, b. No visible wind direction inhomogeneities remain. The inhomogeneities found may have contributed to the apparent strong wind anomalies found by Brönnimann et al. (2009) during the dust bowl drought. They would likely be weaker if homogenized data

had been used. This just shows how important it is to eliminate inhomogeneities before doing climate studies.

Wind speed adjustments are not constant in time, since they depend on wind speed itself. The breaks in the early 1960s are no longer visible in the adjusted innovation time series, only one shift in 1972 has not been adjusted. The adjustments for wind speed and direction can be split into U and V wind component adjustments, with a simple vectorial decomposition, and these can be applied in order to adjust U and V wind components. Due to the predominantly zonal wind direction, the wind direction adjustments are projected more onto the V wind components whereas wind speed adjustments affect mainly the U component. Figure 8 shows unadjusted innovations, adjustments and adjusted innovations of U and V for the 700 hPa level. Note that the V adjustments (panel d) have a negative mean because of the negative wind direction adjustment and the mostly westerly winds. The adjusted time series have no more shifts but also

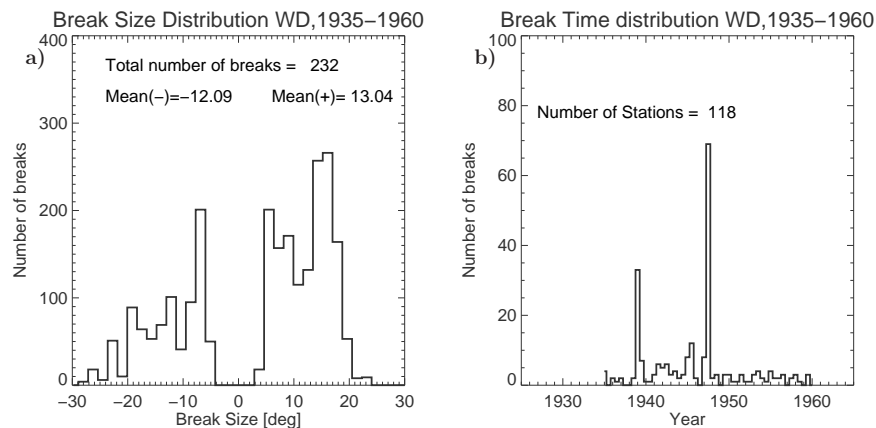


Figure 11. (a) size and (b) temporal distribution of wind direction breaks at North American stations (WMO numbers between 70 000 and 75 000) in the period 1935–1960; all available stations are analyzed. The means of positive and negative breaks are indicated.

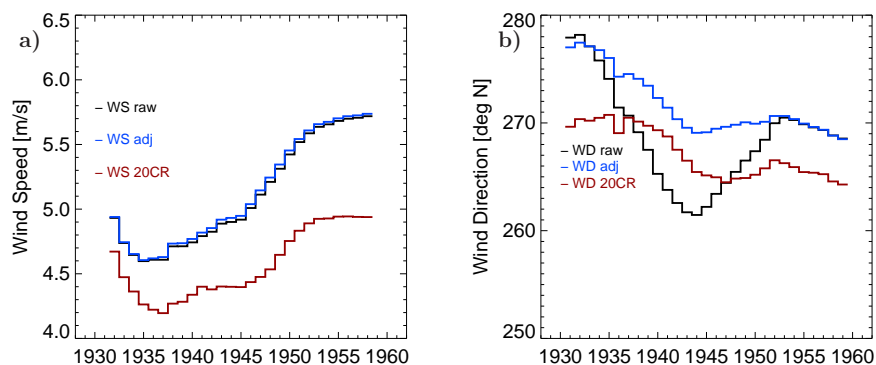


Figure 12. Unadjusted (raw), adjusted and NOAA-20CR wind speeds (a) and directions (b) in the period 1940–1960 at 700 hPa, over a selected group of stations with long and complete time series (WMO numbers: 70261, 72206, 72208, 72250, 72261, 72293, 72317, 72363, 72365, 72405, 72469, 72493, 72518, 72528, 72562, 72572, 72597, 72632, 72681, 72698, 72764, 74626, 72231, 72334, 72374). Running mean: 8 years.

have reduced variance. Generally it has been found that wind speed breaks over the US are relatively rare and relatively weak. Already the unadjusted innovations often look homogeneous, which indicates good quality of both observations and NOAA-20CR.

Wind speed breaks are weak at Bismarck, but at other places they can be quite strong, e.g., in Athens (016716, Greece). This station has already been studied by Gruber and Haimberger (2008). Figure 9 shows the innovation time series at 300 hPa at 00:00 and 12:00 UTC. In 1993, 1987, 1983 and 1979, four massive breaks are detected by the SNHT. The resulting adjustments calculated by RAOBCORE 2.0 and the adjusted innovation time series are shown in the middle and lower panels of Fig. 9. All breaks already detected by Gruber and Haimberger (2008) could be detected again, although a less accurate reference (NOAA-20CR instead of ERA-40) was used. Also, the wind direction series at Athens seems to suffer from two inhomogeneities, but these are not removed

since they are not vertically constant (close to linear growth) and they change sign. As such they are not attributable to wrong north alignment.

4.2 Regional and global trends

The overall beneficial impact of the applied homogeneity adjustments is best visible in maps of trends of both wind direction and speed before and after the data have been treated with RAOBCORE 2.0. The raw, the adjusted and adjustment time series are available at daily resolution, but for trend calculations monthly averages have been used, taking particular care of the sampling problem as noted above. The trend calculation is easy for wind speed (scalar variable), but more challenging for wind direction, which is derived from U and V trends, as explained in Appendix A.

While maps of trends do not reveal all inhomogeneities, they are rather sensitive to inhomogeneities and the comparison with trends at neighboring stations helps to understand

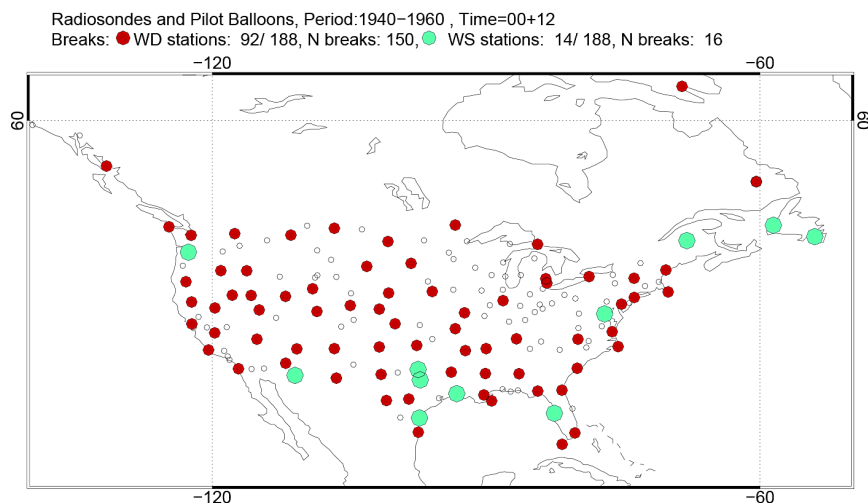


Figure 13. Stations with breaks in wind direction (red bullets) and speed (green bullets) for the period 1940–1960, as well as stations with no breaks (open circles). 188 stations with at least 10 years of observations were analyzed. For wind direction, 92 stations show 150 breaks in this period, whereas only stations with 16 wind speed breaks were found.

where the raw data are affected by them. To estimate the spatial consistency of the trends, the *cost* function introduced by Haimberger (2007) has been used. In this way, smaller improvements in spatial homogeneity can also be objectively measured.

4.2.1 Wind trends over the US in the early period 1940–1960

In 1940 the US already had a well established upper-air network, whereas observations were very rare in other regions. Pilot balloons and radiosondes were launched twice daily, typically reaching the 500 hPa level.

As our first example, we show wind direction trends at 700 hPa in the period 1940–1960 over the US in Fig. 10a. The arrows indicate the mean wind speed over the considered period and point to the mean wind direction. The color scale tells us about the wind direction trend for the investigated period. The figure shows suspiciously strong trends (more than 10° over 10 years, mainly located over the central US; station Bismarck, North Dakota, 072764, belongs to this group, see Fig. 6). Applying RAOBCORE2.0 and using the NOAA-20CR as a reference, around 150 wind direction breaks were detected in over 45 station records in the period 1935–1958. The applied adjustments are shown in Fig. 10b, where the arrows represent the adjustment vectors. For the period 1940–1960, the adjustments are such that winds change from westerly to more northwesterly in most cases (since the breaks in the opposite direction mostly occur before 1940), stressing that all the stations are affected by a similar north-alignment-related bias. The colors show how the adjustments affect the wind direction trends. The adjusted trends in Fig. 10c look much more homogeneous and the cost function has also been

reduced by a factor of 3 due to the improved spatial and temporal homogeneity.

The nature of the breaks affecting the USA in the period 1935–1960 is highlighted in Fig. 11, which shows that the break distribution is clearly bimodal with absolute values of break sizes definitely greater than 0. This indicates that the adjustments are applied only where the break significance has been carefully verified. Moreover, the break time distribution shows that most breaks occurred in 1939 and 1948. S. Schroeder’s metadata database (Tschudin and Schroeder, 2013) indicates a change from theodolite pilot balloons to first-generation radiosondes in 1939, as was the case at Bismarck. In many cases there are metadata events indicating measurement system changes in this database in the above cited years. However, the information does not reveal what exactly caused these changes in the north alignment. According to our estimates, this problem was corrected more than a decade later. If one investigates the break distributions shown in Fig. 11 for the years 1938–1941 and separately for 1947–1951, one obtains two tight and approximately Gaussian distributions, with means of -12° and $+13^\circ$, respectively.

In order to get an idea of how the observed mean wind speed and direction looked like before and after the break analysis, a subset of central US stations was averaged year by year for both wind speed and direction. As is well visible in Fig. 12, wind directions have been strongly adjusted in the period 1935–1948, whereas wind speed shows only slight changes due to the homogenization. The sampling problem does not play a major role for this figure, since, at 700 hPa, most series involved were almost complete. Thus, and because it is visible also in the NOAA-20CR, the increase in wind speed during this period is trusted. Some in-stationarity in wind direction is visible as well. However, this is also

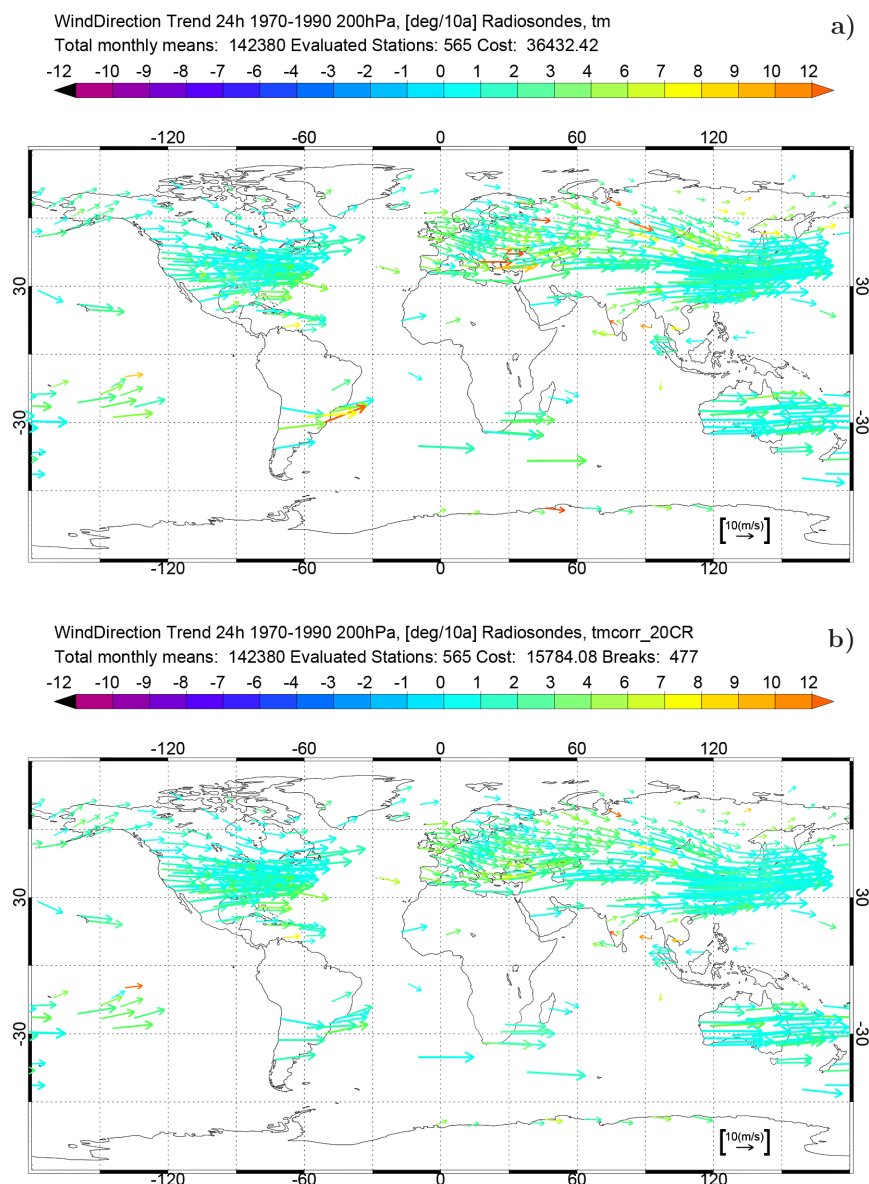


Figure 14. Global observed wind direction trends at 200hPa for the period 1970–1990, (a) before adjustment, (b) after adjustment with RAOBCORE. 565 WMO stations with less than three missing years in the inquired period have been used. The length, direction and color of the arrows have the same meaning as in Fig. 10.

found in the NOAA-20CR. The offset by several degrees is less than the measurement increment of wind direction (5–10°).

Figure 13 shows that 92 out of 188 US stations reporting wind observations in the period 1940–1960 with at least 10 years of observations had breaks in wind direction (150 breaks in total). Only 14 stations were affected by 16 wind speed breaks.

4.2.2 Global trends in more recent times

The upper-air wind observation coverage is fairly global from 1950 onward, with a significant improvement in 1958, the International Geophysical Year. The inclusion of pilot balloon data is essential to get acceptable coverage in the Tropics and Southern Hemisphere in the early years. Inhomogeneities do, however, also occur in later periods. Figure 14 shows global wind direction trend maps at 200hPa for the period 1970–1990. Quite a few stations show suspiciously strong trends compared to their neighbors. 477

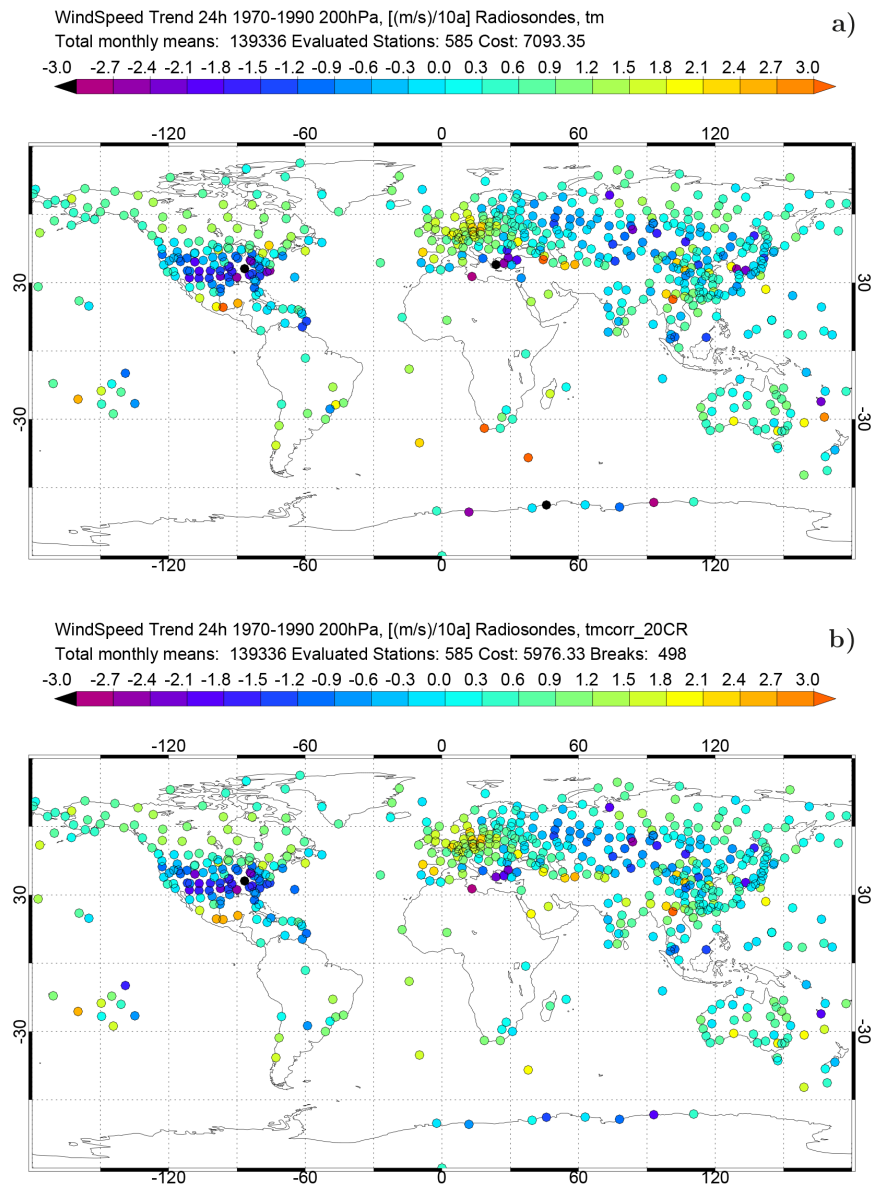


Figure 15. Global observed wind speed trends at 200hPa for the period 1970–1990, (a) before adjustment, (b) after adjustment with RAOBCORE. 585 WMO stations with less than three missing years in the inquired period have been used. Cost values in legend indicate moderate reduction of trend heterogeneity.

breaks have been detected and adjusted by RAOBCORE and the cost function is reduced to about 40 %, which is substantial. The adjusted trends in Fig. 14 show only very few remaining outliers.

Wind speed trend patterns are already relatively smooth without homogenization, as shown in Fig. 15 at 200hPa. Isolated outliers such as Athens (see Fig. 9) or stations in Turkey, Algeria, the Republic of South Africa, California, Mexico and Antarctica are detected and in most cases adjusted. The cost function is reduced only slightly, by 15 %

(Fig. 15). One could have achieved a lower cost function value by setting wind speed break thresholds lower, but we decided to be more conservative. Some strong trend features are also present in the NOAA-20CR (which has a cost value of 3900) as well, such as the strong deceleration of winds over the US, so we do not expect the cost function to become much lower.

Figure 16a shows the size distribution of wind direction breaks over the whole investigated period (1920–2010), whereas (b) shows the temporal distribution of the breaks.

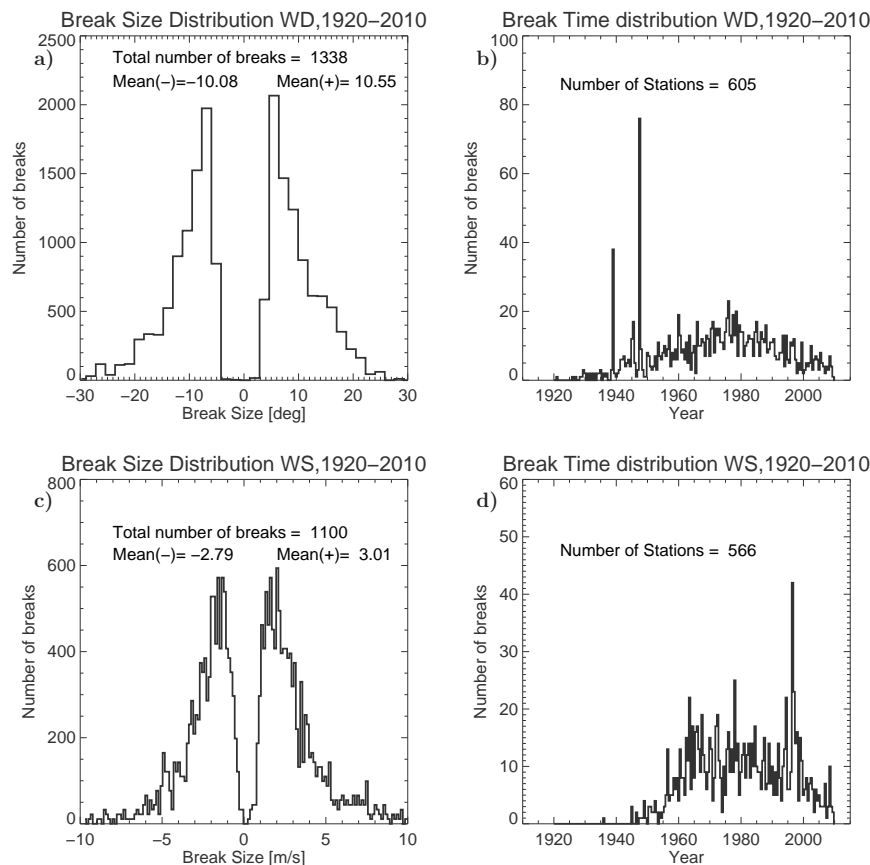


Figure 16. (a) Wind direction break size and (b) time distributions for the whole period investigated (1900–2010), for all available stations. (c) shows corresponding wind speed break size and (d) break time distributions.

The two peaks around 1937/8 and 1947/8 stem from the problems of the early US stations. Afterwards the temporal distribution is smooth. The size distribution shows that really only larger wind direction breaks have been adjusted. Wind speed break sizes in Fig. 16a again show a bimodal break size distribution. Regarding the time distribution in (b), we observe sizeable break numbers only after 1945, most probably because, before, the sparse (only in the USA) soundings did not reach high levels where the wind speed is higher and problems with speed measurements are more likely. The prominent peak in 1998 can be attributed mainly to stations with breaks in the Middle East, northern Africa and South Asia (together ≈ 25 stations). We found no indication of a break in the NOAA-20CR when we compared difference series of ERA-Interim and NOAA-20CR wind speeds (not shown). A total of 1100 wind speed breaks at 566 stations (out of 2924 stations with more than 1 year of data) were detected. In addition, 1338 wind direction breaks at 605 stations have been found.

5 Conclusions

This paper documents our efforts to homogenize the global wind radiosonde and pilot balloon archive described in Part 1 (Ramella-Pralungo et al., 2014), using the NOAA-20CR (Compo et al., 2011) as reference. Since this reanalysis was produced using only surface data it is independent of upper-air data. The already well-known RAOBCORE method (Haimberger, 2007; Gruber and Haimberger, 2008) has been extended and reinforced such that it is able to treat temperature (results are not shown in this work) and wind together.

In contrast to Gruber and Haimberger (2008), we analyzed innovation time series of wind speed and direction only (not U and V) for break detection, since the measurement instruments report speed and direction and the breaks are related to biases linked to the instrument itself. For wind direction we looked specifically for north alignment errors. Regarding wind speed, one expects breaks at those levels where the mean wind speed is particularly large, i.e., near jet streams. When a break was detected, the adjustments were made by

applying a constant factor estimated from comparing the wind speeds and wind speed innovations before and after the break. Combining information from wind speed and direction, the U and V wind components could also be adjusted.

Since the NOAA-20CR was used as reference and since a much more comprehensive input data set was used, several inhomogeneities in the period before 1958 could be detected and adjusted, the most prominent being a pervasive wind direction bias of up to 15° over the central US between 1938 and 1948. After 1960, inhomogeneities are relatively rare compared to temperature inhomogeneities. Fewer breaks have been detected and adjusted compared to Gruber and Haimberger (2008). The reasons are, on the one hand, inhomogeneities in the reference used then (ERA-40, which has some shifts, e.g., in 1972, 1974, 1976, 1979, 1986, mostly related to the satellite observing system; Uppala et al., 2005). Therefore, we did not consider the breaks detected by Gruber and Haimberger (2008) as metadata for the present adjustment procedure. On the other hand, the ERA-40 background departures were much smaller than the NOAA-20CR analysis departures used here. For example σ_u in the period 1979–2001 at 200 hPa at station 35 229 (Aktyubinsk) is 8.1 m s^{-1} for NOAA-20CR analysis departures, 5.9 m s^{-1} for ERA-40 background departures and 4.1 m s^{-1} for ERA-Interim departures. This is simply because upper-air observations have been assimilated in the latter two reanalyses. It is quite likely that some of the smaller shifts that could be detected with ERA-40 could not be detected with our adjustment system simply because of the higher noise level, which makes the SNHT less sensitive (σ is in the denominator of Eq. 4).

The adjustments could be used as input in a reanalysis bias correction scheme or they could be used as a reference to test a future variational wind bias adjustment scheme for radiosonde wind biases with the basic algorithm similar to the one used for adjusting satellite radiances (Dee and Uppala, 2009). In particular, wind direction biases seem good candidates for variational adjustment since wind direction is well constrained in a state-of-the-art multivariate data assimilation system and expected model biases in wind direction are much smaller than the biases found in some of the observation records.

The wind data set developed is the most comprehensive homogenized data set of its kind. It is an ideal basis for estimating the tropical zonal mean warming maximum through exploiting the thermal wind relationship, as pioneered by Allen and Sherwood (2008). The large number of pilot balloon records should allow us to extend these estimates back to 1950, and, because of the more complete data, higher accuracy can be expected compared to their study. It may be very interesting as well to check whether the global mean kinetic energy has increased in the past decades (Bengtsson et al., 2004; Kung, 1966).

Although the data are now homogenized, one should be aware that observed wind speeds have a sampling bias. In the early period, high wind speeds are underrepresented because of measurement limitations. This effect still has to be taken into account when calculating monthly means and trends.

Appendix A: Wind direction trend

While estimating trends of scalar variables is straightforward, it is more challenging for wind variables, especially wind direction. The wind vector in polar coordinates can be expressed as $ff e^{i(dd \cdot \pi/180)}$, which is a nonlinear product. Calculating the wind direction trends just from regressing dd values over time will not always work, amongst other things because of its periodicity. To avoid such problems we split the wind vector into its orthogonal U and V components and regress those independently over time. Then we transform them back to dd and ff . The detailed steps are as follows:

1. For the selected time window (normally chosen to be 20 years), \bar{U}_{raw} , \bar{V}_{raw} , \bar{U}_{adj} and \bar{V}_{adj} are calculated using unadjusted (raw) and adjusted (adj) data (where the mean is taken over the selected time window).
2. From the U_{raw} , V_{raw} and U_{adj} , V_{adj} , time series, the linear trends are calculated. These are multiplied with the length of the time interval to yield differences $\Delta \bar{U}_{\text{raw}}$, $\Delta \bar{V}_{\text{raw}}$, $\Delta \bar{U}_{\text{adj}}$ and $\Delta \bar{V}_{\text{adj}}$.
3. Using the standard inner product definition, the wind direction difference Δdd can be calculated as

$$\Delta dd = \arccos \left(\frac{\left(\frac{\bar{U}}{\bar{V}} \right) \cdot \left(\frac{\bar{U} + \Delta \bar{U}}{\bar{V} + \Delta \bar{V}} \right)}{ff(\bar{ff} + \Delta ff)} \right) \quad (\text{A1})$$

for raw and adj observations.

Dividing Δdd by the length of the time interval used for calculating ΔU , ΔV yields the wind direction trend as it is shown color-coded, e.g., in Fig. 14.

Wind speed trends are calculated similarly, by calculating first the wind speed difference

$$\Delta \bar{ff} = \sqrt{(U + \Delta U)^2 + (V + \Delta V)^2} - \sqrt{U^2 + V^2} \quad (\text{A2})$$

and then dividing it by the time interval.

Appendix B: NetCDF file structure

This Appendix only describes the format of the netCDF adjustment files. The format of the merged archive, which is very similar, has already been described in Part 1 of this paper. The netCDF adjustment files contain the time series with daily resolution (00:00 and 12:00 UTC ascents) at 16 standard pressure levels (10, 20, 30, 50, 70, 100, 150, 200, 250, 300, 400, 500, 700, 850, 925 and 1000 hPa); one file for each variable (temperature, U wind and V wind components) and station. The file names are self-explanatory, such as

123456_corr_t_X.nc for daily adjustments

123456_corr_monthly_t_X.nc for monthly adjustments.

The first digit is either 0 or 1:

- 0: the station has been identified as a WMO station
- 1: the station does not have a WMO identifier.

The next five digits are the WMO station identification number if the first is a 0; otherwise they are the progressive number with which the station has been saved in the respective archive (The Comprehensive Historical Upper-Air Network (CHUAN version 1.7) or the ERA-CLIM historical upper air data sets (ECUD), since only those two archives contain unknown stations). The X refers to the variable reported in the file, and it can be

- $T \rightarrow$ temperature
- $U \rightarrow U$ wind component
- $V \rightarrow V$ wind component
- $WS \rightarrow$ wind speed
- $WD \rightarrow$ wind direction.

The $_t$ refers to *time series*, as this is the form in which the data have been stored. The following variables list specifies data type (float or int) and the name of the variable and provides some explanations:

- *integer* \rightarrow **station** \rightarrow station ID, the same as the first six digits in the file name;
- *float* \rightarrow **lat** \rightarrow station latitude, in degrees north, range $[-90^\circ, 90^\circ]$;
- *float* \rightarrow **lon** \rightarrow station longitude, in degrees east, range $[-180^\circ, 180^\circ]$;
- *float* \rightarrow **alt** \rightarrow station altitude, in m.a.s.l., range $[-400, 8000]$ m;
- *integer* \rightarrow **press(pressure_levels)** \rightarrow array with the 16 standard pressure levels;
- *integer* \rightarrow **obs_time(obs_time)** \rightarrow array with launch times (00:00 and 12:00) UTC;
- *integer* \rightarrow **dates(n_g_values)** \rightarrow progressive day index from 1900-01-01 with Gregorian calendar, range [19000101, 20230316];
- *float* \rightarrow **X_AN_raso_corrections(obs_time, pressure_levels, n_g_values)** \rightarrow this variable contains the actual adjustments; **X** could be either **T**, **U**, **V**, **WS**, **WD**, as for the file names.

The arrays have dimensions

$$\text{obs}(\text{obs_time}, \text{pressure_levels}, \text{n_g_values})$$

. In this way, we use the minimum number of days in order to map the time series. Note that for wind speed and direction only the adjustment files are available. If one

wants to also have the raw data in terms of wind speed and wind direction, one has to calculate those from U and V .

With the same conventions, we also have

- *float* → *X_AN_break_uncertainties(obs_time, pressure_levels, n_g_values)* → the standard errors of the break size estimates
- *float* → *X_AN_breaks(obs_time, pressure_levels, n_g_values)* → the break profiles; these are identical with adjustments for temperature but are different from adjustments for wind direction.

The monthly files have one additional variable:

- *integer* → *dates(n_g_values)* → Number of data used for producing the monthly mean

Both daily and monthly files have the following global attributes:

- *conventions* = “CF-1.4” → NetCDF files conventions;
- *title* → project title;
- *institution* → file owner “University of Vienna”;
- *history* → when the file has been produced;
- *data_type* → “radiosonde measurement bias corrections”;
- *source* → source archive;
- *references*: → www.univie.ac.at/theoret-met/research/raobcore.

Routines for reading the archived NetCDF files are available in FORTRAN and IDL and can be downloaded from [doi:10.1594/PANGAEA.823609](https://doi.org/10.1594/PANGAEA.823609).

3 A global radiosonde and tracked balloon archive on 16 pressure levels (GRASP) back to 1905 - Part 2: Homogeneity adjustments for PILOT and radiosonde wind data

L. Ramella Pralungo and L. Haimberger: Homogeneity adjustments for pilot balloon and radiosonde wind data

315

Acknowledgements. This work has been funded by projects P21772-N22 and P25260-N29 of the Austrian Fonds zur Förderung der wissenschaftlichen Forschung (FWF), as well as by the EU 7th Framework Programme collaborative project ERA-CLIM (Grant No. 265229). The authors thank the collaborators within ERA-CLIM, most notably Hans Hersbach, Alexander Stickler and Stefan Brönnimann, for their support and constructive comments. The comments of two anonymous reviewers, also regarding the format of the adjustment files, substantially improved the manuscript.

Edited by: G. König-Langlo

References

- Alexandersson, H.: A homogeneity test applied to precipitation data, *Int. J. Climatol.*, 6, 661–675, 1986.
- Allan, R., Brohan, P., Compo, G. P., Stone, R., Luterbacher, J., and Brönnimann, S.: The international atmospheric circulation reconstructions over the earth (ACRE) initiative, *B. Am. Meteorol. Soc.*, 92, 1421–1425, doi:10.1175/2011BAMS3218.1, 2011.
- Allan, R. J. and Ansell, T. J.: A new globally complete monthly historical mean sea level pressure data set (HadSLP2): 1850–2004, *J. Climate*, 19, 5816–5842, 2006.
- Allen, R. J. and Sherwood, S. C.: Warming maximum in the tropical upper troposphere deduced from thermal winds, *Nat. Geosci.*, 1, 399–403, 2008.
- Bengtsson, L., Hagemann, S., and Hodges, K. I.: Can climate trends be calculated from reanalysis data?, *J. Geophys. Res.*, 109, D11111–D11119, 2004.
- Brönnimann, S.: A historical upper air-data set for the 1939–44 period, *Int. J. Climatol.*, 23, 769–791, 2003.
- Brönnimann, S., Stickler, A., Griesser, T., Ewen, T., Grant, A. N., Fischer, A. M., Schraner, M., Peter, T., Rozanov, E., and Ross, T.: Exceptional atmospheric circulation during the “Dust Bowl”, 36, L08802, doi:10.1029/2009GL037612, 2009.
- Compo, G. P., Whitaker, J. S., Sardeshmukh, P. D., Matsui, N., Allan, R. J., Yin, X., Gleason, B. E., Vose, R. S., Rutledge, G., Bessemoulin, P., Brönnimann, S., Brunet, M., Crouthamel, R. I., Grant, A. N., Groisman, P. Y., Jones, P. D., Kruk, M. C., Kruger, A. C., Marshall, G. J., Maugeri, M., Mok, H. Y., Nordli, Å., Ross, T. F., Trigo, R. M., Wang, X. L., Woodruff, S. D., and Worley, S. J.: The twentieth century reanalysis project, *Q. J. Roy. Meteor. Soc.*, 137A, 1–28, doi:10.1002/qj.776, 2011.
- Dee, D. P. and Uppala, S. M.: Variational bias correction of satellite radiance data in the ERA-Interim reanalysis, *Q. J. Roy. Meteor. Soc.*, 135, 1830–1841, 2009.
- Dee, D. P., Uppala, S. M., Simmons, A. J., Berrisford, P., Poli, P., Kobayashi, S., Andrae, U., Balmaseda, M. A., Balsamo, G., Bauer, P., Bechtold, P., Beljaars, A. C. M., van de Berg, L., Bidlot, J., Bormann, N., Delsol, C., Dragani, R., Fuentes, M., Geer, A. J., Haimberger, L., Healy, S. B., Hersbach, H., Hólm, E. V., Isaksen, I., Kallberg, P., Köhler, M., Matricardi, M., McNally, A. P., Monge-Sanz, B. M., Morcrette, J. J., Park, B. K., Peubey, C., de Rosnay, P., Tavolato, C., Thépaut, J. N., and Vitart, F.: The ERA-Interim reanalysis: configuration and performance of the data assimilation system, *Q. J. Roy. Meteor. Soc.*, 137, 553–597, doi:10.1002/qj.828, 2011.
- Durre, I., Vose, R., and Wuertz, D. B.: Overview of the Integrated Global Radiosonde Archive, *J. Climate*, 19, 53–68, 2006.
- Ebita, A., Kobayashi, S., Ota, Y., Moriya, M., Kumabe, R., Onogi, K., Harada, Y., Yasui, S., Miyaoka, K., Takahashi, K., Kama-hori, H., Kobayashi, C., Endo, H., Soma, M., Oikawa, Y., and Ishimizu, T.: The Japanese 55-year reanalysis “JRA-55”: An interim report, *SOLA*, 7, 149–152, doi:10.2151/sola.2011-038, 2011.
- Ewen, T., Brönnimann, S., and Annis, J. L.: An extended Pacific North American index from upper air historical data back to 1922, *J. Climate*, 21, 1295–1308, 2008a.
- Ewen, T., Grant, A., and Brönnimann, S.: A monthly upperair data set for north america back to 1922, *Mon. Weather Rev.*, 136, 1792–1805, 2008b.
- Ferguson, C. R. and Villarini, G.: An evaluation of the statistical homogeneity of the twentieth century reanalysis, *Clim. Dynam.*, 42, 2841–2866, doi:10.1007/s00382-013-1996-1, 2013.
- Graystone, P.: Meteorological office discussion on tropical meteorology, *Met. Magazine*, 88, 117ff., 1959.
- Gruber, C. and Haimberger, L.: On the homogeneity of radiosonde wind time series, *Meteorol. Z.*, 17, 631–643, 2008.
- Haimberger, L.: Homogenization of radiosonde temperature time series using innovation statistics, *J. Climate*, 20, 1377–1403, 2007.
- Haimberger, L., Gruber, C., Sperka, S., and Tavolato, C.: Homogenization of the global radiosonde temperature and wind dataset using innovation statistics from reanalyses, in: *Proceedings of the Third WCRP International Conference on Reanalyses*, 5 pp., http://wcrp.ipsl.jussieu.fr/Workshops/Reanalysis2008/Documents/G4-411_ea.pdf, 2008.
- Haimberger, L., Tavolato, C., and Sperka, S.: Homogenization of the global radiosonde temperature dataset through combined comparison with reanalysis background series and neighboring stations, *J. Climate*, 25, 8108–8131, 2012.
- Hartmann, D. L., Klein Tank, A. M. G., and Rusticucci, M. (Eds.): *IPCC 2013: The Physical Science Basis, Chapter Observations: Atmosphere and Surface*, 159–254, IPCC, 2013.
- Hollingsworth, A., Shaw, D. B., Lönnberg, P., Illari, L., and Simmons, A. J.: Monitoring of observation and analysis quality by a data assimilation system, *Mon. Weather Rev.*, 114, 861–879, 1986.
- Kistler, R., Kalnay, E., Collins, W., Saha, S., White, G., Woollen, J., Chelliah, M., Ebisuzaki, W., Kanamitsu, M., Kousky, V., van den Dool, H., Jenne, R., and Fiorino, M.: The NCEP/NCAR 50-year Reanalysis: Monthly Mean CDROM and Documentation, *B. Am. Meteorol. Soc.*, 82, 247–267, 2001.
- Kung, E. C.: Large-scale balance of kinetic energy in the atmosphere, *Mon. Weather Rev.*, 94, 627–640, 1966.
- Luers, J. K. and Eskridge, R. E.: Temperature corrections for the VIZ and Vaisala radiosondes, *J. Appl. Meteorol.*, 34, 1241–1253, 1995.
- Poli, P., Hersbach, H., Tan, D., Dee, D., Thépaut, J. N., Simmons, A., Peubey, C., Laloyaux, P., Komori, T., Berrisford, P., Dragani, R., Tremolet, Y., Holm, E., Bonavita, M., Isaksen, I., and Fisher, M.: The data assimilation system and initial performance evaluation of the ECMWF pilot reanalysis of the 20th-century assimilating surface observations only (ERA-20C), ECMWF, 2013.
- Ramella Pralungo, L., Haimberger, L., Stickler, A., and Brönnimann, S.: A global radiosonde and tracked balloon archive on 16 pressure levels (GRASP) back to 1905 – Part 1: Merging and

- interpolation to 00:00 and 12:00 GMT, *Earth Syst. Sci. Data*, 6, 185–200, doi:10.5194/essd-6-185-2014, 2014.
- Santer, B. D., Hnilo, J., Wigley, T. M. L., Boyle, J. S., Doutriaux, C., Fiorino, M., Parker, D. E., and Taylor, K. E.: Uncertainties in observationally based estimates of temperature change in the free atmosphere, *J. Geophys. Res.*, 104, 6305–6333, 1999.
- Santer, B. D., Wigley, T. M. L., Mears, C., Wentz, F. J., Klein, S. A., Seidel, D. J., Taylor, K. E., Thorne, P. W., Wehner, M. F., Geckler, P. J., Boyle, J. S., Collins, W. D., Dixon, K. W., Doutriaux, C., Free, M., Fu, Q., Hansen, J. E., Jones, G. S., Ruedy, R., Karl, T. R., Lanzante, J. R., Meehl, G. A., Ramaswamy, V., Russell, G., and Schmidt, G. A.: Amplification of surface temperature trends and variability in the tropical atmosphere, *Science*, 309, 1551–1556, 2005.
- Scherhag, R.: Langperiodische Schwankungen der Stratosphärenzirkulation, *Beitr. Phys. Atmos.*, 35, 245–251, 1962.
- Stickler, A. and Brönnimann, S.: Significant bias of the ncep/ncar and twentieth century reanalyses relative to pilot balloon observations over the west african monsoon region (1940–57), *Q. J. Roy. Meteor. Soc.*, 137, 1400–1416, doi:10.1002/qj.854, 2011.
- Stickler, A., Grant, A. N., Ewen, T., Ross, T. F., Vose, R. S., Comeaux, J., Bessemoulin, P., Jylhä, K., Adam, W. K., Jeannet, P., Nagurny, A., Sterin, A. M., Allan, R., Compo, G. P., Griesser, T., and Brönnimann, S.: The comprehensive historical upper air network (CHUAN), *B. Am. Meteorol. Soc.*, 91, 741–751, doi:10.1175/2009BAMS2852.1, 2010.
- Stickler, A., Brönnimann, S., Jourdain, S., Roucaute, E., Sterin, A., Nikolaev, D., Valente, M. A., Wartenburger, R., Hersbach, H., Ramella-Pralungo, L., and Dee, D.: Description of the ERA-CLIM historical upper-air data, *Earth Syst. Sci. Data*, 6, 29–48, doi:10.5194/essd-6-29-2014, 2014.
- Thorne, P., Parker, D. E., Tett, S. F. B., Jones, P. D., McCarthy, M., Coleman, H., and Brohan, P.: Revisiting radiosonde upper-air temperatures from 1958 to 2002, *J. Geophys. Res.*, 110, D18105, doi:10.1029/2004JD005753, 2005.
- Tschudin, M. E. and Schroeder, S. R.: Time constant estimates for radiosonde temperature sensors, *J. Atmos. Ocean. Tech.*, 30, 40–56, doi:10.1175/JTECH-D-11-00181.1, 2013.
- Uppala, S. M., Källberg, P. W., Simmons, A. J., Andrae, U., da Costa Bechtold, V., Fiorino, M., Gibson, J. K., Haseler, J., Hernandez, A., Kelly, G. A., Li, X., Onogi, K., Saarinen, S., Sokka, N., Allan, R. P., Andersson, E., Arpe, K., Balmaseda, M. A., Beljaars, A. C. M., van de Berg, L., Bidlot, J., Bormann, N., Caires, S., Chevallier, F., Dethof, A., Dragosavac, M., Fisher, M., Fuentes, M., Hagemann, S., Hólm, E., Hoskins, B. J., Isaksen, I., Janssen, P. A. E. M., Jenne, R., McNally, A. P., Mahfouf, J. F., Morcrette, J. J., Rayner, N. A., Saunders, R. W., Simon, P., Sterl, A., Trenberth, K., Untch, A., Vasiljevic, D., Viterbo, P., and Woollen, J.: The ERA-40 Re-analysis, *Q. J. Roy. Meteor. Soc.*, 131, 2961–3012, 2005.
- Vautard, R., Cattiaux, J., Yiou, P., Thépaut, J. N., and Ciais, P.: Northern hemisphere atmospheric stilling partly attributed to an increase in surface roughness, *Nat. Geosci.*, 3, 756–761, 2010.

4 New estimates of tropical mean temperature trend profiles from zonal mean historical radiosonde and pilot balloon wind shear observations

This paper presents a direct, using radiosondes temperature profiles, and indirect, using wind PILOT balloon and radiosonde wind profiles, comparison of vertical temperature trends in the tropics [20N, 20S]. The vertical temperature trend is an important indicator of climate change. Due to the discrepancies between climate models and observations, this subject was and is still matter of scientific debate. In this study, particular care has been taken to determine the trends using two weakly dependent methods that are fed with the GRASP data and the adjustments coming from RAOBCORE2.0.

The goal is to reduce the existing gap between the temperature trends derived from climate models and the temperature and wind (employing the thermal wind relation) observations.

My contributions to this work was to prepare the gridded input data and to develop the *IDL* routines to handle the data, to calculate and visualize all the presented results. Leopold Haimberger supported my work offering some *IDL* routines, bringing smart ideas and with productive brainstorming sessions.

The paper text has been written mainly by Leopold Haimberger with my active contribution.

The paper has been submitted on October 3, 2014 to the Journal of Geophysical Research.

RamellaPralungo, L. and Haimberger, L., 2014:

New estimates of tropical mean temperature trend profiles from zonal mean historical radiosonde and pilot balloon wind shear observations.,

Journal of Geophysical Research,

Submitted

4 *New estimates of tropical mean temperature trend profiles from zonal mean historical
radiosonde and pilot balloon wind shear observations*

New estimates of tropical mean temperature trend profiles from zonal mean historical radiosonde and PILOT wind shear observations

1 New estimates of tropical mean temperature trend profiles from zonal mean
2 historical radiosonde and pilot balloon wind shear observations.

3 Lorenzo Ramella Pralungo¹ and Leopold Haimberger¹
4

5 submitted to Journal of Geophysical Research, October 3, 2014

¹DEPARTMENT OF METEOROLOGY AND GEOPHYSICS, UNIVERSITY OF VIENNA, ALTHANSTRASSE 14,
A-1090 VIENNA, AUSTRIA
Email address: lorenzo.ramella-pralungo@univie.ac.at

New estimates of tropical mean temperature trend profiles from zonal mean historical radiosonde and PILOT wind shear observations

2

Abstract

6 Estimation of global scale trends and low frequency variability directly from radiosonde
7 temperature records is challenging particularly in the Tropics due to large biases in the
8 earlier parts of the records that need to be adjusted. Zonal mean zonal winds and wind
9 shear observations are less prone to time varying biases. Together with a zonal mean refer-
10 ence temperature trend profile in the extra-tropics the wind data can be used to estimate
11 zonal mean temperature trends in the tropics using the thermal wind relationship. Earlier
12 estimates using this approach for the periods 1970-2005 and 1979-2005 showed strong trend
13 amplification in the tropical upper troposphere but also very large uncertainties because
14 the latitude for the reference profile was chosen very far north and due to a lack of data in
15 the tropics.

16 Both sources of uncertainties have been addressed by i) using reference temperature
17 profiles from homogenized radiosonde temperature data sets, ii) using the new Global his-
18 torical Radiosondes and Tracked Balloons Archive on standard pressure levels (GRASP) as
19 data source that includes not only radiosondes but also pilot balloons, iii) more accurate
20 vertical discretization and sampling of wind data. The new trend estimates are extended
21 back to 1958 and are considerably less noisy. Trend amplification factors between 1.3 and
22 2.6 were found in the intervals 1979-2005 and 1958-2010, respectively, when using wind
23 shear information. The best estimates for the warming maxima in the upper tropical tro-
24 posphere agree well with those directly from temperatures but tend to be located at higher
25 altitudes.

New estimates of tropical mean temperature trend profiles from zonal mean historical radiosonde and PILOT wind shear observations

3

26

1. INTRODUCTION

27 The vertical profile of upper air temperature trends in the tropics is still a matter
28 of debate. While climate models predict strong (factor 1.5-2.5) amplification of surface
29 temperature trends (as defined by Santer et al. 2005) in the tropics (20S-20N), those are
30 found in a lesser extent in reanalyses and satellite based data sets (Thorne et al. 2011;
31 Hartmann et al. 2013; Mitchell et al. 2013). In raw radiosonde data this amplification is
32 absent (factor < 1 or even negative). It has only been found after comprehensive homog-
33 enization efforts (e.g. Titchner et al. 2009; Randel et al. 2008; Haimberger et al. 2008;
34 Haimberger et al. 2012) and was still weaker than the amplification factors found in CMIP3
35 (Meehl et al. 2007) climate model runs. Only in the most recent of these comparisons
36 (Mitchell et al. 2013) involving radiosonde records adjusted with the Radiosonde Innova-
37 tion Composite Homogenization (RICH) method (Haimberger et al. 2012) and an ensemble
38 of CMIP5 model runs driven by assimilated surface temperatures found good agreement
39 between observed and modeled data up to levels of 200 hPa (12km).

40 At a time when the trend discrepancies were still large (Trenberth et al. 2007;
41 Douglass et al. 2007; Santer et al. 2008), it was demonstrated in a pioneering study by
42 Allen and Sherwood (2008) (henceforth abbreviated as AS08) that wind data can be used
43 as a zonal mean temperature proxy applying the thermal wind equation. They converted
44 zonal mean wind shear trends into temperature gradient trend and those could be compared
45 to trends from measured radiosonde temperature. Their approach is valuable because it
46 exploits a new and independent data source for estimating tropical temperature trends.
47 AS08 found very strong tropical temperature trends (maxima of 0.65 K/10a in the period
48 1970-2005, more than 0.4K/10a in the period 1979-2005) at very high levels between 150
49 and 200 hPa, although with large uncertainty bounds.

50 Their evaluations were restricted to the period 1970-2005 (mostly even 1979-2005) and
51 they used only wind speed data from radiosondes, not pilot balloons. However, there

New estimates of tropical mean temperature trend profiles from zonal mean historical radiosonde and PILOT wind shear observations

4

52 were quite many pilot balloon reports particularly in the Tropics, which could help re-
53 duce the large spatial sampling errors there. Thanks to inclusion of pilot balloons data
54 and also of some newly digitized records in the Global historical Radiosondes and tracked
55 balloons Archive on Standard Pressure levels (GRASP, Ramella-Pralungo et al. 2014;
56 Ramella-Pralungo and Haimberger 2014) a much more comprehensive upper air wind
57 archive is now available from the 1920s to 2013. It also contains homogeneity adjustments
58 for the wind data and it has daily resolution. This is a major improvement compared to
59 AS08, who had to assume that the radiosonde winds are unbiased and who used monthly
60 means as input data, who could potentially be affected by a sampling bias due to the fact
61 that balloons could often not be tracked to high pressure levels under high wind conditions.
62 Ramella-Pralungo and Haimberger (2014) have shown that this sampling bias is affecting
63 monthly means at pressure levels above 500 hPa mostly up to the late 1950s, before RADAR
64 tracking became standard. Especially these measurements are, however, crucial to sample
65 the subtropical jet and its associated vertical wind shear.

66 The above progress appears significant enough to lead to more accurate results com-
67 pared to AS08. As will be outlined below, also the numerical calculation method could be
68 improved by employing second order finite differences in the vertical. Our ambition is to
69 demonstrate that these new trend evaluations with wind data, which do not rely strongly
70 on temperature homogeneity adjustments, are consistent with trends solely from homogene-
71 ity adjusted temperature records such as the RAOBCORE and RICH (Haimberger 2007;
72 Haimberger et al. 2008; Haimberger et al. 2012) data sets.

73 After a short discussion of the input data in section 2, the vertical and horizontal
74 discretization of the thermal wind relationship are described in section 3. In results section
75 4 the various sources of uncertainty are assessed and temperature trend estimates for the
76 periods 1979-2005 and 1958-2010 are presented. Conclusions are drawn in sections 5.

New estimates of tropical mean temperature trend profiles from zonal mean historical radiosonde and PILOT wind shear observations

5

77

2. INPUT DATA

78 The zonal wind data are taken from the GRASP archive
 79 (Ramella-Pralungo et al. 2014) including homogeneity adjustments for wind as de-
 80 scribed in (Ramella-Pralungo and Haimberger 2014). It contains zonal wind from
 81 radiosondes as well as pilot balloons on 16 pressure levels with daily resolution at 00GMT
 82 and 12GMT, respectively and reaches from 1905 up to 2013.

83 In addition, the RAOBCORE and RICH homogenized radiosonde data sets have been
 84 used for calculation of the necessary extra-tropical reference trend profile and for comparison
 85 purposes. They reach back to 1958. A sizable number of radiosonde data back to the
 86 late 1940s exists (Stickler et al. 2014), at least in the extra-tropics, but those are yet to
 87 be homogenized. Fig. 1 shows the distribution of stations which contain enough wind and
 88 temperature data to be useful for the following analysis. In the Tropics there are noticeably
 89 more wind data than temperature data since pilot balloons have been used extensively over
 90 South America, Africa and Australia.

91 The NOAA 20th Century Reanalysis (NOAA-20CR, Compo et al. 2011) has been used
 92 implicitly by Ramella-Pralungo and Haimberger (2014) as reference for wind homogeniza-
 93 tion. In addition it is used here for estimating sampling and discretization errors when
 94 calculating zonal mean temperature trends from vertical wind shear trends. For this pur-
 95 pose we use the standard analysis data on a 2 degree grid on 20 pressure levels which are
 96 then aggregated to $10 \times 10^\circ$ box values to match the resolution of the gridded radiosonde
 97 and pilot balloon data.

98

3. METHOD

99 The zonal mean temperature trends at some latitude ϕ can be calculated by meridional
 100 integration of the well known thermal wind relation:

$$(1) \quad T(\phi, p, t) = T(\phi_o, p, t) + \int_{\phi_o}^{\phi} \frac{af(\phi')}{R} \frac{\partial u(\phi', p, t)}{\partial \log p} d\phi'$$

New estimates of tropical mean temperature trend profiles from zonal mean historical radiosonde and PILOT wind shear observations

6

101 The temperature trend profile must be known only at some reference latitude ϕ_o . The
 102 symbol a is Earth's radius, R is the specific gas constant of dry air, f is the Coriolis
 103 parameter, p is pressure, T is zonal mean temperature, u is zonal mean zonal wind speed.

104 In order to evaluate this integral, however, several specifications have to be made that
 105 affect the uncertainty of the results. The most obvious choice to be made is the reference
 106 latitude ϕ_o . It should be one where the temperature trend derived directly from temperature
 107 is reliable. In general this is the case in the northern mid-latitudes. We chose 45°N, but
 108 experimented also with 35°N which is closer to the equator but less well covered with data.

109 The choice of temporal and spatial resolution is a compromise between numerical ac-
 110 curacy and data availability. Following Thorne et al. (2005) and several others, we chose
 111 10° as spatial resolution, resulting in 18x36 grid boxes. The vertical resolution is inevitably
 112 non-equidistant, since the standard pressure levels are equidistant neither in pressure nor
 113 in log-pressure. The temporal resolution of the gridded data is chosen to be monthly.

114 The wind records themselves are homogenized and the filling procedure as described
 115 in Ramella-Pralungo and Haimberger (2014) has been applied (affecting mostly pre-1960
 116 data) to avoid a negative wind speed sampling bias. Scaled NOAA-20CR winds have been
 117 substituted for missing values if more than 15 valid values per month are available per
 118 pressure level. If less valid values were available no monthly values were calculated. This
 119 strategy allowed maximum backwards extension of the global records. In order to be sure
 120 that no spurious trend had been introduced, we compared the results to those without
 121 filling, just to see how much uncertainty is incurred by the temporal sampling problem. At
 122 least for the periods shown later (1958-2010, 1979-2005) the effect is negligible.

123 **3.1. Averaging and discretization.** When a record has enough values in a particular
 124 month at either 00GMT or 12GMT, its monthly mean is combined with values from other
 125 stations within a grid box to yield a grid box average. One valid monthly value within
 126 a grid box either at 00GMT or 12GMT is already deemed sufficient to define a grid box
 127 average. This rather liberal data policy helps to find enough grid box means at low latitudes.

New estimates of tropical mean temperature trend profiles from zonal mean historical radiosonde and PILOT wind shear observations

7

128 Further there is no evidence of a diurnal cycle of wind speed or wind speed errors at higher
129 altitudes (Ramella-Pralungo and Haimberger 2014). Two grid box values either at 00GMT
130 or 12GMT (out of 72 possible) have been required to define a valid zonal mean. It is
131 therefore necessary to sub-sample data sets on a full grid to the grid boxes where station
132 data are available in order to ensure comparability between those (model generated or
133 assimilated) data and the observation data (Free and Seidel 2005; McCarthy 2008). Fig. 1
134 indicates that especially in the tropics and in large parts of the southern hemisphere there
135 are many grid boxes with only one station that has enough data within the chosen time
136 period.

137 Since data availability allows only coarse spatial resolution, the discretization is of some
138 importance to avoid large errors. After zonal averaging, we have functions of ϕ and $\log p$,
139 which need to be discretized. In meridional direction we use second order centered differ-
140 encing with T and $\partial u / \partial \log p$ given at 85, 75, ... - 85 degrees N.

141 In vertical direction we use second order differencing for non-equidistant grid points in
142 $\log p$, as described e.g. by Sundqvist and Veronis (1970):

$$(2) \quad \left(\frac{\partial u}{\partial p} \right)_i \approx \frac{u_{i+1} - \left(\frac{h_i}{h_{i-1}} \right)^2 u_{i-1} - \left[1 - \left(\frac{h_i}{h_{i-1}} \right)^2 \right] u_i}{h_i \left(1 - \frac{h_i}{h_{i-1}} \right)}$$

143 where $h_i = \log(p_{i+1}/p_i)$. The discretization error is $h_i h_{i-1} / 6 \times \partial^3 u / \partial \log p^3$. Evaluation of
144 wind shear starts at 20 hPa and goes down to 1000 hPa where the surface wind is assumed
145 zero (non-slip condition) or equal to the 10m wind (slip condition) or equal to the 850
146 hPa wind ("free" slip condition). The lower boundary has some impact on near surface
147 temperature trends. The free slip condition is considered more consistent with the thermal
148 wind relationship, which holds only when friction can be neglected, and it also yielded
149 the best results for the lower troposphere. Using the non-slip condition led to unrealistic
150 temperature trends in the tropics near the surface.

New estimates of tropical mean temperature trend profiles from zonal mean historical radiosonde and PILOT wind shear observations

8

The impact of the discretization on accuracy can be seen by comparing a zonal mean temperature trend field taken from NOAA-20CR temperatures with trends gained by integrating dT/dy or $\partial U/\partial p$ meridionally in both directions starting at a reference latitude. Fig. 2a),b) shows differences between temperature trends calculated from the full NOAA-20CR grid, using $10^\circ \times 10^\circ$ grid boxes. One sees that the differences vanish at the reference latitude (45N, the vertical zero contour). In general the differences are quite small, with the exception of Antarctica. Overall the trend differences are mostly below 0.05K/decade which is smaller than the differences due to the coarse spatial sampling shown in panel c). The vertical discretization of $\partial U/\partial p$ is thus considered accurate enough for trend calculation.

Panels c),d) show that the sub-sampling required by the location of the radiosondes has a stronger effect of trends than the calculation method. Yet the combined effect of sub-sampling and coarse vertical and meridional discretization rarely exceeds 0.1K/10a between 45N and 30S, especially in panel d). However one must expect that the pattern shown is projected onto the trend estimates using vertical wind shear, i.e. that trends are underestimated in the lower troposphere but overestimated around 150 hPa.

3.2. Choice of the reference trend profile. The successful application of the approach taken in this paper depends largely on the quality of the temperature trend profile at the reference latitude. Errors in the profiles there propagate directly into errors in the tropical trend profiles. The error when sampling the zonal mean is best avoided at latitudes between 30N and 60N. Thus we made tests starting the integration with zonal mean temperature trends centered at 35N or 45N. Whereas 45N is best in terms of data availability, 35N has the advantage of a shorter integration path into the tropics.

Fig. 3 shows that the unadjusted extra-tropical temperature trends are about 0.1K/10a more positive than the unadjusted trends for both considered periods. The effect of homogenization is much smaller than found in the tropics e.g. in (Haimberger et al. 2008) where the homogenization increases the trends in the tropical upper troposphere and stratosphere by up to 0.5K/decade during some periods, particularly 1979-2005. In the extra-tropics

New estimates of tropical mean temperature trend profiles from zonal mean historical radiosonde and PILOT wind shear observations

9

178 there is also a relatively high level of consensus regarding the effect of the homogenization
179 and good agreement with trend estimates from MSU (Haimberger et al. 2012).

180 **3.3. Zonal mean wind trends.** The vertical wind shear trends determine how much
181 stronger the warming in the tropics can be compared to the extra-tropics. Fig. 4 depicts
182 clearly positive $\partial U/\partial p$ trends estimated from the radiosonde and pilot balloon data in
183 the upper troposphere and lower stratosphere between 45N and the equator during both
184 investigated time periods, but particularly in 1979-2005. In the lower troposphere the wind
185 shear trends are neutral or negative, indicating that the tropical temperature trends are
186 smaller than in the extra-tropics. This is consistent with trends from direct temperature
187 measurements.

188 In the southern hemisphere, there are very strong wind shear trends, consistent
189 with the strong cooling of the southern polar cap, partly caused by Ozone depletion
190 (Ramaswamy et al. 1996). Particularly for 1958-2010, there are large sampling problems
191 south of 50S. Therefore we do not recommend interpretation of trends from wind shear
192 south of 30S.

193 The wind shear integration method has some potential even before 1958. Fig. 5 shows
194 zonal mean temperature and zonal wind trends for the period 1950-1970. The plots indicate
195 that it is feasible to define a reference temperature trend profile in the extra-tropics since
196 there are valid trend estimates at these latitudes. There is only the problem that the
197 temperature data in this early period are not yet adequately homogenized. The zonal wind
198 trends in panel b) indicate that there are enough wind data to integrate southward to the
199 Equator. The main problem is that pilot balloon ascents traced by theodolites often do not
200 reach the upper troposphere in the tropics. We expect that the picture will improve further
201 in the next two years once the recently digitized upper air data from former French colonies
202 become available (Jourdain and Roucaute 2013) which have been digitized but have yet to
203 be assimilated.

New estimates of tropical mean temperature trend profiles from zonal mean historical radiosonde and PILOT wind shear observations

10

204

4. RESULTS

205 In this section we assess the uncertainty of linear temperature trends. Fig. 6 gives an
206 overview of temperature trends calculated from different data sources in the period 1979-
207 2005. This time interval was chosen for comparison with the results of AS08. First of all,
208 one sees that much smaller regions had to be masked out than in AS08 because of the
209 improved data coverage. The fields are spatially quite smooth except in the South Polar
210 region. Panel a) shows trends using a RAOBCORE-adjusted temperature profile at 45N
211 and wind shear from adjusted winds. Panel b) shows the same quantity except that a
212 RICH-adjusted profile was used at 45N. Both panels show a distinct warming maximum in
213 the tropical upper troposphere exceeding 0.3K/10a, with a somewhat stronger maximum
214 when using the RAOBCORE-adjusted reference profile. It is interesting to compare this
215 to zonal means inferred directly from unadjusted and adjusted radiosonde temperatures.
216 As discussed e.g. in Santer et al. (2005) the trend pattern from unadjusted temperatures
217 shows no warming maximum at all due to large biases exceeding 0.5K in upper tropospheric
218 temperature measurements in the 1980s and 1990s. Panel d) shows trends from RICH-
219 adjusted temperatures. A moderately strong upper tropospheric warming maximum is
220 again visible.

221 Fig. 7 summarizes the global mean trends 1979-2005 estimated directly from unadjusted
222 radiosonde temperatures, from radiosonde temperatures adjusted with RAOBCORE (pan-
223 els a,c) and RICH(the ensemble mean,panels b,d)) as well as trends derived from vertical
224 wind shear and reference profiles at 35N (panels a,b) and 45N (panels c,d). The gray shaded
225 areas denote the $\pm 1.96\sigma$ uncertainties estimated as described in the appendix. These are
226 generally smaller for trends derived directly from temperatures and larger for those involv-
227 ing vertical wind shear integrations.

228 Apart from the unrealistic trends obtained directly from unadjusted temperature ob-
229 servations, there is reasonable agreement between trends calculated directly from adjusted

New estimates of tropical mean temperature trend profiles from zonal mean historical radiosonde and PILOT wind shear observations

11

230 temperatures and trends calculated with wind shear data, particular in the upper tropo-
231 sphere. When employing vertical wind shear, the warming trends are clearly dependent on
232 the temperature adjustment performed at the reference latitude, particularly if a reference
233 profile at 35N is used. Using unadjusted temperatures at 35N and vertical wind shear does
234 not yield an upper tropospheric warming maximum (see orange curves in panels a,b). The
235 situation changes when using 45N as reference profile. In this case employing vertical wind
236 shear always yields a warming maximum, even when unadjusted temperatures are used at
237 45N. The maxima from wind shear trends are located higher (ca. 200 hPa) than for tem-
238 perature (ca. 300 hPa). The reason might be either still too weak homogeneity adjustments
239 for radiosonde temperatures or exaggerated warming from wind shear derived trends due
240 to sub-sampling effects, as suggested by Fig. 2-d.

241 If a reference profile at 45N is used, the upper tropospheric trend maxima from wind
242 shear tend to be stronger and interestingly also the correspondence between trends derived
243 directly from adjusted temperature datasets and those from wind shear is improved. It
244 is also interesting to see that almost all trend profiles except those obtained directly from
245 RICH-adjusted temperatures, show relatively weak trends in the lower troposphere, albeit
246 with large spread.

247 The numbers given in the plot legends are amplification factors defined as:

$$\alpha = \frac{\max(dT/dt)|_{100-500hPa}}{(dT/dt)_{HadCRUT4_{med}}}$$

248 This measure is very sensitive and can only be calculated if the surface trend signal is signif-
249 icant (typically at least 0.1 K/decade), as is the case for the investigated periods 1979-2005
250 and 1958-2010. $(dT/dt)_{HadCRUT4_{med}}$ is the tropical belt mean surface trend of the me-
251 dian of the 100 HadCRUT4 surface temperature field realizations. $\max(dT/dt)|_{100-500hPa}$
252 is the maximum belt mean upper air temperature trend value occurring between the 100
253 and 500 hPa levels, respectively. The lower uncertainty bound is obtained by dividing
254 $\max(dT/dt - \sigma)|_{100-500hPa}$ through the upper quartile $(dT/dt)_{HadCRUT4_{75}}$, the upper uncer-
255 tainty bound is obtained by dividing $\max(dT/dt + \sigma)|_{100-500hPa}$ through $(dT/dt)_{HadCRUT4_{25}}$.

New estimates of tropical mean temperature trend profiles from zonal mean historical radiosonde and PILOT wind shear observations

12

256 σ is the standard deviation of the trend estimates, visible as half of the shaded area around
 257 each profile. The factor α is found to be larger than one in most cases, with reasonable
 258 uncertainty bounds, for all except the unadjusted temperature trends. Amplification fac-
 259 tors involving wind shear and an adjusted temperature trend profile have values between
 260 1.1 and 2.3, which is lower than predicted by most of the CMIP3 climate model ensemble
 261 (Santer et al. 2008) but fits quite well into the range of amplification factors of the most
 262 advanced CMIP5 simulations (1.7-2.4, Mitchell et al. 2013).

263 Fig. 8 extends the trend evaluations from temperature and wind shear data to the pe-
 264 riod 1958-2010. For this long time interval, the existence of a warming maximum is more
 265 robust, particularly when using 45N as reference latitude. Warming maxima are found even
 266 when the trends are calculated from an unadjusted temperature profile at 45N plus wind
 267 shear. The amplification factors are also slightly higher, more often reaching a value above
 268 2.0 for this period. As such they agree well with the most advanced CMIP5 predictions
 269 (Mitchell et al. 2013). The estimated amplification factors are also in accord with measure-
 270 ments from satellite data Po-Chedley and Fu (2012) and reanalyses (Simmons et al. 2014).

271 While these new results estimated from wind shear are not different from those obtained
 272 directly from temperatures, it is reassuring to see that they can be estimated with much
 273 smaller uncertainty bounds than before and that they independently support the weak
 274 tropospheric trend amplification observed in homogenized pure temperature data sets.

275 5. CONCLUSIONS

276 Despite considerable progress in developing a stable and accurate global monitoring
 277 system, estimating long term trends of basic essential climate variables is still challenging.
 278 Building upon a much more comprehensive temperature and wind data set than previ-
 279 ously available, the amplification of surface low frequency variability in the tropical upper
 280 troposphere could be estimated with smaller uncertainties. Using HadCRUT4 surface tem-
 281 peratures, RAOBCORE v1.5 and RICH adjusted extra-tropical temperature trends and
 282 GRASP homogenized zonal wind data, we found amplification factors in the range 1.2-2.5

New estimates of tropical mean temperature trend profiles from zonal mean historical radiosonde and PILOT wind shear observations

13

283 the maximum being at the 200 hPa level. These factors are smaller than the best estimates
284 found by Allen and Sherwood (2008) (amplification factor 4).

285 The amplification factors derived from a reference trend profile plus vertical wind
286 shear are now in better agreement with those solely from temperature, if adjusted tem-
287 perature data are used. Considering also the estimates from recent satellite data eval-
288 uations, reanalyses and climate models (Po-Chedley and Fu 2012; Simmons et al. 2014;
289 Mitchell et al. 2013) we conclude that the tropical temperature trend discrepancies between
290 these data sets have been largely reconciled, at least up to 200 hPa. In the stratosphere
291 there are still significant differences.

292 Backwards extension of the present evaluations to the early 1950s seems feasible given
293 the amount of new but not yet homogenized upper air data particularly in tropical regions
294 (Stickler et al. 2014).

ACKNOWLEDGMENTS

296 This work has been funded by projects P25260-N29 of the Austrian Fonds zur
297 Förderung der wissenschaftlichen Forschung (FWF), as well as by the EU 7th Framework
298 Programme collaborative project ERA-CLIM (Grant No. 265229).

299 The input data used in this study can be downloaded
300 from <http://doi.pangaea.de/10.1594/PANGAEA.823617>(GRASP),
301 <http://www.univie.ac.at/theoret-met/research/raobcore>
302 (RAOBCORE/RICH), <http://data.ecmwf.int> (ERA-Interim, used for homogenization
303 by RAOBCORE/RICH), http://www.esrl.noaa.gov/psd/data/gridded/data.20thC_ReanV2.html
304 (NOAA 20th century reanalysis).

305 The authors have complied with AGU's Data Policy by providing information on how to
306 obtain the data used to produce the results of this paper (whether the data is available for
307 free or for purchase).

New estimates of tropical mean temperature trend profiles from zonal mean historical radiosonde and PILOT wind shear observations

14

APPENDIX A. UNCERTAINTIES ESTIMATION

For the trend uncertainty estimation in this paper we consider three types of uncertainty: Sampling uncertainty, parametric uncertainty and structural uncertainty (Thorne et al. 2005).

One is sampling uncertainty, which can be estimated directly from the available time series. We do this assuming normal distribution and taking autocorrelation into account. Both temperature and wind shear are approximately normal distributed. Under these assumptions the standard confidence interval of the slope as calculated by many statistical software packages can be estimated as

$$(3) \quad \sigma_{SL} = \sqrt{\sum_1^n (y_i - \bar{y}_i)^2 / (n - 2)} / \sqrt{\sum_1^n (t_i - \bar{t})^2}$$

where $\bar{y}_i = \beta_0 + \beta_1 t_i$ and \bar{t} are the respective means of time and the dependent variable (e.g. U , T , $\partial U / \partial p$). In this text we use monthly time series for trend estimation, thus n is the number of months of the considered interval. If the residuals of the trend estimate are autocorrelated, the sample size n has to be replaced by the *effective* sample size n_{eff} . It can be in most cases well approximated by $n_{eff} = n(1 - \alpha) / (1 + \alpha)$, where α is the estimated lag 1 autocorrelation of monthly mean series.

This estimate can be given for every $10^\circ \times 10^\circ$ grid box. The zonal and belt mean sampling error standard deviations can be estimated by adequately summing the variances of the slopes in individual grid boxes, assuming that the sampling errors in the individual grid boxes are uncorrelated. This yields belt mean sampling errors at each pressure level.

It should be noted that the belt mean errors of $\partial U / \partial p$ trends cannot be estimated from the errors of the U trends, since there is strong compensation of errors when calculating the gradients. Instead, one has to calculate $\partial U / \partial p$ first and then estimate the sampling error from the regression as above.

Besides the sampling error of the trend in a grid box, there are also the sampling errors when calculating the zonal means. These can be estimated by comparing zonal mean

New estimates of tropical mean temperature trend profiles from zonal mean historical radiosonde and PILOT wind shear observations

15

333 trends from reanalysis data sub-sampled to grid boxes with radiosondes and those with full
 334 coverage. This error is assumed independent of the time sampling error and is added to
 335 the total sampling error. In the plots the sampling error $\pm 1.96\sigma$ is visualized in Figs. 7-8
 336 as gray shading.

337 Alternatively one could also calculate zonal mean T and $\partial U/\partial p$ time series first and
 338 then calculate the trends from those.

339 In addition to that, one has to deal with parametric uncertainties, which arise from
 340 uncertainties in the settings of the adjustment method, e.g. thresholds used for break
 341 detection, minimum length of the averaging intervals, etc. Those can be estimated by
 342 varying the parameters within reasonable bounds. On top of that there are structural
 343 uncertainties. These arise from the choice of the adjustment method, the choice of the
 344 reference and the breaks in the measurement biases to be adjusted. These can be tackled
 345 by using different adjustment methods and different references. The individual realizations
 346 gained by the different methods are shown as individual lines with their respective sampling
 347 errors. For assessment of structural uncertainties, we used the RAOBCORE and RICH
 348 adjustment methods as well as the unadjusted temperature records. While RAOBCORE
 349 adjustments yield trends more similar to those obtained from ERA-Interim reanalysis data,
 350 RICH is more strongly based on the radiosonde archive. However, in RICH there are
 351 more choices to be made during the adjustment process. Therefore an ensemble of 32
 352 RICH ensembles has been generated by Haimberger et al. (2012). This is reflected by the
 353 larger uncertainty bounds around the best estimates for trends directly from RICH-adjusted
 354 temperature data but also around the best estimates from wind shear based trends that
 355 use RICH adjusted reference profiles (see Figs. 7,8 and table 1).

356 The temperature trends at the reference latitude are of particular importance when
 357 trends are calculated by integration of $\partial T/\partial \phi$ or $\partial U/\partial p$. The adjustment of the 45 degree
 358 profiles with RAOBCORE/RICH are essential for the final results. Without adjustments
 359 the warming maximum in the tropics cannot be reproduced. Sampling errors are minor at

New estimates of tropical mean temperature trend profiles from zonal mean historical radiosonde and PILOT wind shear observations

16

References

this latitude since there are plenty radiosondes over the US and Eurasia. We calculate the trend uncertainties at these latitudes from the sampling errors of the 45N time series for RAOBCORE. For RICH we have the ensemble of realizations whose spread is considered independent of the sampling error and is therefore added to the sampling uncertainty.

Overall we find uncertainties on the order of ± 0.1 K/10a in the troposphere and of ± 0.2 K/10a in the stratosphere. Exceptions are the southern extra-tropics where we get excessive errors south of 50S when using wind shear data.

REFERENCES

- Allen, R.J., and S.C. Sherwood, 2008: Warming maximum in the tropical upper troposphere deduced from thermal winds. *Nature Geoscience*, **1**, 399–403.
- Compo, G.P., J.S. Whitaker, P.D. Sardeshmukh, N. Matsui, R.J. Allan, X. Yin, B.E. Gleason, R.S. Vose, G. Rutledge, P. Bessemoulin, S. Brönnimann, M. Brunet, R.I. Crouthamel, A.N. Grant, P.Y. Groisman, P.D. Jones, M.C. Kruk, A.C. Kruger, G.J. Marshall, M. Maugeri, H.Y. Mok, Å. Nordli, T.F. Ross, R.M. Trigo, X.L. Wang, S.D. Woodruff, and S.J. Worley, 2011: The twentieth century reanalysis project. *Quart. J. Roy. Meteor. Soc.*, **137A**, 1–28. DOI: 10.1002/qj.776.
- Douglass, D.H., J.R. Christy, B.D. Pearson, and S.F. Singer, 2007: A comparison of tropical temperature trends with model predictions. *Int. J. Climatol.*, **27**. doi: 10.1002/joc.1651.
- Free, M., and D.J. Seidel, 2005: Causes of differing temperature trends in radiosonde upper air data sets. *J. Geophys. Res.*, **110**, D07101.
- Haimberger, L., 2007: Bias correction of radiosonde observations. In: *Proceedings of the ECMWF/GEO Workshop on Atmospheric Re-analysis, 19-22 June 2006*, RG2 9AX Shinfield Park, Reading, U.K., pp. 123–126. ECMWF.

New estimates of tropical mean temperature trend profiles from zonal mean historical radiosonde and PILOT wind shear observations

References

17

- 384 Haimberger, L., C. Gruber, S. Sperka, and C. Tavalato, 2008: Homogenization of the
385 global radiosonde temperature and wind dataset using innovation statistics from re-
386 analyses. In: *Proceedings of the Third WCRP International Conference on Reanal-*
387 *yses*, pp. 5. [http://wcrp.ipsl.jussieu.fr/Workshops/Reanalysis2008/Documents/G4-](http://wcrp.ipsl.jussieu.fr/Workshops/Reanalysis2008/Documents/G4-411_ea.pdf)
388 [411_ea.pdf](http://wcrp.ipsl.jussieu.fr/Workshops/Reanalysis2008/Documents/G4-411_ea.pdf).
- 389 Haimberger, L., C. Tavalato, and S. Sperka, 2012: Homogenization of the global ra-
390 diosonde temperature dataset through combined comparison with reanalysis back-
391 ground series and neighboring stations. *J. Climate*, **25**, 8108–8131.
- 392 Hartmann, D.L., A.M.G. Klein Tank, and M. Rusticucci (Eds.), 2013: *IPCC 2013: The*
393 *Physical Science Basis*, Chapter Observations: Atmosphere and Surface, pp. 159–254.
394 IPCC.
- 395 Jourdain, S., and E. Roucaute, 2013: Historical upper air data rescue at météo-france
396 for era-clim. In: *EMS Annual Meeting Abstracts*, Volume 10, pp. EMS2013–97. EMS.
397 <http://meetingorganizer.copernicus.org/EMS2013/EMS2013-97.pdf>.
- 398 McCarthy, M.P., 2008: Spatial sampling requirements for monitoring upper-air climate
399 change with radiosondes. *Int. J. Climatol.*, **28**, 985–993. 10.1002/joc.1611.
- 400 Meehl, G.A., C. Covey, T. Delworth, M. Latif, B. McAvaney, J.F.B. Mitchell, R.J. Stouf-
401 fer, and K.E. Taylor, 2007: The WCRP CMIP3 multi-model dataset: A new era in
402 climate change research. *Bull. Amer. Meteorol. Soc.*, **88**, 1383–1394.
- 403 Mitchell, D.M., P.W. Thorne, P.A. Stott, and L.J. Gray, 2013: Revisiting the controver-
404 sial issue of tropical tropospheric temperature trends. , **40**, 1–6. doi:10.1002/grl.50465.
- 405 Po-Chedley, S., and Q. Fu, 2012: Discrepancies in tropical upper tropospheric warming
406 between atmospheric circulation models and satellites. *Environ. Res. Lett.*, **7**, 044018.
- 407 Ramaswamy, V., M.D. Schwarzkopf, and W.J. Randel, 1996: Fingerprint of ozone de-
408 pletion in the spatial and temporal pattern of recent lower-stratospheric cooling. *na-*
409 *ture*, **382**, 616–618.

New estimates of tropical mean temperature trend profiles from zonal mean historical radiosonde and PILOT wind shear observations

18

References

- 410 Ramella-Pralungo, L., and L. Haimberger, 2014: A global radiosonde and tracked balloon
411 archive on 16 pressure levels (grasp) back to 1905:
412 part ii: Homogeneity adjustments for pilot and radiosonde wind data. *ESSD*, **6**, 297–
413 316. doi:10.5194/essd-6-297-2014.
- 414 Ramella-Pralungo, L., L. Haimberger, A. Stickler, and S. Brönnimann, 2014: A global
415 radiosonde and tracked balloon archive on 16 pressure levels (grasp) back to 1905:
416 part i: Merging and interpolation to 00 and 12gmt. *ESSD*, **6**, 185–200.
417 doi:10.5194/essd-6-185-2014.
- 418 Randel, W.J., K.P. Shine, J. Austin, J. Barnett, C. Claud, N.P. Gillet, P. Keckhut,
419 U. Langematz, R. Lin, C. Long, C. Mears, A. Miller, J. Nash, D.J. Seidel, D.W.J.
420 Thompson, F. Wu, and S. Yoden, 2008: An update of observed stratospheric temper-
421 ature trends. *JGR*, **114**, D02107.
- 422 Santer, B., P. Thorne, L. Haimberger, K. Taylor, T. Wigley, J. Lanzante, S. Solomon,
423 M. Free, P. Gleckler, P. Jones, T. Karl, S. Klein, C. Mears, D. Nychka, G. Schmidt,
424 S. Sherwood, and F. Wentz, 2008: Consistency of modelled and observed temperature
425 trends in the tropical troposphere. *Int. J. Climatol.*, **28**. DOI: 10.1002/joc.1756.
- 426 Santer, B.D., T.M.L. Wigley, C. Mears, F.J. Wentz, S.A. Klein, D.J. Seidel, K.E. Taylor,
427 P.W. Thorne, M.F. Wehner, P.J. Geckler, J.S. Boyle, W.D. Collins, K.W. Dixon,
428 C. Doutriaux, M. Free, Q. Fu, J.E. Hansen, G.S. Jones, R. Ruedy, T.R. Karl, J.R.
429 Lanzante, G.A. Meehl, V. Ramaswamy, G. Russell, and G.A. Schmidt, 2005: Am-
430 plification of surface temperature trends and variability in the tropical atmosphere.
431 *Science*, **309**, 1551–1556.
- 432 Simmons, A.J., P. Poli, D.P. Dee, P. Berrisford, H. Hersbach, S. Kobayashi, and
433 C. Peubey, 2014: Estimating low-frequency variability and trends in atmospheric
434 temperature using ERA-Interim. *Quart. J. Roy. Meteor. Soc.*, **140**, 323–353. DOI:
435 10.1002/qj.2317.

New estimates of tropical mean temperature trend profiles from zonal mean historical radiosonde and PILOT wind shear observations

References

19

- 436 Stickler, A., S. Brönnimann, S. Jourdain, E. Roucaute, A. Sterin, D. Nikolaev,
437 M.A. Valente, R. Wartenburger, H. Hersbach, L. Ramella-Pralungo, and D. Dee,
438 2014: Description of the ERA-CLIM historical upper-air dataset. *ESSD*, **6**, 29–48.
439 doi:10.5194/essd-6-29-2014.
- 440 Sundqvist, H., and G. Veronis, 1970: A simple finite-difference grid with non-constant
441 intervals. *Tellus*, **22**, 26–31.
- 442 Thorne, P., D.E. Parker, S.F.B. Tett, P.D. Jones, M. McCarthy, H. Coleman, and P. Bro-
443 han, 2005: Revisiting radiosonde upper-air temperatures from 1958 to 2002. *J. Geo-
444 phys. Res.*, **110**, D18105.
- 445 Thorne, P.W., D.E. Parker, J.R. Christy, and C.A. Mears, 2005: Uncertainties in climate
446 trends: Lessons from upper-air temperature records. *Bull. Amer. Meteorol. Soc.*, **86**,
447 1437–1442.
- 448 Thorne, P.W., K.M. Willett, R.J. Allan, S. Bojinski, J.R. Christy, N. Fox, S. Gilbert,
449 I. Jolliffe, J.J. Kennedy, E. Kent, A. Klein Tank, J. Lawrimore, D.E. Parker,
450 N. Rayner, A. Simmons, L. Song, P.A. Stott, and B. Trewin, 2011: Guiding the
451 creation of a comprehensive surface temperature resource for 21st century climate
452 science. *Bull. Amer. Meteorol. Soc.*, **92**, ES40–ES47. doi:10.1175/2011BAMS3124.1.
- 453 Titchner, H., M. McCarthy, P.W. Thorne, S.F.B. Tett, L. Haimberger, and D.E. Parker,
454 2009: Critically reassessing tropospheric temperature trends from radiosondes using
455 complex validation experiments. *J. Climate*, **22**, 465–485.
- 456 Trenberth, K.E., P.D. Jones, P. Ambenje, R. Bojariu, D. Easterling, A. Klein-Tank,
457 D. Parker, F. Rahimzadeh, J.A. Renwick, M. Rusticucci, B. Soden, and P. Zhai,
458 2007: *Climate Change 2007: The Physical Science Basis*, Chapter 3 Observations:
459 Surface and Atmospheric Climate Change, pp. 235–336. Cambridge University Press,
460 Cambridge, United Kingdom and New York, NY, USA. Contribution of Working
461 Group I to the Fourth Assessment Report of the Intergovernmental Panel on Climate
462 Change.

New estimates of tropical mean temperature trend profiles from zonal mean historical radiosonde and PILOT wind shear observations

20

References

463

TABLES

1979-2005	CRUT4 [°C/10a]	UNADJ	RICH	RAOBCORE
T	0.15±0.02	0.05±0.05	0.21±0.06	0.26±0.06
35N,∂u/∂p		0.05±0.05	0.21±0.06	0.17±0.05
45N,∂u/∂p		0.21±0.07	0.34±0.07	0.22±0.07
1958-2010	CRUT4 [°C/10a]	UNADJ	RICH	RAOBCORE
T	0.11±0.02	0.06±0.03	0.22±0.03	0.21±0.03
35N,∂u/∂p		0.15±0.03	0.25±0.03	0.25±0.03
45N,∂u/∂p		0.16±0.04	0.29±0.04	0.27±0.04

Table 1: Tropical mean temperature trends for the intervals 1979-2005 and 1958-2010. Best estimates and uncertainties given for HadCRUT4 surface trends and maximum trends aloft (between 100 and 500 hPa). Trends using wind shear data have used the respective column temperature data set at reference latitude.

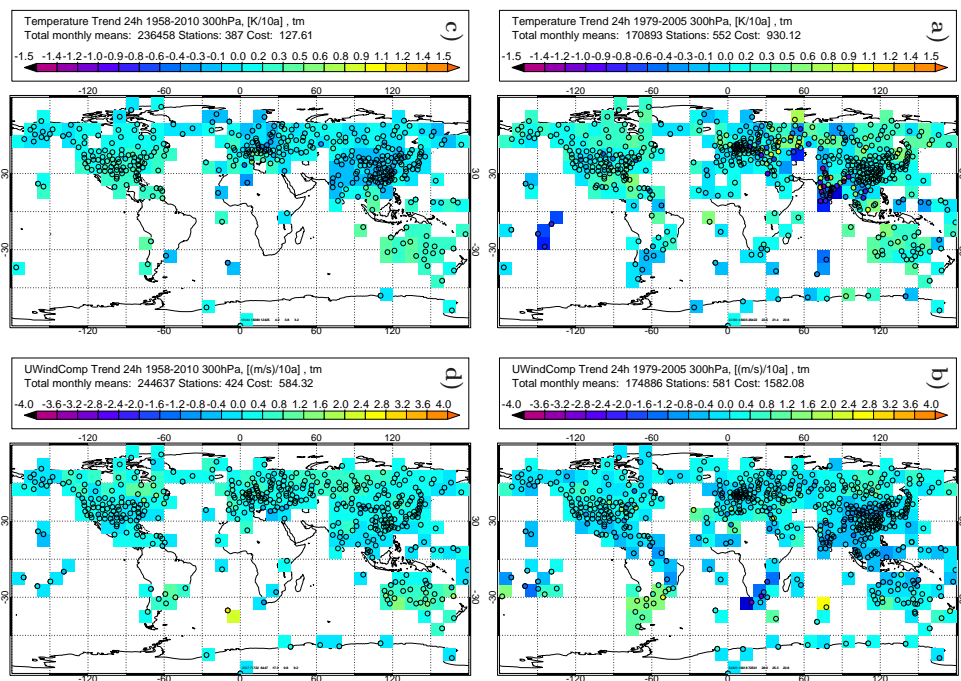
464

FIGURES

4 New estimates of tropical mean temperature trend profiles from zonal mean historical radiosonde and pilot balloon wind shear observations

New estimates of tropical mean temperature trend profiles from zonal mean historical radiosonde and PILOT wind shear observations

Figure 1: Observed and unadjusted T-trends (panels a, c) and U-wind trends (panels b, d) at individual stations (circles) and gridded to $10 \times 10^\circ$ boxes. Time intervals are 1979-2005 (panels a,b) and 1958-2010 (panels c,d), respectively. Only trends time series with less than 15% of missing data in the respective periods are included. Data filling according to Ramella-Pralungo and Haimberger (2014) data filling has been applied before calculating monthly means and trends.



References

21

New estimates of tropical mean temperature trend profiles from zonal mean historical radiosonde and PILOT wind shear observations

22

References

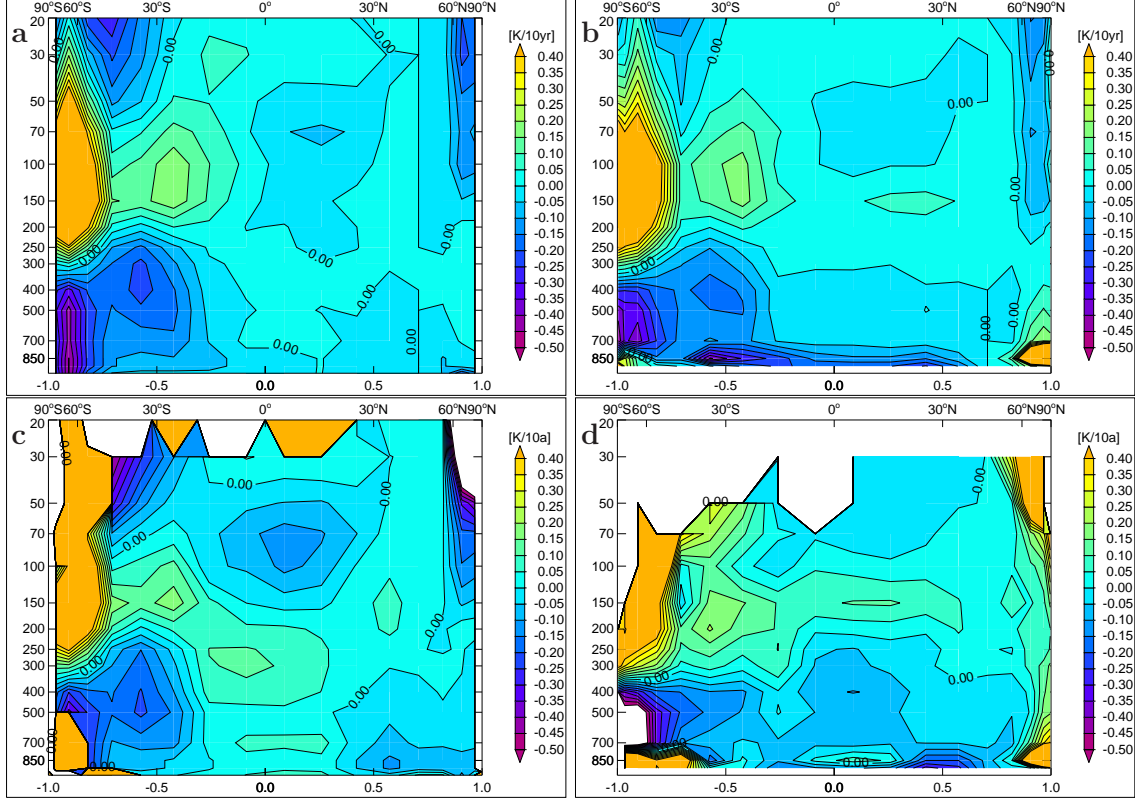


Figure 2: Zonal mean temperature trend reconstruction errors due to sub-sampling and due to meridional integration in the period 1979-2005. The trends from fully sampled NOAA-20CR temperatures are used as reference. a) shows error due to integration over $\partial T/\partial \phi$, using the trends at 45N as reference. b) shows errors due to integration over y and using $\partial U/\partial p$ instead of $\partial T/\partial \phi$. c) shows "error" due to sub-sampling temperatures to locations with radiosondes (see also Fig. 1-c), d) shows the combined error of y and using $\partial U/\partial p$ and sub-sampling to radiosonde station locations. Sampling errors may be larger in pre-1958 periods due to sparser network.

4 New estimates of tropical mean temperature trend profiles from zonal mean historical radiosonde and pilot balloon wind shear observations

New estimates of tropical mean temperature trend profiles from zonal mean historical radiosonde and PILOT wind shear observations

References

23

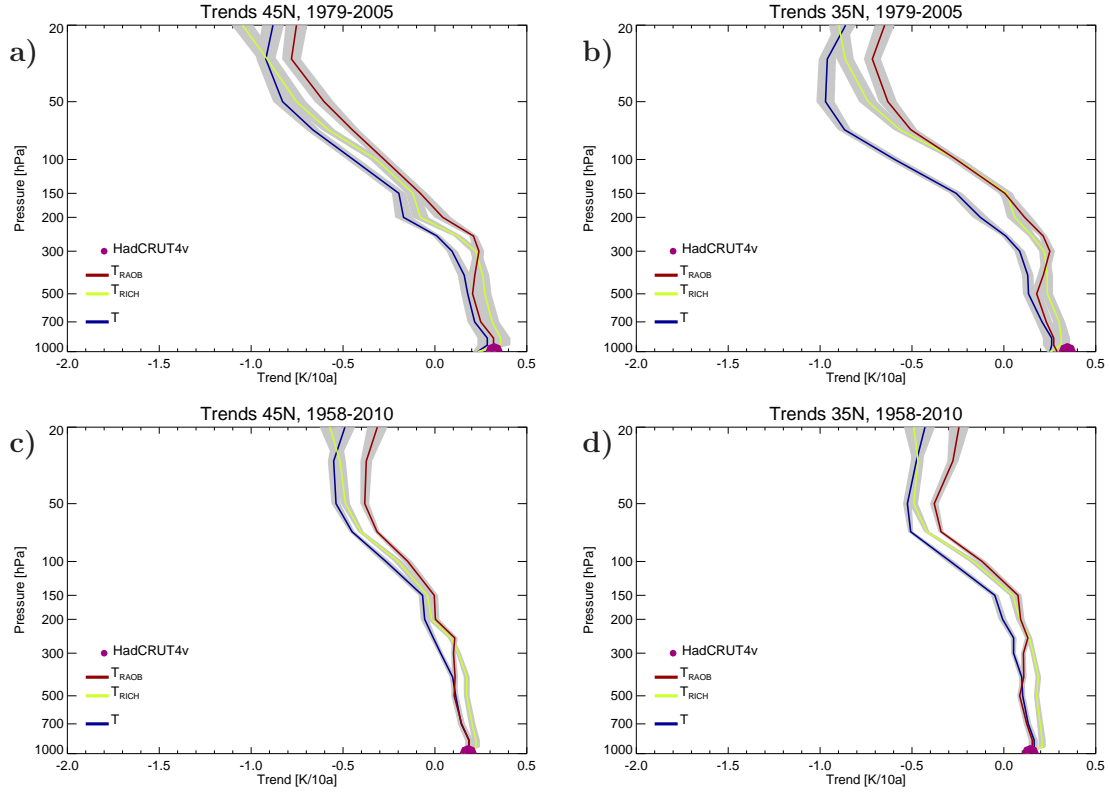


Figure 3: Zonal mean trends 1979-2005 (upper panels) and 1958-2010 (below panels) from unadjusted radiosonde temperatures, RAOBCORE adjusted temperatures and RICH adjusted temperatures at reference latitude belts a) $45\pm5^\circ\text{N}$ and b) $35\pm5^\circ\text{N}$. Surface trend values from HadCRUT4 at these latitude belts are given as well.

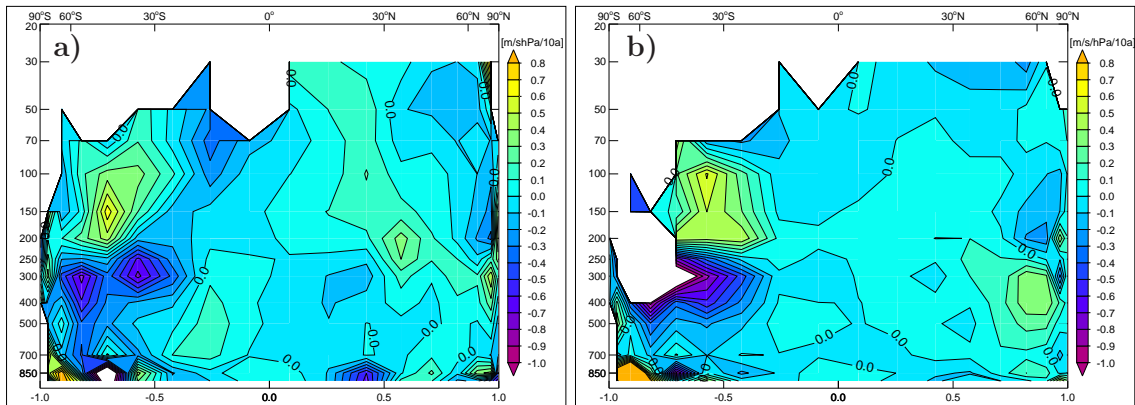


Figure 4: Zonal mean $\partial U \partial p$ trends for periods a) 1979-2005, b) 1958-2010.

New estimates of tropical mean temperature trend profiles from zonal mean historical radiosonde and PILOT wind shear observations

24

References

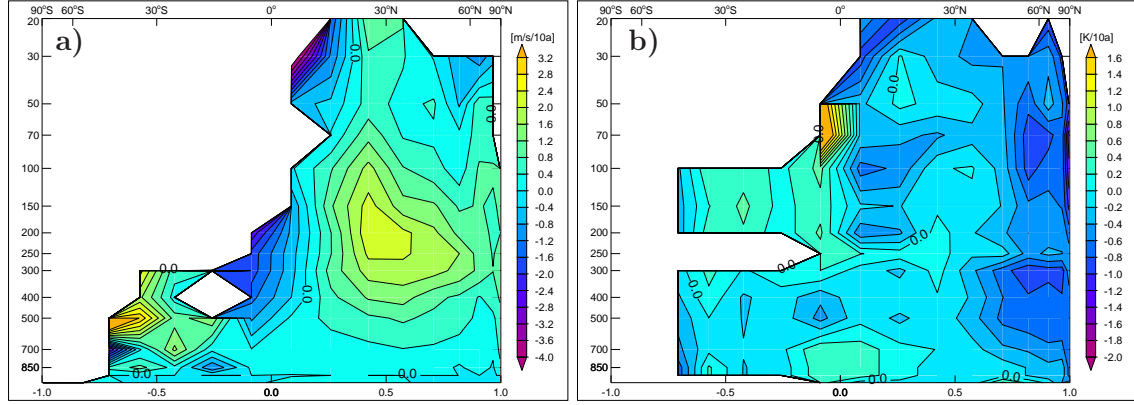


Figure 5: a) zonal mean U -trends for period 1950-1970 and b) zonal mean T -trends for 1950-1970, derived from stations with records longer than 16 years in this period. Values in at least 2 (out of 36) grid boxes are required in a 10° latitude belt to yield a valid zonal mean value.

4 New estimates of tropical mean temperature trend profiles from zonal mean historical radiosonde and pilot balloon wind shear observations

New estimates of tropical mean temperature trend profiles from zonal mean historical radiosonde and PILOT wind shear observations

References

25

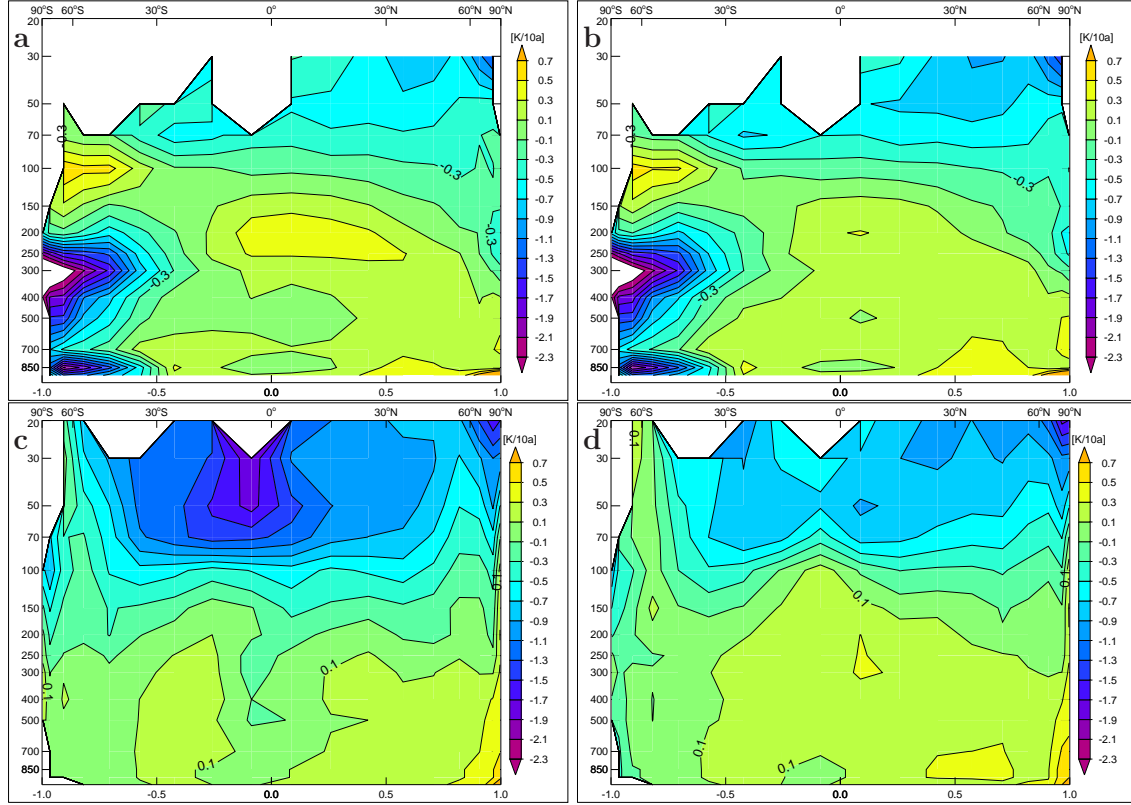


Figure 6: Temperature trend for the period 1979-2005 calculated, a) from integrating $\partial U / \partial p$ using a RAOBCORE 1.5 reference profile at 45N b) from integrating $\partial U / \partial p$ using a RICH 1.5 reference profile at 45N, c) directly from unadjusted temperatures, d) directly from RICH-adjusted temperatures.

New estimates of tropical mean temperature trend profiles from zonal mean historical radiosonde and PILOT wind shear observations

26

References

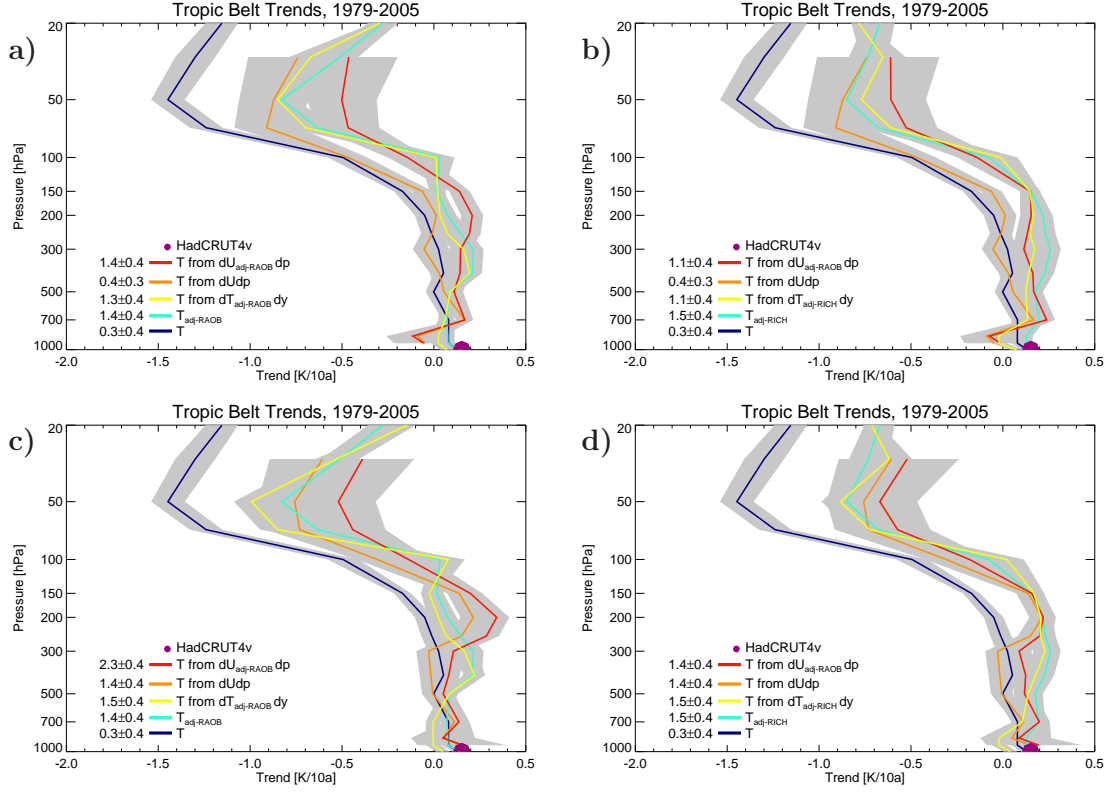


Figure 7: Global mean temperature trends in the tropical belt (20N-20S) inferred from zonal wind vertical wind shear for the period 1979-2005, a) integrating from 35N, using a RAOBCORE reference temperature trend profile for lines with index adj , b) as a) but with a RICH reference temperature profile, c) same as a) but integrating from 45N, d) same as b) but integrating from 45N. The numbers in the legends are trend amplification factors (max of tropospheric trend/surface trend).

4 New estimates of tropical mean temperature trend profiles from zonal mean historical radiosonde and pilot balloon wind shear observations

New estimates of tropical mean temperature trend profiles from zonal mean historical radiosonde and PILOT wind shear observations

References

27

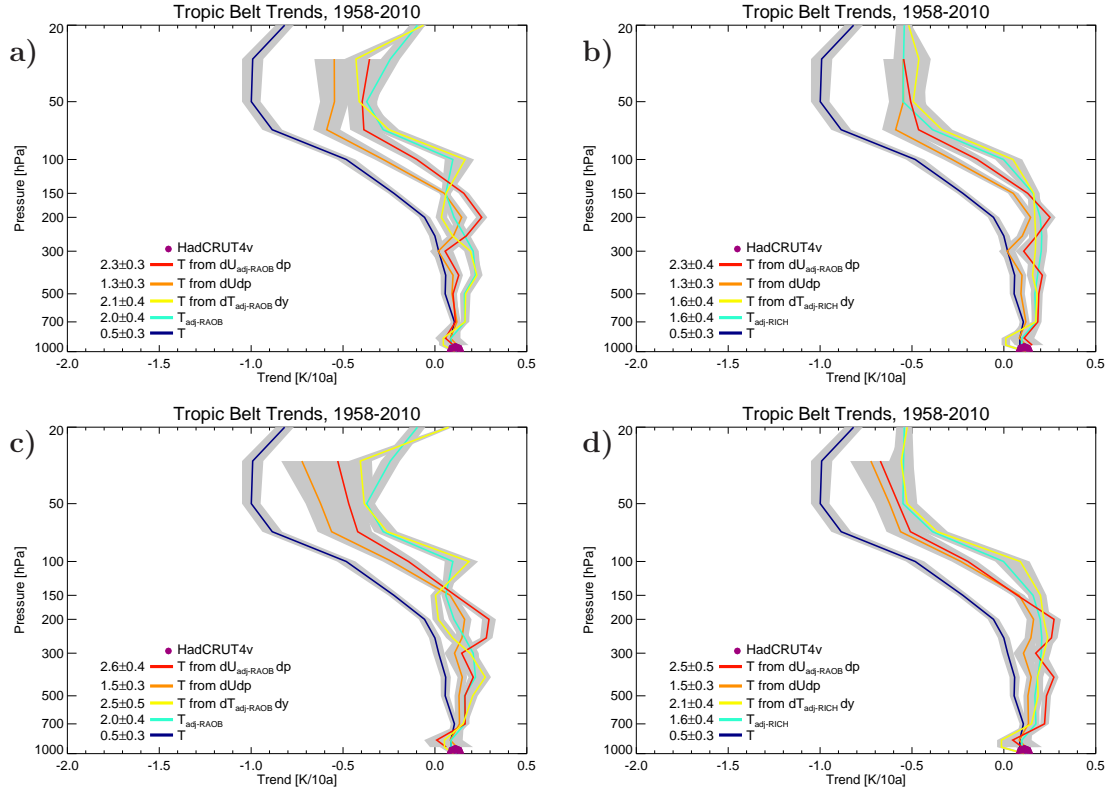


Figure 8: As Fig. 7 but for period 1958-2010.

5 Conclusions

In the introduction of this thesis two main research goals were highlighted:

- (i) To generate a comprehensive archive of the available digitalized upper air data sets which contains PILOT balloons and radiosondes coming from the existing fragmentary archives;
- (ii) To develop a unified automatic homogenization system that analyzes and adjusts upper air temperature and wind data-sets together, using reanalysis information as reference.

In addition, a further investigation became natural to test the value of the efforts made in (i) and (ii):

- (iii) To estimate the tropical mean temperature trend profile from radiosonde and PILOT wind shear observations and compare them with radiosonde temperature trend and the climate models results.

The point (i) was accomplished by collecting and merging all the available in situ upper air data so far digitalized. The involved input sources are the ERA-Interim and ERA-40 input data, IGRA, CHUAN and ECUD, which contain mainly radiosondes and PILOT balloons reports. Those catalogues are precious but, unfortunately they contain fragmented information, at pressure and altitude levels and, especially for the period prior to 1958, they report observations at a-synoptic time and the stations were not identified with a common and unique identifier. The classification and merging of the sparse data in long and homogeneous observed time series is an essential prerequisite for state of the art climatological studies.

As first step, all the stations have been identified via automatic cross checking (latitude/longitude, station name and identifier, if available) plus an additional manual check. After the identification procedure a WMO ID has been assigned to ca. 95% of the CHUAN/ECUD stations. To non WMO stations, a local ID above 100000 has been assigned. As second step, the raw data have been interpolated from altitude to pressure, from pressure to standard pressure levels, and from a-synoptic to synoptic time. As reference, the NOAA-20CR has been employed. To guarantee the maximum data reliability, a consistency check has been performed comparing the overlap between observed time series coming from different sources and comparing single series with the NOAA-20CR synthetic time series. Suspicious data (larger than 4 standard deviations σ) have been discarded. As a final step, the raw time series gained from input archives have been merged.

The outcome is the Global Radiosonde and tracked balloon Archive on 16 Standard Pressure levels (GRASP), presented to the scientific community in Ramella-Pralungo et al. (2014). The GRASP and the input archives have been organized in the user-friendly time series format and stored as NetCDF and ASCII files available in the PANGEA web portal.

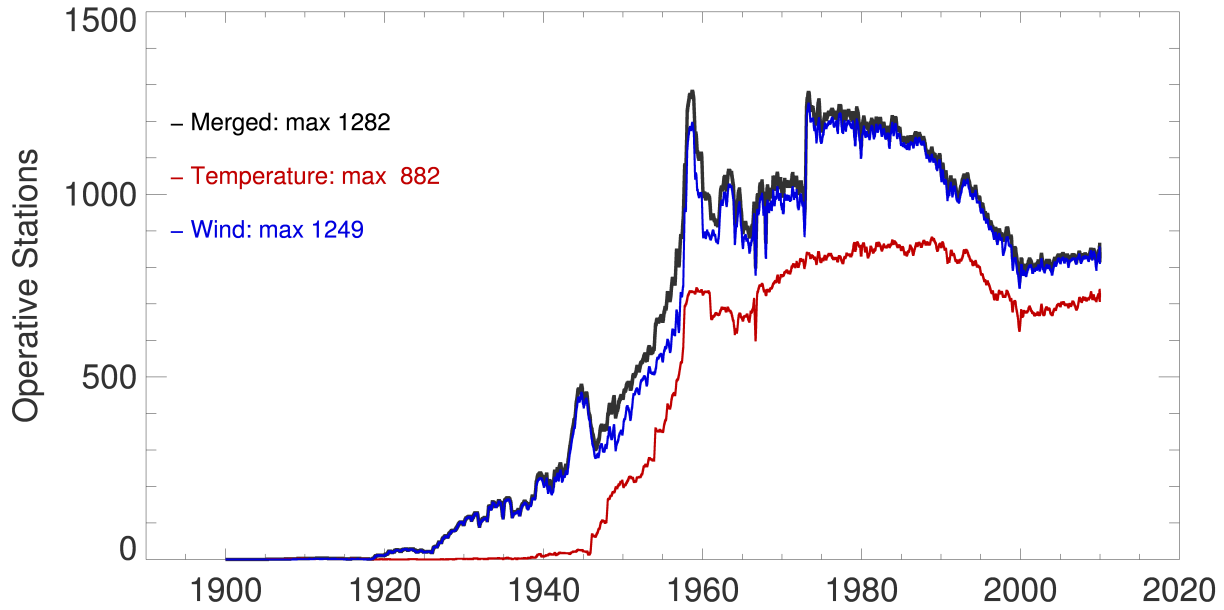


Figure 4: Temporal distributions of stations with at least 365 days of data, at the pressure levels of 850, 700 and 500hPa, contained in the GRASP archive. Only WMO stations have been used.

The GRASP contains 3217 stations with time series longer than 365 days (minimum number of days allowed to process the time series), where roughly 3020 stations have been recognized as WMO stations with a valid WMO ID. 1598 stations contain temperature information and 3152 wind data (stored as U and V components). The oldest temperature record starts the 4th April 1900 and belongs to the Lindenberg observatory (WMO ID 10393, CHUAN archive) but the observation practice was quite fragmentary and became continuous only in 1905. As consequence of the world wars, data are missing from 1918 till 1922 and again from 1939 till 1956. The longest continuous temperature record comes from Moscow with data available from 1938 onward. The longest and most complete wind time series (several stations) belong to the USA and they start from the 1920s up to days. Globally, the GRASP contains 37 wind records longer than 70 years (mainly located in USA) and 139 temperature records (mainly located over USA, Europe and some in Japan) longer than 60 years.

A relative abundance of wind reports (mainly from PILOT balloons) in respect to temperature report is visible in Fig.4 prior the 1940s when the wind measurements were already quite consolidated over the USA, Europe and Japan. The peak visible in Fig.4 for the wind reports around 1960s is the result of the IGY scientific campaigns in remote regions that unfortunately have been closed after few years.

The soundings spatial coverage, presented in Fig.5, is much more dense for wind than for temperature, especially over the tropics, which are key regions for climate change understanding. The northern hemisphere has a good coverage in comparison with the southern hemisphere, where only after the late 1970s a satisfactory coverage has been gained.

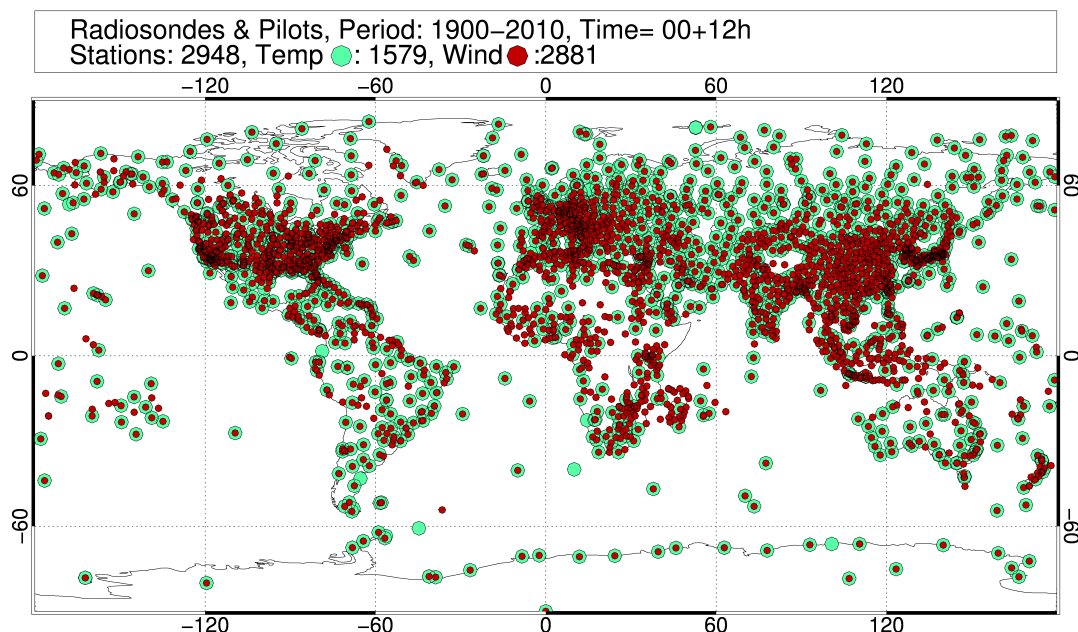


Figure 5: Spatial distributions of stations with at least 365 days of data, at the pressure levels of 850, 700 and 500hPa, contained in the GRASP archive for the period 1900-2010. Only WMO stations have been used.

The weak coverage in the southern hemisphere gives to the available stations a strategic importance: those are the only upper air observation sites available in the range of thousands of kilometers and they are necessarily employed for any kind of analysis or study. The availability of new and homogeneous series coming from the CHUAN and ECUD archives in the remote regions is crucial to improve this lack. Unfortunately, in the last two decades the number of pilots has been decreasing in remote regions. Still in our days the oceans lack soundings due to the difficulties in maintaining regular measurements.

The GRASP is the most comprehensive source of long time series at standard pressure levels and synoptic time. It represents a powerful base for further data processing steps, most notably homogenization and gridding, after which it should be a valuable input source for climatological studies.

In order to exploit the full potential of the data contained in the GRASP, it is essential to remove spurious biases and shifts from the records. This task is known as homogenization process. It refers to the research point (ii) announced in the introduction. The University of Vienna has a long and consolidated tradition in radiosonde homogenization processes: here was brought to the light the RAOBCORE (acronym for “RADiosonde OBServation CORrection using REanalyzes”, (Haimberger et al. (2008))). With RAOBCORE the first attempt to homogenize the whole temperature radiosonde network since the 1958 (first year available in ERA-40) was conducted. It relies on ERA-40 and ERA-Interim ECMWF Reanalysis background information, employing for the first time the so called innovations for break detection and correction.

The approach was particularly appreciated by the scientific community due to the daily resolution and the full automation of the method that, after properly set, can treat the whole radiosonde database.

Based on the RAOBCORE experience, few months later another attempt was carried out by Gruber and Haimberger (2008), aiming at wind radiosondes time series homogenization, using the same back ground reference.

Both works stress that the raw time series are often not homogeneous and that, in some cases, artificial shifts are strong enough to compromise the short (few years) and long (up to several decades) trends: before any climatological application, these artificial biases have to be removed or minimized. At the same time, they pointed out that the wind data should be more robust and relatively less break-affected than the temperature data.

The RAOBCORE method has the major disadvantage of using ECMWF ERA-40 and ERA-Interim reanalysis products for break detection and correction. Indeed, these reanalyzes products ingested themselves the radiosonde and pilot balloons as input data. In order to avoid this kind of potentially dangerous recursion, the RICH method was presented in (Haimberger et al. (2012)). It employs ECMWF reanalysis for break detection and information from neighboring stations for break adjustment. In this way, RICH is only slightly dependent on the background information, although it works efficiently only if neighboring stations are not too far and are not affected by the same kind of inhomogeneities. Unfortunately, these two weakness are quite common in the period prior 1960.

Based on the knowledge accumulated with the previous experiences, the new RAOBCORE 2.0 has been designed from scratch: a novel approach to treat temperature and wind data together using background information from the NOAA-20CR. This product is the pioneer of the new generation of surface-data-only reanalysis and it contains atmospheric fields from the 1871s onwards, thus allowing the analysis of all in situ upper air data sets (the oldest record in GRASP goes back to 1905, at the Lindenberg observatory, WMO ID 10393). The main advantages are the simultaneous treatments of wind and temperature data and the complete independency between analyzed data and the reference used; on the other hand, the NOAA-20CR is an ensemble mean and its analysis departures have higher variance than ERA-Interim and ERA-40. This combination drives to set a relative low threshold for break detection in the SNHT and accordingly a relatively high number of points may be flagged as potential breaks. In a second phase, based on the nature of the shift, a check based on the physics of the shifts is performed in order to adjust only the significant breaks.

The homogenization effort presented here is the most comprehensive attempt to reduce artificial biases in the temperature and wind, spanning the whole time series lifetime of the available time series stored in the GRASP.

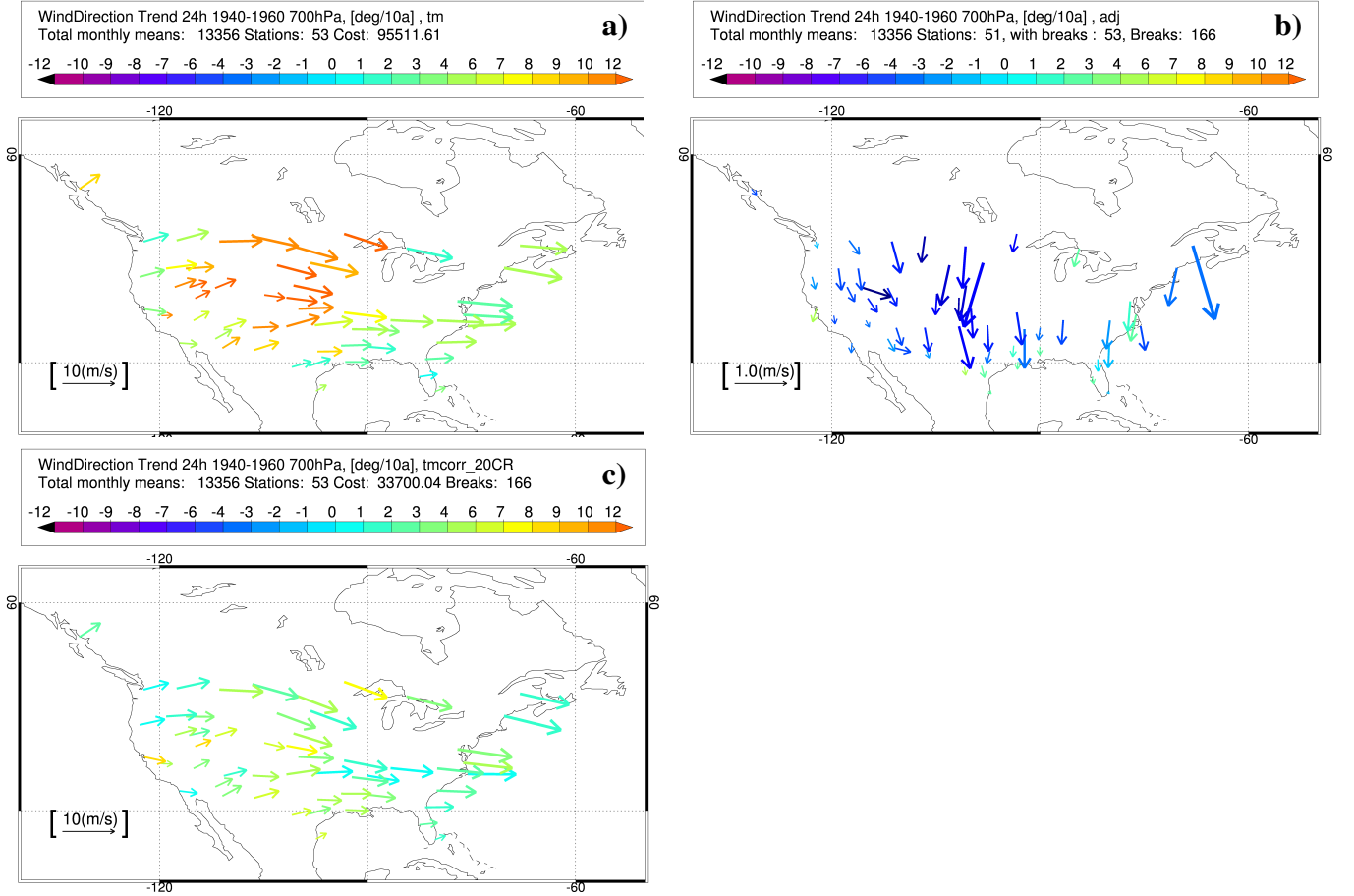


Figure 6: a) Raw wind direction trends at 700hPa at US stations (WMO numbers between 71000 and 73000) for the period 1940-1960 averaged over both 00 and 12 GMT (most stations reported twice daily). Arrows depict the mean wind speed and direction over this period. Arrow color indicates wind direction trend over the investigated period. Only stations with less than 1 year of missing values are shown. b) Wind direction adjustments ($\Delta \bar{U}$, $\Delta \bar{V}$) as estimated by RAOBCORE 2.0. The arrows show size and direction of the adjustments, the colors show how much the wind direction trend has been changed due to the adjustments. Note scale difference in arrow length compared to a) and c). 166 shifts have been adjusted in total. c) shows wind direction trends after adjustment. The cost function measuring spatial trend heterogeneity (see Haimberger et al. (2008, 2012)) has been reduced by a factor of 3 compared to a)

The homogenization of data prior to 1958 is particularly challenging and innovative since no precedent automatized and global homogenization efforts have been computed. A big regional inhomogeneity has been found over the USA for wind direction measurements: between 1935 and 1960, 118 stations shows anomalous wind direction trends. The situation is summarized in the Fig. 6(a) where the red arrows indicate stations with suspicious strong wind direction trends. The Fig. 7 reports the Bismark station (North Dakota, USA, WMO ID 072764) time series: in the upper panel (a), the innovation time series attests the direction break typically attributed to wrong north alignment. RAOBCORE2.0 detects the anomalous breaks in 1938 and 1948 (yellow dashed peaks in the SNHT blue curve, Fig. 7(a), right scale axes) and calculates the appropriate adjustments (Fig. 7(b)). Applying the gained adjustment the shift is reduced, as

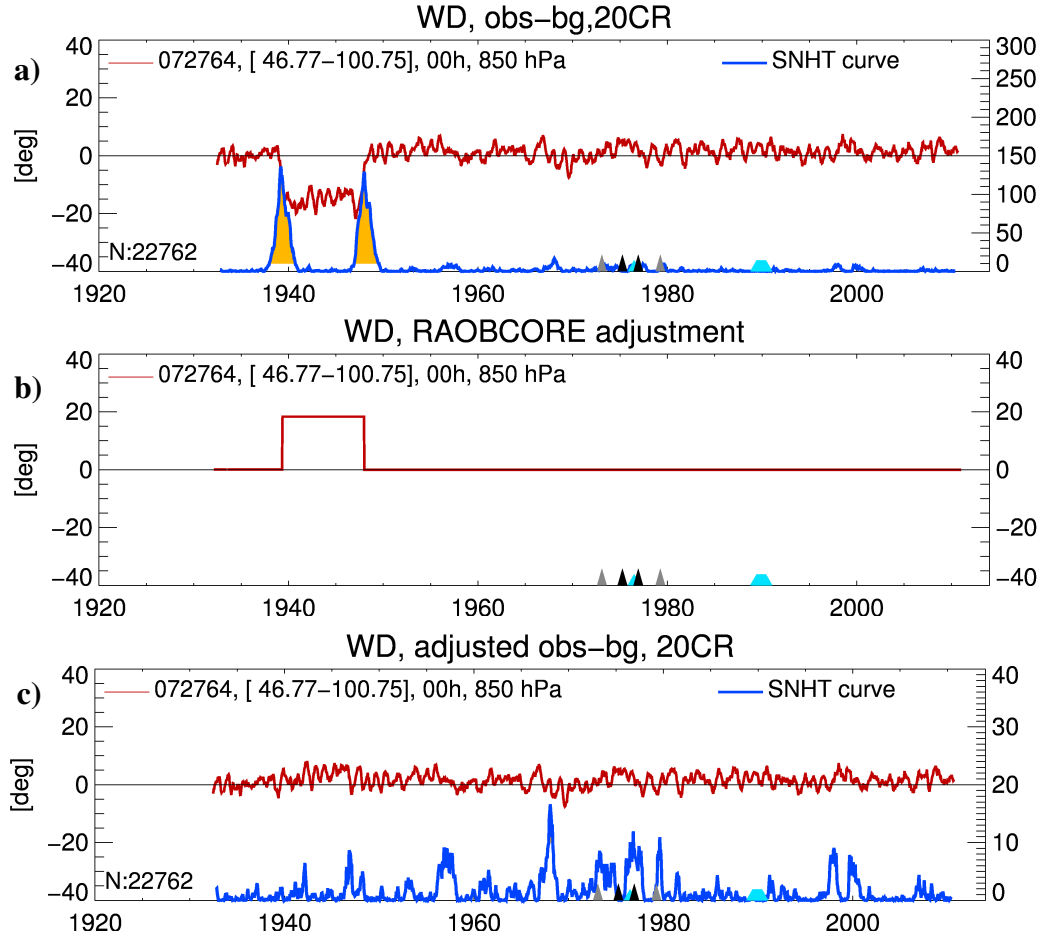


Figure 7: Upper row: a) wind direction analysis departure (Obs-NOAA-20CR) time series at time 00 GMT at 850hPa at station Bismarck (North Dakota, USA, WMO ID 072764, red curves). The blue curves (right axes) show the modified SNHT (applied as described in Ramella-Pralungo and Haimberger (2014a)) time series. Values above $CriticalValue = 10$ are statistically significant and are shaded. The small colored triangles on the x-axes indicate changes of the radiosonde type. Metadata from IGRA are indicated as light blue trapezoids or triangles. Middle row: b) wind direction adjustments calculated by RAOBCORE2.0 from analysis of the departure time series in upper row. Wind direction biases are constant in pressure and time between breakpoints. Lower row: c) analysis departures after adding the adjustments in middle row to upper row. Note smaller right axis scales compared to the upper panel, indicating better homogeneity.

visible in Fig7(c). All the stations in the Fig.6(a) are affected by similar breaks and the relative adjustments (see Fig.6(b)) are pointing southward, meaning that the shift is common through the region, even if with different amplitude. After the adjustments, a more smooth trend pattern is gained as shown in the Fig.6(c): the cost function measuring spatial trend heterogeneity has been reduced almost by a factor 3. On average the detected breaks in the period 1935-1960 have a symmetrical shape with mean over the 118 stations, ca. -12° and $+13^\circ$, respectively in 1938 and 1948. In more recent time sparse breaks are still detected and adjusted, especially over former Soviet Union, South America and South Africa.

Wind speed is more robust and it doesn't show any wide regional breaks at any time, but several severe inhomogeneities affecting sparse stations have been found confirming the results of Gruber and Haimberger (2008) in the overlapping period. The total number of adjusted breaks for wind direction and speed is comparable: 605 stations with roughly 1300 breaks for wind direction and ca. 1100 breaks over 566 stations for wind speed.

Albeit wind speed is less affected by breaks, it suffers from a sampling bias in the early period, especially before 1960. Indeed, the early wind measurement systems uses theodolites to track the balloon; this technique requires good visibility and only moderate winds at the upper levels: under fair weather conditions the balloon could be tracked up to 200hPa or even higher, but with storms the balloons were lost soon. As a result, the wind records in severe weather conditions are underrepresented. It has been found the wind speed monthly mean is strongly underestimated since only low winds are recorded. To calculate unbiased monthly wind speed, a "filling" technique has been developed: missing observations can be replaced by scaled NOAA-20CR values. Since the NOAA-20CR wind speeds are known to be low biased (Compo et al. (2011)), they have to be adjusted by a factor λ_{20CR} , derived as the wind speed quotient between the most recent part of the observation time series (treated as unbiased since the instruments are tracked via radar) and the corresponding NOAA-20CR time series. With this precaution, when at least 50% of the monthly values are already present, a missing observation can be synthetically replaced using as proxy the scaled NOAA-20CR value. This approach allows the reduction of the wind speed low bias mainly in the period prior to 1960, when the balloons were tracked via theodolites.

The Fig. 8(a) shows the suspicious strong U wind anomalies trend ($+4.66m/s/10years$) at 200hPa in a composite over USA and Canada stations for the period 1940-1960. The "filling" expedient reduces the sampling bias, as visible in 8(b), where the trend has been lowered to $+0.72m/s/10years$. Employing this technique the wind speed observations, and the derived monthly means are more accurate and precise.

Also temperature time series have been analyzed with RAOBOCRE 2.0. Severe inhomogeneities have been detected through the whole period 1905-2011 (end of NOAA-20CR project) but, particularly interesting was the period prior 1970s when the observation practice was not uniform and the radiosondes were suffering from severe systematic instrumental inefficiency. These inaccuracies "comprised several kelvin in the stratosphere during the 1960s and 1970s" have been already detected by Haimberger et al. (2008). Now, it is possible to go further back in time, till the beginning of time series, and to confirm that heavy temperature biases are affecting the observation also at the lower pressure levels (below 500hPa). In particular the Russian network (already known as strong biased in stratosphere) has a continuous radiation error from the pioneering ascents (early 1940) till 1980, most probably induced by the type of probe used

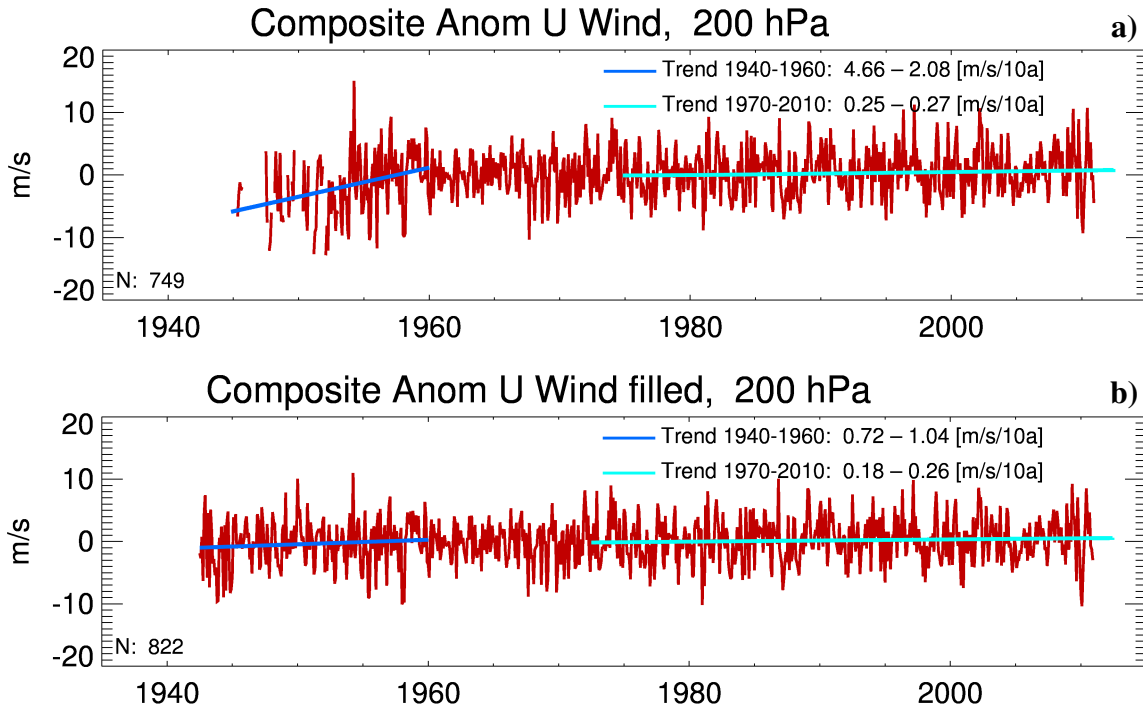


Figure 8: Monthly mean wind speed at 200hPa, averaged over WMO stations with IDs between 70000 and 75000 (most USA and Canada), a) without filling, b) with replacing missing data with NOAA-20CR scaled wind values.

(Haimberger (2007)). Still in more recent times, significant inhomogenities can be detected at the upper levels (above 300hPa) and they should be removed before exploiting the data for climate related studies.

Unfortunately, the NOAA-20CR stratospheric temperature trends are unrealistic and temperature fields show biases up to several kelvin over the Poles and in the Stratosphere (Compo et al. (2011)). Thus, temperature adjustments may be unreliable for the upper levels (above 300hPa) if NOAA-20CR is used as reference for temperature homogenization. However, this homogenization effort has the primary focus on the early data, prior to 1958, when only sporadically soundings reached the 200hPa. On the other hand, ERA-Interim and ERA-40 reanalysis, used as reference in RAOBCORE, show some biases in the upper-troposphere caused by the increasing number of warm-biased temperature reports from aircraft (Dee and Uppala (2009)) and due to the not homogeneous radiosondes information that has been assimilated (Dee et al. (2011)). For the most recent part of the time series (after 1979, where no regional biases are expected), the RICH method, that bases the adjustments on a composite of neighbors stations, should lead to more realistic estimates than RAOBCORE2.0.

To summarize, RAOBCORE2.0 extends the previous efforts to homogenize the global in situ upper air data set back in time till the beginning of the 20th century. It uses as input data the GRASP archive, the most comprehensive collection of the digitalized PILOT balloons and radiosondes, that contains temperature and wind data, supplemented with analysis departures from NOAA-20CR. Compared to previous attempts to homogenize the upper air data sets

archive, RAOBOCORE2.0 has the advantages to analyze, temperature and wind time series together, and in comparison to its ancestors (RAOBCORE and RICH), it is upper air data reference free, since the NOAA-20CR is a surface-data-only reanalysis.

The homogenized wind data sets has been presented in Ramella-Pralungo and Haimberger (2014a), and the adjustments are fully downloadable from the PANGAEA web archive.

The GRASP with the wind and temperature adjustments establishes a new standard for upper air data quality that can be particularly appreciated for climate related studies.

In the third section of this thesis, the GRASP archive and the wind adjustments are used to calculate temperature trends and to compare them with the trends directly derived from temperature radiosondes unadjusted and after homogenization efforts (RAOBCORE and RICH, both). Zonal mean temperature trends can be calculated either directly from temperature information or indirectly by integrating the vertical wind shear over latitude interval. Temperature trends inferred by the wind shear $\partial U / \partial \log p$, at the pressure p , time t and latitude ϕ , can be summarized as:

$$T(\phi, p, t) = T(\phi_o, p, t) + \int_{\phi_o}^{\phi} \frac{af(\phi')}{R} \frac{\partial u(\phi', p, t)}{\partial \log p} d\phi' \quad (5.1)$$

where ϕ_o is some reference latitude, a is Earth's radius, R is the specific gas constant of dry air, f is the Coriolis parameter, p is pressure, T is zonal mean temperature, and u is zonal mean zonal wind speed.

Nevertheless, in order to evaluate the integral, some crucial simplifications are required:

- the reference latitude ϕ_o plays an important role since any error in the reference temperature profile is translated into errors in the tropical trend. Thus, ϕ_o should be selected according to the region where the most accurate direct temperature trend can be estimated. The northern middle latitudes match this criteria and $45^\circ N$ has been chosen (although other references have been tested, for instance $35^\circ N$ is also particularly promising, due to the relative good observations density and the advantage of shorter integration path to the tropics).
- the homogenization plays an active role to define the reference temperature profile $T(\phi_o, p, t)$ and different homogenized data sets have been tested: RAOBOCORE2.0, RAOBCORE and RICH. As previously described, the temperature trends from NOAA-20CR above 300hPa are particularly poor and the RAOBOCORE2.0 outcomes are not fully reliable above this threshold, thus only the RAOBCORE and RICH homogenized data sets are used to calculate the reference temperature trend at $45^\circ N$ (and $35^\circ N$).

- $10^\circ \times 10^\circ$ grid boxes have been introduced, a compromise between numerical accuracy and data availability to grid the available data. When a wind or temperature record contains more than 15 days in a month, the monthly mean is performed. One valid month value either at 00 or 12GMT, coming from one single station, is sufficient to define a grid box average. Two grid boxes are required in order to calculate a longitudinal belt. These criteria are quite crude but they help finding satisfactory grid box coverage in the rather data sparse tropical regions.
- in order to reduce the discretization-induced errors for vertical coordinates, second order finite differences for non-equidistant grid points in $\log p$ have been adopted, as described in Sundqvist and Veronis (1970).

The discretization procedure is particularly decisive and its impact has been tested comparing a zonal mean temperature trend with trends gained by meridionally integrating of dT/dy or $\partial U/\partial p$. All fields are taken directly from NOAA-20CR, once with full sample and once sampled accordingly to the GRASP input data density. As presented in Ramella-Pralungo and Haimberger (2014b), the differences between the inferred trends are quite small, with the exception of Antarctica. Thus, the simplifications introduced are considered accurate and safe enough for trend estimation.

The Fig. 9 gives an overview of the temperature trends calculated from the different data sources employed in this study for the two periods 1979-2005 (chosen as reference period to compare the results with Allen and Sherwood (2008) and Mitchell et al. (2013)) and 1958-2010. The second period is the longest trend that can be calculated employing a reliable temperature reference profile (RICH starts in 1958). However, it seems feasible to go further back in time, since there are sufficient wind data, back to the beginning of the 1950s, but a homogeneous temperature reference profile above 300hPa has yet to be prepared. In the Fig.9(a), apart from the unrealistic trends obtained directly from unadjusted temperature observations (dark blue line), a reasonable agreement is visible between trends calculated directly from adjusted temperature (RICH method) and trends inferred with wind shear data, particularly in the upper troposphere. Both have been obtained by integrating dT/dy and $\partial U/\partial p$ using RICH ensemble mean profile as reference at $45^\circ N$. Employing wind data, the warming maximum is well visible for the period 1979-2005 also employing unadjusted data, while it tends to be weak in the period 1958-2010, most probably due to the wind speed low bias and the non-negligible inhomogeneities that are filled with RAOBCORE 2.0 (Ramella-Pralungo and Haimberger (2014a)). The trend derived from adjusted temperature and wind data are fitting quite well each other considering the estimated uncertainty (gray dashed areas denote the $\pm 1.96\sigma$). The maximum trends are located higher when using wind shear (ca. 200hPa) than temperature (ca. 300hPa).

A possible explanation may be the still too weak temperature homogeneity adjustments for the upper levels or too strong wind shear estimate due to the station scarcity in the tropical region.

The table 1 reports the summary of the deduced trends. After homogenization all the trends are

1979-2005				
	<i>HadCRUT_{v4}</i>	UNADJ	RICH	RAOBCORE
T	0.15 ± 0.02	0.05 ± 0.05	0.21 ± 0.06	0.16 ± 0.06
$45^\circ \partial U / \partial p$		0.21 ± 0.07	0.34 ± 0.07	0.22 ± 0.07
1958-2010				
	<i>HadCRT_{v4}</i>	UNADJ	RICH	RAOBCORE
T	0.11 ± 0.02	0.06 ± 0.03	0.22 ± 0.03	0.21 ± 0.03
$45^\circ \partial U / \partial p$		0.16 ± 0.04	0.29 ± 0.04	0.27 ± 0.04

Table 1: Tropical mean temperature trends for the intervals 1979-2005 and 1958-2010. Best estimates and uncertainties given for *HadCRUT_{v4}* surface trends and maximum trends aloft (between 100 and 500hPa). Trends using wind shear data have used $45^\circ N$ as temperature reference.

in agreement within the uncertainty bounds ($\pm 1.96\sigma$), and the wind deducted trends are always more generous than the direct temperature ones.

To better wrap up the results, the amplification factor, defined as the ratio between the maximum trend in the range 100-500hPa and the surface *HadCRUT_{v4}*¹¹(Morice et al. (2012)) ensemble mean trend, has been introduced:

$$\alpha = \frac{\max(dT/dt)|_{100-500hPa}}{(dT/dt)_{HadCRUTv4_{med}}} \quad (5.2)$$

α is a sensitive measure of the amplification of the surface trend signal and it can be calculated only if the surface trend is significant.

The Fig. 9 reports also the amplification factors: with unadjusted temperatures, they are unrealistic (less than 1) and all the others factors (adjusted temperature, unadjusted and adjusted inferred by wind shear), between 1.5 and 2.5, are fitting well with the recent CIMP5 model predictions (Mitchell et al. (2013)).

Considering the present results and recent satellite data evaluations (Po-Chedley and Fu (2012)), reanalyses (Simmons et al. (2014)) and models (Mitchell et al. (2013)), it is possible to conclude that the tropical temperature trend discrepancies between these data sets have been largely reconciled up to 150hPa (in the stratosphere there are still persisting large differences). In particular, for temperature and wind, the encouraging result has been obtained thanks to satisfactory data coverage over the tropics of the GRASP archive, that includes historical data

¹¹ <http://www.cru.uea.ac.uk/cru/data/temperature/>

and PILOT balloons not previously used, and employing the state of the art homogenization techniques.

The past upper air data are a precious source of information that have been endorsed and made available to the scientific community with the presented thesis. Upcoming in situ upper air data digitization campaign and homogenization efforts will improve the current data availability and reliability, giving new horizons new scientific challenges.

This work has concentrated on extending and improving the data sets backwards. The difficulties seen made clear that measurement homogeneity should be ensured in the future for the rescued historical data. However, the GCOS-Reference Upper-Air Network¹² (GRUAN, Seidel et al. (2009)) campaign for radiosondes climate requirements and, from 1979, the GPS-Radio Occultation (GPS-RO Steiner et al. (2011)) showed that it is feasible to obtain climate quality upper air records without homogenization.

¹² Global Climate Observing System (GCOS) evolved in the GCOS-Reference Upper-Air Network (GRUAN)

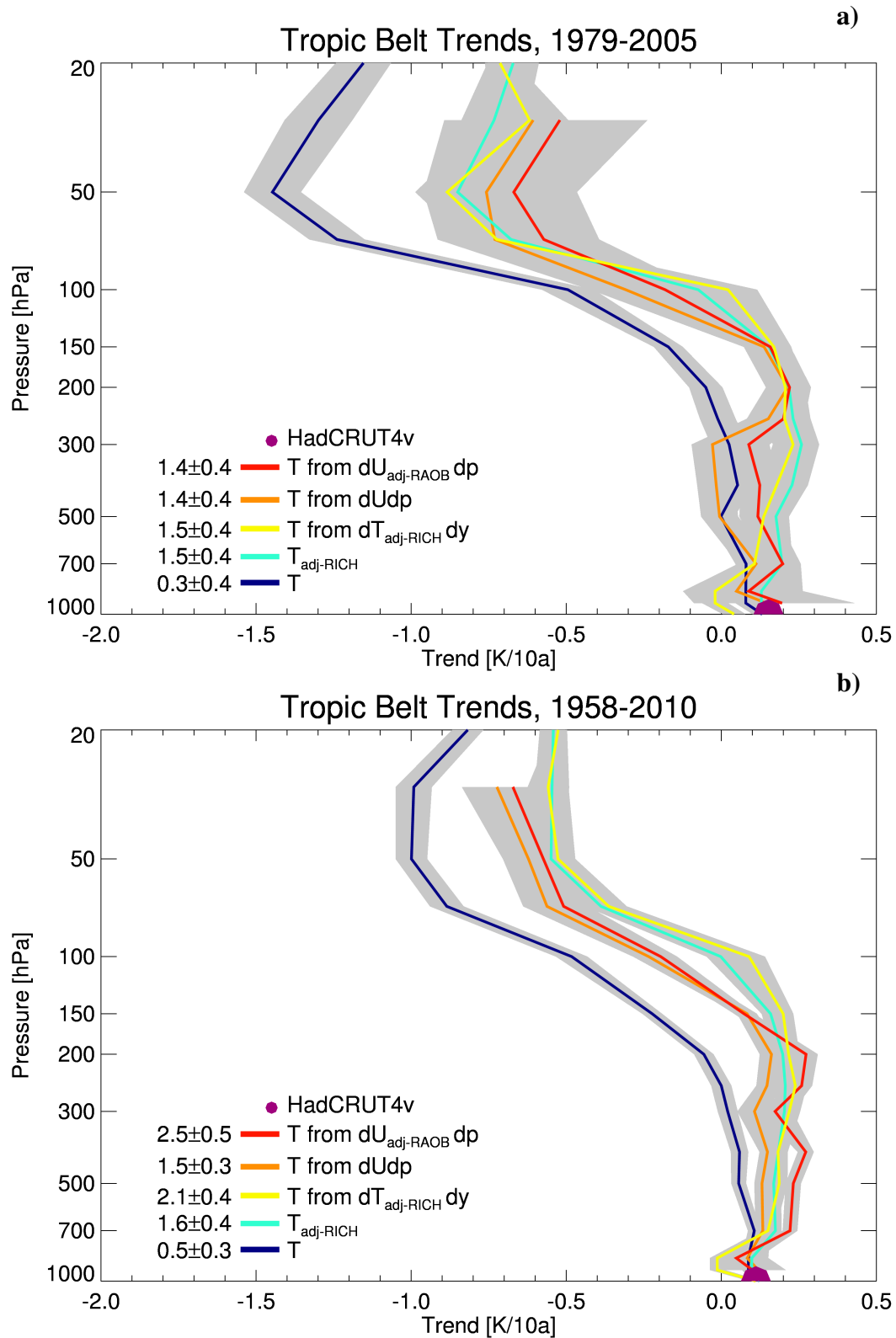


Figure 9: Global mean temperature trends in the tropical belt (20N-20S) inferred from zonal wind vertical wind shear and directly gained from temperature profiles (dark blue unadjusted and light blue adjusted) for the period a) 1979-2005 and b) 1958-2010; integrating from 45N, using RICH reference temperature profile and RAOBCORE2.0 for wind homogenization. The grey shaded areas denote the $\pm 1.96\sigma$ uncertainty. The numbers in the legends are trend amplification factors (max of tropospheric trend/surface trend).

6 Outlook

The results presented in Ramella-Pralungo et al. (2014); Ramella-Pralungo and Haimberger (2014a) and Ramella-Pralungo and Haimberger (2014b) and summarized in this thesis motivate several ideas for next researches.

First, the Atmospheric Circulation Reconstructions over the Earth (ACRE¹³) and the ECMWF ERA-CLIM¹⁴ data-rescuing activities, started in the last years, are still fully operational and, in the upcoming years, will bring to the light new in situ upper air data mainly coming from remote regions like tropical or polar (Jourdain and Roucaute (2013), Stickler et al. (2014)). As soon as the new stations will be digitized, the GRASP archive can be extended and also complementary adjustments can be calculated by RAOBCORE2.0. On the other hand, RAOBCORE 2.0 could be slightly improved adding more physical constrains to allow more sophisticated techniques for adjustments. This point could help temperature homogenization that now suffers due the poor NOAA-20CR temperature trend in the Stratosphere. Also test the RICH method performance for temperature and wind in the early day conditions could be promising even if the station scarcity problem should be treated carefully. A substantial improvement in the ability to detect and adjust breaks is strictly linked with the availability of new reanalysis products that span the whole 20th century. Preferably, these reanalysis should rely only on surface data to preserve the independence between reference and analyzed data. It would be interesting to compare the presented results with a new reanalysis. The new ECMWF ERA-20C (Poli et al. (2013)) seems to be promising.

The extension of the temperature and wind time series and the more dense station coverage in the tropical regions will actively contribute to extend the temperature trend estimation backward and to reduce the uncertainties. At the current state, the availability of wind homogeneous data would lead to satisfactory reliable trends estimation back to the late 1940s (see Ramella-Pralungo and Haimberger (2014b)), but it has to wait for an adequate temperature reference that needs to be prepared in future campaigns of data rescue, digitization and homogenization.

The positive RAOBCORE2.0 experience lets open the humidity data homogenization topic. The time is ripe to include also this important parameter too long forgotten but important to quantify the human impact on climate change (Santer et al. (2007)). In the past, Dai et al. (2011) were able to globally and automatically homogenize the dew point depression radiosonde data coming from the IGRA archive gaining more coherent trends during 1973-2009 than the raw data. In the presented work it was planned to insert also humidity in GRASP and RAOB-

¹³ <http://www.met-acre.org/>

¹⁴ <http://www.era-clim.eu/>

CORE2.0 projects, but due to the lack of a suitable reference, it was not possible to collocate not-standard altitude and time data contained in the CHUAN and ECUD to standard pressure and synoptic time and to homogenize them.

For the most recent part of the series (from 1993 onwards) MSU information could be employed as reference series (Santer et al. (2007)). Challenging is also the homogenization in the modern era where the Satellite radiance GPS-RO (Steiner et al. (2011)) could be used as background reference in addition to the reanalysis information.

Having a long and homogeneous set of upper air temperature, wind and humidity time series covering the whole globe would represent a top quality archive that could be suitable for climate change studies and could be used as input data for future reanalysis efforts.

References

- Alexandersson, H. and Moberg, A. (1997). Homogenization of Swedish temperature data. part I: Homogeneity test for linear trends. *Int. J. Climatol.*, 17:25–34.
- Allen, R. J. and Sherwood, S. C. (2008). Warming maximum in the tropical upper troposphere deduced from thermal winds. *Nature Geoscience*, 1:399–403.
- Brönnimann, S. and Luterbacher, J. (2004). Reconstructing northern hemisphere upper-level fields during World War II. *Clim. Dyn.*, 22:499–510. DOI 10.1007/s00382-004-0391-3.
- Brönnimann, S., Martius, O., Franke, J., Stickler, A., and Auchmann, R. (2013). Historical weather extremes in the "twentieth century reanalysis". *Geographica Bernensia*, G89:7–17. doi:10.4480/GB2013.G89.01.
- Brönnimann, S., Stickler, A., Griesser, T., Ewen, T., Grant, A. N., Fischer, A. M., Schraner, M., Peter, T., Rozanov, E., and Ross, T. (2009). Exceptional atmospheric circulation during the "Dust Bowl". *Geophys. Res. Lett.*, 36:L08802. doi:10.1029/2009GL037612.
- Compo, G. P., Whitaker, J. S., Sardeshmukh, P. D., Matsui, N., Allan, R. J., Yin, X., Gleason, B. E., Vose, R. S., Rutledge, G., Bessemoulin, P., Brönnimann, S., Brunet, M., Crouthamel, R. I., Grant, A. N., Groisman, P. Y., Jones, P. D., Kruk, M. C., Kruger, A. C., Marshall, G. J., Maugeri, M., Mok, H. Y., Nordli, Å., Ross, T. F., Trigo, R. M., Wang, X. L., Woodruff, S. D., and Worley, S. J. (2011). The twentieth century reanalysis project. *Q.J.R. Meteorol. Soc.*, 137A:1–28. DOI: 10.1002/qj.776.
- Dai, A., Wang, J., Thorne, P. W., Parker, D. E., Haimberger, L., and Wang, X. L. (2011). A new approach to homogenize daily radiosonde humidity data. *J. Climate*, 24:965–991. doi: <http://dx.doi.org/10.1175/2010JCLI3816.1>.
- Dee, D. and Uppala, S. (2009). Variational bias correction of satellite radiance data in the era-interim reanalysis. *Q.J.R. Meteorol. Soc.*, 135:1830–1841. doi:10.1002/qj.493.
- Dee, D. P., Uppala, S. M., Simmons, A. J., Berrisford, P., Poli, P., Kobayashi, S., Andrae, U., Balmaseda, M. A., Balsamo, G., Bauer, P., Bechtold, P., Beljaars, A. C. M., van de Berg, L., Bidlot, J., Bormann, N., Delsol, C., Dragani, R., Fuentes, M., Geer, A. J., Haimberger, L., Healy, S. B., Hersbach, H., Hólm, E. V., Isaksen, L., Kallberg, P., Köhler, M., Matricardi, M., McNally, A. P., Monge-Sanz, B. M., Morcrette, J.-J., Park, B.-K., Peubey, C., de Rosnay, P., Tavolato, C., Thépaut, J.-N., and Vitart, F. (2011). The ERA-Interim reanalysis: configuration and performance of the data assimilation system. *Q.J.R. Meteorol. Soc.*, 137:553–597. doi: 10.1002/qj.828.
- Douglass, D. H., Christy, J. R., Pearson, B. D., and Singer, S. F. (2007). A comparison of tropical temperature trends with model predictions. *R. Meteorol. Soc.*, 27. doi: 10.1002/joc.1651.
- DuBois, J. L., Multhauf, P. R., and Ziegler, A. C. (2002). *The Invention and Development of the Radiosonde*. Smithsonian Institution Press. http://www.sil.si.edu/smithsoniancontributions/HistoryTechnology/pdf_lo/SSHT-0053.pdf.
- Durre, I., Vose, R., and Wuertz, D. B. (2006). Overview of the integrated global radiosonde archive. *J. Climate*, 19:53–68. <http://dx.doi.org/10.1175/JCLI3594.1>.

- Gruber, C. and Haimberger, L. (2008). On the homogeneity of radiosonde wind time series. *Meteorol. Z.*, 17:631–643. DOI: 10.1127/0941-2948/2008/0298.
- Haimberger, L. (2007). Homogenization of radiosonde temperature time series using innovation statistics. *J. Climate*, 20:1377–1403. doi: <http://dx.doi.org/10.1175/JCLI4050.1>.
- Haimberger, L., Gruber, C., Sperka, S., and Tavolato, C. (2008). Homogenization of the global radiosonde temperature and wind dataset using innovation statistics from reanalyses. In *Proceedings of the Third WCRP International Conference on Reanalyses*, page 5. http://wcrp.ipsl.jussieu.fr/Workshops/Reanalysis2008/Documents/G4-411_ea.pdf.
- Haimberger, L., Tavolato, C., and Sperka, S. (2012). Homogenization of the global radiosonde temperature dataset through combined comparison with reanalysis background series and neighboring stations. *J. Climate*, 25:8108–8131. doi: <http://dx.doi.org/10.1175/JCLI-D-11-00668.1>.
- Hartmann, D. L., Klein Tank, A. M. G., and Rusticucci, M., editors (2013). *IPCC 2013: The Physical Science Basis*, chapter Observations: Atmosphere and Surface, pages 159–254. IPCC. <http://www.ipcc.ch/report/ar5/wg1/>.
- Hoinka, P. K. (1997). The tropopause: discovery, definition and demarcation. *Meteorolo. Zeitschrift*, 6:281–303. <http://empslocal.ex.ac.uk/people/staff/gv219/classics.d/Hoinka-tropo97.pdf>.
- Jourdain, S. and Roucaute, E. (2013). Historical upper air data rescue at météo-france for ERA-CLIM. In *EMS Annual Meeting Abstracts*, volume 10, pages EMS2013–97. EMS. <http://meetingorganizer.copernicus.org/EMS2013/EMS2013-97.pdf>.
- Kington, J. (1988). *The Weather of the 1780s Over Europe*. Cambridge University Press. ISBN: 9780521113076.
- Le Treut, H., Somerville, R., Cubasch, U., Ding, Y., Mauritzen, C., Mokssit, A., Peterson, T., and Prather, M. (2007). Historical overview of climate change. in: Climate change 2007: The physical science basis. contribution of working group i to the fourth assessment report of the intergovernmental panel on climate change. *Cambridge University Press, Cambridge, United Kingdom and New York, NY, USA.*, pages 1–36. <http://www.ipcc.ch/pdf/assessment-report/ar4/wg1/ar4-wg1-chapter1.pdf>.
- Meehl, G. A., Covey, C., Delworth, T., Latif, M., McAvaney, B., Mitchell, J. F. B., Stouffer, R. J., and Taylor, K. E. (2007). The WCRP CMIP3 multi-model dataset: A new era in climate change research. *Bull. Amer. Meteor. Soc.*, 88:1383–1394. doi: <http://dx.doi.org/10.1175/BAMS-88-9-1383>.
- Mitchell, D., Thorne, P., Stott, P., and Gray, L. (2013). Revisiting the controversial issue of tropical tropospheric temperature trends. *Geo. Res. Lett.*, 40:1–6. doi:10.1002/grl.50465.
- Morice, C. P., Kennedy, J. J., Rayner, N. A., and D., J. P. (2012). Quantifying uncertainties in global and regional temperature change using an ensemble of observational estimates: The HadCRUT4 dataset. *J. Geophys. Res.*, 117:1–22. doi:10.1029/2011JD017187.

- Po-Chedley, S. and Fu, Q. (2012). Discrepancies in tropical upper tropospheric warming between atmospheric circulation models and satellites. *Environ. Res. Lett.*, 7:044018. doi:10.1088/1748-9326/7/4/044018.
- Poli, P., Hersbach, H., Tan, D., Dee, D., Thépaut, J.-N., Simmons, A., Peubey, C., Laloyaux, P., Komori, T., Berrisford, P., Dragani, R., Tremolet, Y., Holm, E., Bonavita, M., Isaksen, L., and Fisher, M. (2013). The data assimilation system and initial performance evaluation of the ECMWF pilot reanalysis of the 20th-century assimilating surface observations only (ERA-20C). Technical Report 14, ECMWF.
- Ramella-Pralungo, L. and Haimberger, L. (2014a). A global radiosonde and tracked balloon archive on 16 pressure levels (grasp) back to 1905: part II: Homogeneity adjustments for pilot and radiosonde wind data. *ESSD*, 6:297–316. doi:10.5194/essd-6-297-2014.
- Ramella-Pralungo, L. and Haimberger, L. (2014b). New estimates of tropical mean temperature trend profiles from zonal mean historical radiosonde and pilot balloon wind shear observations. *Journal of Geophysical Research*, ??:?? submitted.
- Ramella-Pralungo, L., Haimberger, L., Stickler, A., and Brönnimann, S. (2014). A global radiosonde and tracked balloon archive on 16 pressure levels (grasp) back to 1905: part I: Merging and interpolation to 00 and 12gmt. *ESSD*, 6:185–200. doi:10.5194/essd-6-185-2014.
- Santer, B., Thorne, P., Haimberger, L., Taylor, K., Wigley, T., Lanzante, J., Solomon, S., Free, M., Gleckler, P., Jones, P., Karl, T., Klein, S., Mears, C., Nychka, D., Schmidt, G., Sherwood, S., and Wentz, F. (2008). Consistency of modelled and observed temperature trends in the tropical troposphere. *Int. J. Climatol.*, 28:1703–1722. DOI: 10.1002/joc.1756.
- Santer, B. D., Mears, C., Wentz, F. J., Taylor, K. E., Gleckler, P. J., Wigley, T. M. L., Barnett, T. P., Boyle, J. S., Brüggemann, W., Gillett, N. P., Klein, S. A., Meehl, G. A., Nozawa, T., Pierce, D. W., Stott, P. A., and Washington, W. M. and Wehner, M. F. (2007). Identification of human-induced changes in atmospheric moisture content. *Proceedings of the National Academy of Sciences of the United States of America*, 104:15248 – 15253. doi: 10.1073/pnas.0702872104.
- Santer, B. D., Wigley, T. M. L., Mears, C., Wentz, F. J., Klein, S. A., Seidel, D. J., Taylor, K. E., Thorne, P. W., Wehner, M. F., Geckler, P. J., Boyle, J. S., Collins, W. D., Dixon, K. W., Doutriaux, C., Free, M., Fu, Q., Hansen, J. E., Jones, G. S., Ruedy, R., Karl, T. R., Lanzante, J. R., Meehl, G. A., Ramaswamy, V., Russell, G., and Schmidt, G. A. (2005). Amplification of surface temperature trends and variability in the tropical atmosphere. *Science*, 309:1551–1556. DOI: 10.1126/science.1114867.
- Seidel, D. J., Berger, F. H., Immler, F., Sommer, M., Vömel, H., Diamond, H. J., Dykema, J., Goodrich, D., Murray, W., Peterson, T., Sisterson, D., Thorne, P., and Wang, J. (2009). Reference upper-air observations for climate: Rationale, progress, and plans. *Bull. Amer. Meteor. Soc.*, 90:361–369. doi: http://dx.doi.org/10.1175/2008BAMS2540.1.
- Sherwood, S., Lanzante, J., and Meyer, C. (2005). Radiosonde daytime biases and late 20th century warming. *Science-express*, 309:1556–1559. doi: 10.1126/science.1115640309.

- Simmons, A. J., Poli, P., Dee, D. P., Berrisford, P., Hersbach, H., Kobayashi, S., and Peubey, C. (2014). Estimating low-frequency variability and trends in atmospheric temperature using ERA-Interim. *Q.J.R. Meteorol. Soc.*, 140:323–353. DOI: 10.1002/qj.2317.
- Solomon, S., Qin, D., Manning, M., Chen, Z., Marquis, M., Averyt, K., Tignor, M., and Miller, H. (2007). Contribution of working group i to the fourth assessment report of the intergovernmental panel on climate change, 2007. *Cambridge University Press, Cambridge, United Kingdom and New York, NY, USA*. http://www.ipcc.ch/publications_and_data/ar4/wg1/en/contents.html.
- Steiner, A. K., Lackner, B. C., Ladstätter, F., Scherllin-Pirscher, B., Foelsche, U., and Kirchengast, G. (2011). GPS radio occultation for climate monitoring and change detection. *Radio Science*, 46:RS0D24. doi:10.1029/2010RS004614.
- Stickler, A. and Brönnimann, S. (2011). Significant bias of the ncep/ncar and twentieth century reanalyses relative to pilot balloon observations over the west african monsoon region (1940–57). *Q.J.R. Meteorol. Soc.*, 137. doi: 10.1002/qj.854.
- Stickler, A., Brönnimann, S., Jourdain, S., Roucaute, E., Sterin, A., Nikolaev, D., Valente, M. A., Wartenburger, R., Hersbach, H., Ramella-Pralungo, L., and Dee, D. (2014). Description of the ERA-CLIM historical upper-air dataset. *ESSD*, 6:29–48. doi:10.5194/essd-6-29-2014.
- Stickler, A., Grant, A. N., Ewen, T., Ross, T. F., Vose, R. S., Comeaux, J., Bessemoulin, P., Jylhä, K., Adam, W. K., Jeannet, P., Nagurny, A., Sterin, A. M., Allan, R., Compo, G. P., Griesser, T., and Brönnimann, S. (2010). The comprehensive historical upper air network (CHUAN). *Bull. Amer. Meteor. Soc.*, 91:741–751. <http://dx.doi.org/10.1175/2009BAMS2852.1>.
- Sundqvist, H. and Veronis, G. (1970). A simple finite-difference grid with non-constant intervals. *Tellus*, 22:26–31. <http://tellusa.net/index.php/tellusa/article/viewFile/10155/11783>.
- Thorne, P. W., Willett, K. M., Allan, R. J., Bojinski, S., Christy, J. R., Fox, N., Gilbert, S., Jolliffe, I., Kennedy, J. J., Kent, E., Klein Tank, A., Lawrimore, J., Parker, D. E., Rayner, N., Simmons, A., Song, L., Stott, P. A., and Trewin, B. (2011). Guiding the creation of a comprehensive surface temperature resource for 21st century climate science. *Bull. Amer. Meteor. Soc.*, 92:ES40–ES47. doi:10.1175/2011BAMS3124.1.
- Trenberth, K. E., Jones, P. D., Ambenje, P., Bojariu, R., Easterling, D., Klein-Tank, A., Parker, D., Rahimzadeh, F., Renwick, J. A., Rusticucci, M., Soden, B., and Zhai, P. (2007). *Climate Change 2007: The Physical Science Basis*, chapter 3 Observations: Surface and Atmospheric Climate Change. Contribution of Working Group I to the Fourth Assessment Report of the Intergovernmental Panel on Climate Change, pages 235–336. Cambridge University Press, Cambridge, United Kingdom and New York, NY, USA. http://www.ipcc.ch/publications_and_data/ar4/wg1/en/contents.html.
- Uppala, S. M., Kållberg, P. W., Simmons, A. J., Andrae, U., da Costa Bechtold, V., Fiorino, M., Gibson, J. K., Haseler, J., Hernandez, A., Kelly, G. A., Li, X., Onogi, K., Saarinen, S., Sokka, N., Allan, R. P., Andersson, E., Arpe, K., Balmaseda, M. A., Beljaars, A. C. M., van de Berg,

L., Bidlot, J., Bormann, N., Caires, S., Chevallier, F., Dethof, A., Dragosavac, M., Fisher, M., Fuentes, M., Hagemann, S., Hólm, E., Hoskins, B. J., Isaksen, L., Janssen, P. A. E. M., Jenne, R., McNally, A. P., Mahfouf, J.-F., Morcrette, J.-J., Rayner, N. A., Saunders, R. W., Simon, P., Sterl, A., Trenberth, K., Untch, A., Vasiljevic, D., Viterbo, P., and Woollen, J. (2005). The ERA-40 Re-analysis. *Q. J. R. Meteorol. Soc.*, 131:2961–3012. doi: 10.1256/qj.04.176.

Wartenburger, R., Brönnimann, S., and Stickler, A. (2013). Observation errors in early historical upper-air observations. *J. Geophys. Res.*, 118:12012–12028. doi: 10.1002/2013JD020156.

Acknowledgments

First of all, I am thankful to my advisor Leo Haimberger. My gratitude to him goes for the capable guidance, the invaluable constructive criticism and the friendly advice during the project work. Leo was always available for constructive brainstorming sessions and he supported me with brilliant ideas. I appreciate his huge willingness during the last months of remote work.

I would also like to thank Hans Hersbach, Alex Stickler, Stefan Brönnimann, Gilbert P. Compo, and Dick Dee, who helped me with scientific and technical hints to finalize the project.

Thanks to all my colleagues, in particular Michael, Christina, Lukas, Stefano, Johannes, Niko, Felizitas, Irene, and Simon that actively contribute to make this experience simply unforgettable.

This is also the right place to thank my Vienna's family: Gloria, Francesca, Elena, Tanja, Mauricio, Alessandro, and Paolo for the great time we had in Vienna, for sharing unique moments of happiness and to cheering up each other during the difficulties. Thanks to my flatmates David, Larissa, Liz, Robert, Stephan, and Rebecca for the nice time we have spent together and the pleasant experience of life.

Special thanks for to my parents, Anna and Giovanni, who supported me to become a meteorologist, for the warm welcome back every time I was visiting home and for the effort to pick me up or bring me to the airport. Gratitude to my brother Stefano that was (almost) always available to accomplish my wish of wild nature, bike and alpinism.

Last but not least, my heart goes out to Olivera, for the unconditioned support and patience during the realization of this thesis, for being understanding when I was absorbed by the work during many evenings and weekends.

I can not forget to mention one more time my gratitude Michael for translating the abstract in German and to Mauricio, Francesca, Olivera, Anna and Stefano for the helpful suggestions to make better this thesis's look.

*Sincere thanks,
you all contribute
to realize this dream
and to make my life better;*

Lorenzo

Europass Curriculum Vitae



Personal information

Surname / First name **Ramella Pralungo, Lorenzo**
Telephone +39-347-95-89109 (ITA) +41-768181084(CH)
Email lore.rame@libero.it
Nationality Italian
Date and place of birth October 14, 1984 in Biella (Italy)
Gender male



Current position

Position Meteo Analyst
Affiliation DufEnergy Trading SA - Duferco
Address Via Bagutti, 9, 6900 Lugano, Switzerland
Telephone / Fax +41 91 822 56 00/ +41 91 822 57 00
Email lorenzo.ramella@dufenergy.com
Web www.duferco.com

Work Experience

October 2009 - February 2014 *PhD Student ("Doktoratsstudent") in Meteorology and Climatology*
Web: <http://img.univie.ac.at/en/research/tm/staff/ramella-pralungo/>
Department of Meteorology and Geophysics, University of Vienna, Austria
September 2008 - May 2009 *Project fellowship: development and calibration of strategies for the gas engine control*
Web: <http://www.crf.it/en-US/Pages/default.aspx>
Centro Ricerche FIAT (CRF), Turin, Italy
January 2008 - June 2008 *Research internship: study and characterisation of suction pipes fluid dynamics*
Web: <http://www.crf.it/en-US/Pages/default.aspx>
Centro Ricerche FIAT (CRF), Turin, Italy

Research interests

Mountain meteorology and clima.

Research projects

April 2013 - February 2014 **As Researcher:**
FWF (Austrian Science Fund) Stand-alone project P25260, "Homogenous atmospheric observations, state and flux quantities of the past 75 years", PI: Ao.Univ.Prof.Dr. Leopold Haimberger.
November 2012 - March 2013 EC FP7 'ERA-CLIM' European project, PI: Ao.Univ.Prof.Dr. Leopold Haimberger.
October 2009 - October 2012 WF (Austrian Science Fund) Stand-alone project P21772, "Global historic in situ upper air data for climate change research", PI: Ao.Univ.Prof.Dr. Leopold Haimberger.

Other scientific activity

Training Courses

- ECMWF training course: 'Predictability, diagnostics and extended-range forecasting', from 8 to 17 May 2013, Shinfield Park, Reading (UK)
- ECMWF training course: 'Data assimilation and use of satellite data', from 4 to 13 May 2011, Shinfield Park, Reading (UK)
- ECMWF training course: 'Computer User Training Course', from 1 to 5 May 2010, Shinfield Park, Reading (UK)

As meteorologist

- Meteorological consulting and translation to Italian for the project:
MetGIS: World-Wide Mountain Weather Forecasts
<http://www.metgis.com>. From October 2012 to June 2013.

Teaching

Courses

Exercise courses

- **Programming in Meteorology** in the B.Sc. program in Meteorology, in the Academic Years 2013-2012-2011-2010. Faculty of Earth Sciences, Geography and Astronomy, University of Vienna.
- **Statistical Methods of Meteorology** in the B.Sc. program in Meteorology, in the Academic Years 2013-2014. Faculty of Earth Sciences, Geography and Astronomy, University of Vienna.
- **Ensemble prediction system** in the M.Sc. program in Meteorology, in the Academic Year 2012. Faculty of Earth Sciences, Geography and Astronomy, University of Vienna.

Curriculum Studiorum

- Master Degree in **Environmental and Biomedical Physic**
University of Turin, Turin (Italy), July 25th 2008, full marks with honours.
Dissertation: *Experimental investigation of the intake duct performance for new generation internal combustion engines*. Supervisor: Prof. Guido Boffetta.
- Degree in **Physic**
University of Turin, Turin (Italy), July 27th 2006, full marks
Dissertation: *Thermal analysis in Alpine environment*. Supervisor: Prof. Claudio Cassardo.
- Diploma di maturità scientifica (Scientific high school leaving certificate)
ITIS "Q. Sella", Biella (Italy), June 2003, marks 100/100.

Language skills

Mother tongue
Self-assessment
European level*

English

German

Italian

Understanding				Speaking				Writing	
Listening		Reading		Spoken interaction		Spoken production			
C1	Proficient user	C1	Proficient user	C1	Proficient user	C1	Proficient user	C1	Proficient user
B1	Independent user	B1	Independent user	B1	Independent user	B1	Independent user	A2	Basic user

* Common European Framework of Reference (CEF) level

Last updated: November 13, 2014

Lorenzo Ramella Pralungo, publications and contributions

Articles on peer-reviewed journals

- [1] **Ramella-Pralungo, L.**, and Haimberger, L. (2014): New estimates of tropical mean temperature trend profiles from zonal mean historical radiosonde and pilot balloon wind shear observations. *Submitted*
- [2] **Ramella-Pralungo, L.**, and Haimberger, L. (2014): A global radiosonde and tracked balloon archive on 16 pressure levels (GRASP) back to 1905: Part II: Homogeneity adjustments for PILOT and radiosonde wind data. *ESSD*, **6**, 297-316.
doi:10.5194/essd-6-297-2014
- [3] **Ramella-Pralungo, L.**, and Haimberger, L. and Stickler, A. and Brönnimann, S. (2014): A global radiosonde and tracked balloon archive on 16 pressure levels (GRASP) back to 1905: Part I: Merging and Interpolation to 00 and 12GMT. *ESSD*, **6**, 185-200.
doi:10.5194/essd-6-185-2014
- [4] Stickler, A. and Brönnimann, S. and Jourdain, S. and Roucaute, E. and Sterin, A. and Nikolaev, D. and Valente, M. A. and Wartenburger, R. and Hersbach, H. and **Ramella-Pralungo, L.** and Dee, D. (2014): Description of the ERA-CLIM historical upper-air dataset *ESSD*, **6**, 29-48.
doi:10.5194/essd-6-29-2014

International conference contributions

- [5] **Ramella-Pralungo, L.**, and Haimberger, L. (2013): Reducing uncertainties of early upper air time series using surface data only reanalyses. *13th EMS Annual Meeting and 11th European Conference on Applications of Meteorology (ECAM)*, 09.-13. September 2013, Reading, United Kingdom.
- [6] **Ramella-Pralungo, L.**, and Haimberger, L. (2013): Quality control and homogenization of early upper air time series using surface data only reanalyses. *DACH 2013: die Deutsch-Österreichisch-Schweizerische Meteorologentagung*, Innsbruck, Austria, 02.-06. September 2013.
- [7] **Ramella-Pralungo, L.**, and Haimberger, L. (2012): Global historic in situ upper air data for climate change research. *5th ACRE Workshop*, Meteo France, Toulouse (France), 28.-30. November, 2012.
- [8] **Ramella-Pralungo, L.**, and Haimberger, L. (2012): Homogenization of radiosonde Temperature and Wind records using 20CR and ERA background information *2nd EC FP7 ERA-CLIM General Assembly*, Meteo France, Toulouse, (FRANCE), 26.-28. November, 2012.
- [9] **Ramella-Pralungo, L.**, and Haimberger, L. (2012): Global historic in situ upper air data for climate change research. *4th WCRP International Conference on Reanalysis*, Silver Spring, Maryland (USA), 07.-11. May, 2012
- [10] **Ramella-Pralungo, L.** and Haimberger, L. (2012): Global historic in situ upper air data for climate change research. *ERA-CLIM work package 4th Workshop on observation errors*, Vienna (Austria), 19.-20. April, 2012.
- [11] Leopold Haimberger, and **Ramella-Pralungo, L.** and Hadzimustafic, J. and Tavalato, C. (2011): Homogenization of the global radiosonde temperature and wind data sets. *European Geosciences Union (EGU) 2011*, Vienna, (Austria), 03.-08. April 2011.

National conference contributions (Austria)

- [12] Haimberger, L. and Tavalato, C. and **Ramella-Pralungo, L.**: Systematische Fehler im globalen Radiosondentemperaturdatensatz 4. *Österreichischer Meteorologentag*, Klagenfurt (A), November 03rd and 04th November 2011.